Some Determinations of the Energy Levels of Light Nuclei

by

J. G. Rutherglen

Department of Natural Philosophy,

University of Glasgow.

Presented as a thesis for the degree of Ph.D.

in the University of Glasgow.

May, 1951.

ProQuest LLC.
789 East Eisenhower Parkway
P.O. Box 1346
Ann Arbor, MI 48106 – 1346

Preface.

In this thesis I have described some of the methods by which data can be obtained on the energy levels of light nuclei. Part I. contains a summary of the fundamental considerations relating to nuclear energy levels, their general properties and the basic methods which are used in the study of them. This part has been largely drawn from Devons (Excited States of Nuclei) and Bethe (Reviews of Modern Physics. Vol.9, 1937).

Part II. describes the methods which are used to accelerate charged particles to high energies for nuclear disintegration experiments. After a general summary, this part contains a description of the design and construction of the 800 kilovolt high tension accelerator set with which the nuclear disintegration experiments presented in this thesis were performed. Much of this work is new, in particular, a new type of positive ion source is described, which has a greatly improved performance compared with sources previously used. I should like to acknowledge the assistance of Mr. J. F. I. Cole during some of the early work on the ion source. The work on the design and construction of the H.T. generator, the accelerator tube, and its associated equipment, was performed in collaboration with Mr. R. D. Smith.

Part III. contains a description of the spectrometer used in measurements on the disintegration products from

nuclear reactions. The work on the design and development of the spectrometer for charged particle measurements was performed solely by myself. The gamma-ray spectrometer was designed by Dr. E. R. Rae and I was only concerned with certain small modifications which had to be made for the particular experiments described in this thesis.

In Part IV. the results of a number of nuclear disintegration experiments are presented, together with a discussion of their significance in relation to the energy levels of the nuclei involved. The matter here is original, but I should like to acknowledge the assistance of Dr. E. R. Rae and Mr. R. D. Smith in the experimental work on the gamma-ray measurements and of Mr. R. D. Smith in the work on the reaction $Al^{27}(p,\alpha)Mg^{24}$.

In Part V. I have concluded by discussing the present state of our knowledge of nuclear energy levels and the attempts which have been made to find a theory of nuclear structure and nuclear forces which will explain the experimental data.

I should like to thank Professor P. I. Dee for his sustained interest and encouragement and for many helpful discussions during the course of the work.

May, 1951. J.G.R.

* * * * * * *

Some Determinations of the Energy Levels of Light Nuclei.

Contents.

II.4./

Contents (Continued)

* * * * * *

Part I. General Discussion of Nuclear Properties.

I.1. Reasons for the Study of Nuclear Energy Levels.

The atomic nucleus consists of an assembly of protons and neutrons which are bound together by forces which are known to be very strong compared with the Coulomb forces which bind the atomic electrons to the nucleus. One of the most fundamental problems which remains to be solved is that of the nature of these nuclear forces. In the case of atomic structure a very complete theory has been developed, based on the original conceptions of Rutherford and Bohr. This theory has led to a very complete understanding of the quantum mechanical processes involved in the interaction of matter and radiation. The principal experimental data on which this theory was based was a knowledge of the excited states of the atomic electrons. This data was obtained from the study, by spectroscopic methods, of the radiation emitted by excited atoms in returning to the ground state, or to excited atates of lower energy.

Now in the case of the nucleus, as in the case of the atom, the principles of quantum mechanics would lead us to expect that the total energy of the nucleons could only assume a set of discrete values, the 'energy levels' of the nucleus. A large amount of experimental data has been obtained to confirm this expectation, for example the

phenomena of resonance absorption of protons and neutrons and the emission of gamma-rays of discrete energy values provide striking confirmation. The particular properties of these energy levels, such as their spacing from the ground state, their angular momentum, energy width etc. must depend upon the forces between individual nucleons and upon the structure of the nucleus. Thus it is clearly desirable to have as complete a knowledge as possible of the energy levels of nuclei in order to provide a basis for comparison with theoretical predictions based on assumptions as to the nature of nuclear forces and nuclear structure.

* * * * * *

I. 2. Methods of Excitation available for Light Nuclei.

In order to make measurements on nuclear energy levels it is clearly necessary to have some method of exciting the nucleus concerned. Now the energy of even the lowest level of most nuclei is of the order of 10^4 volts above the ground state and consequently the normal methods used for the excitation of optical spectra are quite impractical.

The two methods of nuclear excitation which have had the widest use are (a) bombardment of nuclei by nucleons or small groups of nucleons and (b) radio-active decay. In the case (a) the original nucleus may be left excited by an inelastic collison, or a nuclear reaction may occur, leaving a residual nucleus in an excited state. In the case (b) the residual nucleus of β-decay may be left in an excited state. It is also possible to excite nuclei by irradiating them with high energy electromagnetic radiation or electrons, but this method has only had limited application at the present time on account of the technical difficulties involved. The method which has by far the widest field of application, particularly in the case of light nuclei, is that of bombarding the nuclei with high energy particles.

* * * * * *

I.3. Classification of Nuclear Reactions.

Let us consider a nuclear reaction of the following type:

$$A + P \rightarrow C \rightarrow B + R$$

Here a particle P collides with a nucleus A, forming the compound nucleus C, which will normally be in a highly excited state. This compound nucleus may then de-excite in two principal ways, (a) by emitting one or more gamma quanta to the ground state of C, (b) by emitting a particle R and leaving the residual nucleus B in its ground state or in an excited state. We may conveniently illustrate such a reaction by means of the energy level diagram shown in Fig. I (1).

Here we represent energy on a vertical scale and plot the energy levels of the three systems A + P, C and B + R. The solid horizontal lines represent the ground state of the three systems and the dotted horizontal lines represent excited states. We assume that the particles P and R are either elementary particles or simple combinations such as deuterons or alpha-particles for which there are no excited states in the energy region which we are considering. Thus

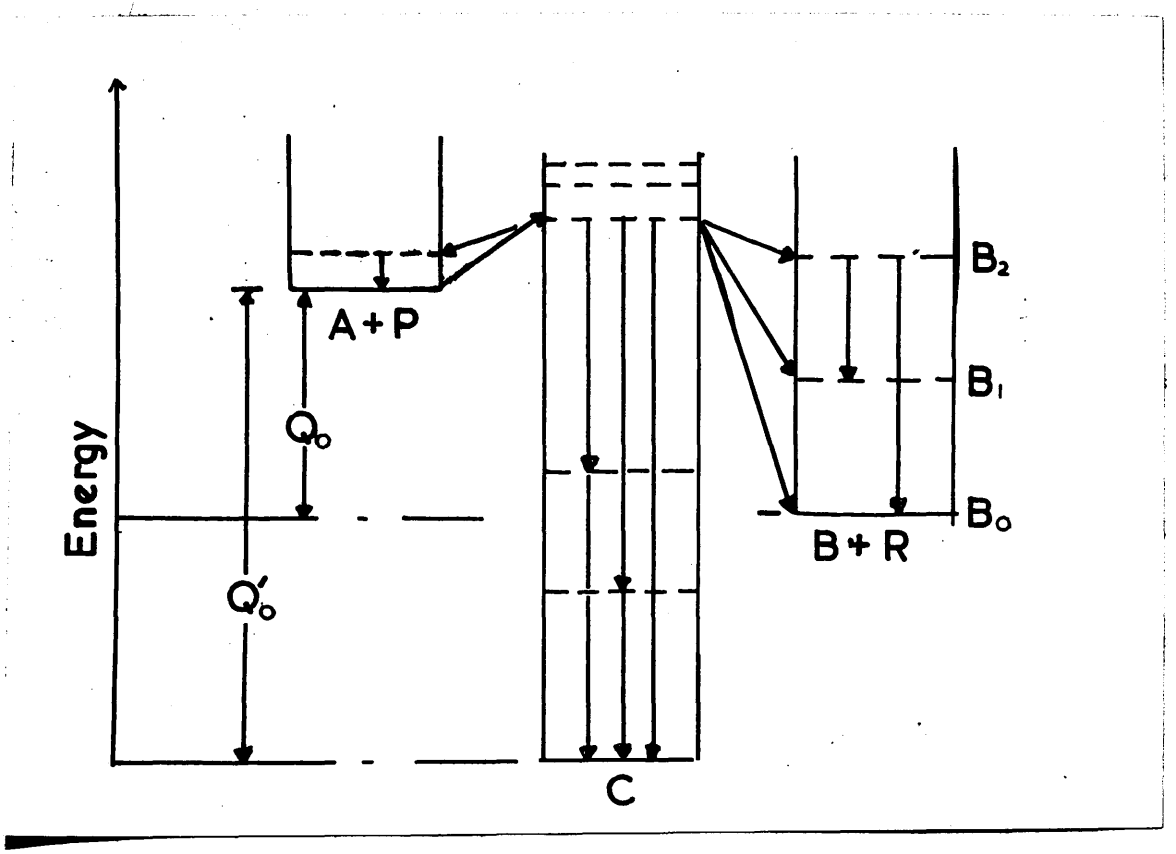

Fig.I(i). Nuclear Energy Level Diagram.

the excited states represented in Fig.1(b) are simply those of the compound nucleus C and the residual nucleus B. The arrows represent transitions from one state to another, the diagonal arrows representing emission or absorption of a particle and the vertical arrows representing the emission of gamma -quanta. The energy liberated during a particular transition is usually denoted by Q. Let us consider the reaction A + P → B + R, which for convenience is usually written A (P,R) B. Then, if B is left in the ground state B_o, we may denote the energy released by Q_o and the total kinetic energy which will be divided between R and B will be $Q_o + E_P$, where E_P is the kinetic energy of the incident particle P. On the energy level diagram Q_o is the vertical separation between the lines representing the ground states of A + P and B + R. If the residual nucleus B is left in an excited state B_1, and the energy released is Q_1, then the total kinetic energy will be $Q_1 + E_P$. In order to measure Q_o and Q_1 it is only necessary to measure the kinetic energy of the particle R in each case, since the geometry of the experiment and the principle of the conservation of momentum define the division of energy between R and B. We may note that, since R is usually of much smaller mass than B, it will usually take up a large fraction of the kinetic energy. Having thus measured Q_o and Q_1, the energy of the excited state B_1 is known to be equal to $Q_o - Q_1$, with respect to the ground state B_o. The value of Q_o may also

be calculated if the mass values of A, B, P and R are known with sufficient accuracy. Thus if ΔM is the mass difference between A + P and B + R, then the theory of relativity predicts that $Q_o = \Delta M\ C^2$ where C is the velocity of light. Much of the early work on nuclear reactions was devoted to verifying this relation between mass and energy, but is now assumed to be correct and the ground state Q-values of nuclear reactions are used to supplement mass spectroscopic data on the exact mass values of stable isotopes and to provide information on the mass values of radio-active isotopes, which are not usually available in sufficient quantities for mass spectroscopic analysis. To return to the measurement of energy levels, we see that by measurement of the energy of particle groups from nuclear reactions we are able to calculate the energy levels of the residual nucleus. This information may be confirmed and supplemented by measurement of the gamma radiation from the residual nucleus. For example, in the case considered above, we should expect to observe gamma rays of energy $Q_o - Q_1$ emitted in transitions from the excited state B_1 to the ground state B_o.

In the case of 'radiative capture', where the nucleus C de-excites by emitting gamma-rays, we can only make measurements on these gamma-rays. Such a process is normally denoted by $A(P,\gamma)C$. If only one gamma quantum is emitted direct to the ground state of the nucleus C, then a

measurement of its energy only serves to measure the ground state Q value for the reaction. However, if more than one gamma quantum is emitted, then we shall obtain information about the energy levels of C through which the transitions take place.

In either of the two general types of reaction discussed above it may be possible to obtain information on the more highly excited energy levels of the compound nucleus C by a study of the 'excitation function' of the nuclear reaction. If the region of excitation energy in which the compound nucleus C is formed by absorption of the particle P is not too high, then there may exist discrete energy levels. If this is the case, then there will only be discrete energies of the incident particle P which can result in the formation of the compound nucleus C in one of its energy levels. Thus the yield, or cross-section, of the reaction will exhibit sharp maxima or 'resonances' at these energies, and a measurement of their energy values, absolute yields, and widths will give corresponding information about the energy levels of the compound nucleus C. It is usual to define the total width of such a level by Γ and to define the 'partial widths' for the emission of a proton, alpha-particle, or gamma-ray by Γ_p, Γ_α, Γ_γ, where:

$$\Gamma = \Gamma_p + \Gamma_\alpha + \Gamma_\gamma + \cdots$$

The partial widths are proportional to the relative probabilities for the decay of the level by the appropriate

processes. It can be shown that the cross-section σ for a reaction of the type A(P, R)B is given by the Breit-Wigner dispersion formula:

$$\sigma = \frac{\lambda^2}{2\pi} \omega \frac{\Gamma_P \Gamma_R}{(E-E_r)^2 + \frac{1}{4}\Gamma^2} \qquad (1)$$

where λ is the de Broglie wave-length of the bombarding particle P , Γ_P and Γ_R are the partial widths for emission of the particles P and R respectively, E is the kinetic energy of P, E_r is the resonance energy and ω is a factor which depends upon the angular momentum changes involved in the transition and which is of the order of unity for small changes of angular momentum. If we integrate equation (1) over all values of E close to E_r for which σ is appreciably different from zero we obtain the following expression for Y , the thick target yield in disintegrations per incident particle.

$$Y = \frac{\hbar^2 \omega}{4ME_r\epsilon} \frac{\Gamma_P \Gamma_R}{\Gamma} \qquad (2)$$

Here ϵ is the rate of loss of energy of the incident particle in the target material per disintegrable nucleus per c.c. and λ^2 has been replaced by $\hbar^2/2ME_r$ where M is the mass of the incident particle and h is Planck's constant. We note that if $\Gamma_P \gg \Gamma_R$, so that $\Gamma = \Gamma_P$, then equation (2) reduces to:

$$Y = \frac{\hbar^2 \omega}{4ME_R\epsilon} \Gamma_R \qquad (3)$$

Similarly, if $\Gamma_R \gg \Gamma_P$ we have:

$$Y = \frac{\lambda^2 \omega}{4\pi E_R \epsilon} \Gamma_P \qquad (4)$$

Thus we see that a measurement of the thick target yield provides a method of measuring the smaller of the two quantities Γ_P and Γ_R. The total width Γ can be measured directly from the width of the thin target excitation curve, provided that it is greater than the experimental resolution.

We see that measurements of the type described above enable us to measure the energy value and the energy width of a nuclear level. Two further parameters are normally introduced to describe the observed characteristics of nuclear energy levels. These are the angular momentum and the parity. According to the principles of quantum mechanics the orbital angular momentum j of an assembly of particles can only assume integral values in units of $\lambda/2\pi$. However, the individual nucleons which constitute an atomic nucleus are known to have an intrinsic spin of $\frac{1}{2}$. The total angular momentum J, of a nucleus in a given state, will be the vector sum of the orbital angular momentum and the spins of the individual particles and can therefore assume integral or half-integral values, depending on whether the number of nucleons in the nucleus is even or odd. The parity of a state is introduced in a wave mechanical description of the state to define its symmetry properties.

The parity is defined as being odd (-) or even (+) according to whether the wave function describing the state does or does not change sign when the co-ordinates of the particles are ~~inter~~changed. in sign.

The angular momentum and parity are important in determining the type of transitions which can take place between different energy levels. In the case of gamma-ray transitions the changes in the value of the angular momentum and of the parity determine the multipole order of the transition (electric dipole, magnetic dipole, electric quadrupole etc.). In the case of particle emission the angular momentum and parity changes determine the probability of the process. The emission of a particle such as a proton, alpha-particle or neutron with an even number of units of angular momentum is only possible if the parity of the initial and final states is the same. Similarly the emission of a particle with odd angular momentum is only possible if the parities are different. In addition to these selection rules, the emission and absorption of charged particles with high angular momentum will be less probable than the emission of particles of low angular momentum because of the increased effective height of the potential barrier for particles of high angular momentum.

* * * * * *

I.4. Consideration of the Requirements for the Beam of Incident Particles.

In the previous discussion we have outlined briefly the type of information which can be obtained from nuclear reactions. We can now consider the general properties which the beam of bombarding particles should have in order that it should be capable of being used for as wide a field of nuclear research as possible.

First, let us consider the energy of the bombarding particles. It is clear that the range of excitation energies of the compound nucleus C which can be investigated by measurement of the excitation function, will extend from the energy Q_o' corresponding to the mass difference between A + P and C, and the energy $Q_o' + E_P$, where E_P is the kinetic energy of the particle P. Thus it would seem desirable to be able to vary E_P from zero to as high a value as possible to cover the widest possible field. However, the spacing between energy levels in a given nucleus tends to decrease as the excitation energy increases until finally they overlap and form a continuum in which it is no longer possible to discern discrete level structure. In general, the most interesting field of investigation of the energy levels of the compound nucleus is covered by the range of E_P from 0 to 3 or 4 Mev. and much useful work can be done in the range from 0 to 1 Mev.

In addition to the measurement of the position of energy levels it is of interest to measure the energy width of these levels. The degree of resolution which can be obtained in such measurements will depend upon the energy homogeneity of the bombarding particles when they collide with the target nuclei. This, in turn, will depend upon (a) the homogeneity of the particles in the beam and (b) the thickness of the target. The latter effect is due to the fact that the particles will lose energy in traversing the target and hence will have a lower energy if they make nuclear reactions at the back of the target. However, the ultimate resolution attainable with a very thin target will depend upon the homogeneity of the beam. The level widths which are concerned in, for example, proton induced reactions range from about 1000 volts up to 100 kilovolts or more. Thus an energy homogeneity of better than 1000 volts is desirable. In practice this degree of homogeneity is most readily attained with a direct type of accelerator such as a cascade generator or Van der Graaf machine and can only be obtained with a multiple accelerator, such as a cyclotron, by the use of energy analysers which reduce the beam intensity by a large factor.

In the case of experiments designed to measure the energy levels of the residual nucleus by measurements of the energy of the reaction products, the homogeneity

requirements of the incident beam are not usually as stringent as in the case of excitation function measurements. There are two main reasons for this, firstly, if the reaction proceeds via a sharply defined energy level in the compound nucleus the energy homogeneity of the incident beam will not affect the energy of the out-going particle, provided that it is sufficiently small to excite only one energy level in the compound nucleus. Secondly, even if a broad state or continuum in the compound nucleus is involved, the techniques for measurement of the energy of the out-going particle do not normally have a sufficiently high resolution to justify a high degree of homogeneity in the energy of the incident particles. However, it must be mentioned that recent developments in the technique of high resolution magnetic spectrometers for heavy particles make an exception to the above statement. If measurements on the energy levels of the residual nucleus are made by observing the gamma-radiation from these levels, then the homogeneity of the incident beam is quite unimportant.

The intensity of the beam of particles is also of great importance in nuclear disintegration experiments, particularly at low bombarding energies, because of the small yield of disintegrations per incident particle. For

example, let us consider the reaction $Li^7(p,\gamma)Be^8$, which is one of the highest yield proton capture reactions in the energy range below 1 Mev. The thick target yield of the 440 kev resonance of this reaction is of the order of magnitude of one disintegration per 10^8 incident protons. To make a precision measurement of the energy of the emitted gamma-rays it may be necessary to use a spectrometer with an efficiency of one count per 10^7 gamma-rays from the source, thus giving an overall counting rate of one count per 10^{15} incident protons. A current of 1 μa. corresponds to a flux of 6×10^{12} protons per second and this current would therefore give a counting rate of about 0.3 counts per minute in the experiment considered above. It would therefore be necessary to count for several hours to obtain reasonable statistical accuracy on a single point. However, a current of 100 μa. would reduce the necessary duration of each measurement to a few minutes. Since many interesting reactions have yields considerably smaller than the one considered above we see that it is desirable that the beam of incident particles should have the highest possible intensity.

* * * * * * *

I.5. The Detection and Measurement of the Reaction Products.

The range of techniques which has been developed for the detection and measurement of the products of nuclear reactions cover such a wide field that we shall make no attempt to discuss them all in this thesis. The discussion will therefore be limited to the techniques relevant to the experimental work to be described later.

5 (a) Charged Particles.

Let us first consider the case of a nuclear reaction in which a charged particle is emitted. The particles which are most frequently involved are the proton (H^1) and the α-particle (He^4), but H^2, H^3 and He^3 are also sometimes observed. The dynamics of such a reaction are illustrated in Fig.I (ii). A bombarding particle P of mass M_1 and energy E_1 collides with a nucleus A which is initially at rest. A nuclear reaction occurs and a particle R of mass M_2 is emitted with energy E_2 in a direction which makes an angle θ with the initial direction of P. The residual nucleus B of mass M_3 recoils with energy E_3 in a direction making an angle ϕ with the initial direction of P. From the principles of the conservation of energy and momentum we can now calculate E_2 as a function of Q, E_1 and θ, where Q is the energy release as defined in section I.3. In the special case where $\theta = 90^\circ$ the relation is easily shown to be:

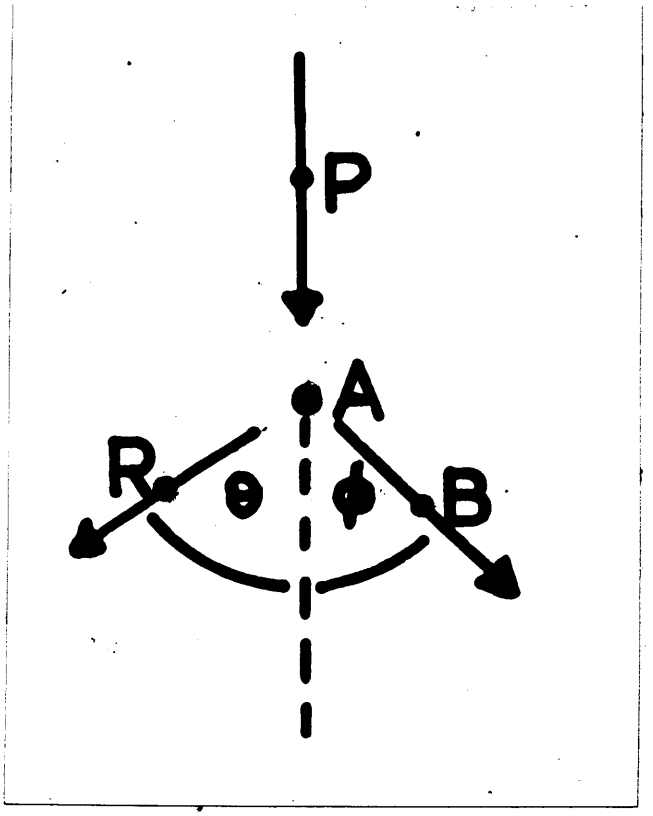

Fig.I(ii). Dynamics of Nuclear Disintegration.

$$(E_2)_{90^\circ} = \frac{M_3}{M_2 + M_3} Q + \frac{M_3 - M_1}{M_2 + M_3} E_1 \qquad (i)$$

Thus we see that we can calculate the energy release Q by measuring E_2.

The most widely used method of measuring the energy E_2 of charged particles has been to measure the 'range' of the particles. In traversing matter, a high energy charged particle loses energy by making ionising collisions with the atoms in its path until finally all its energy has been dissipated and it comes to rest. The distance which the particle travels before coming to rest is termed its 'range'. Because of the statistical nature of the ionisation process there is a small spread on the range of a beam of particles which are initially homogeneous in energy. However, this spread or 'straggling' in range only amounts to a few per cent and hence a measurement of the mean range of a homogeneous group of particles serves to measure the energy of the particles with an accuracy of the order of 1%. It is, of course, necessary to know the relation between range and energy in the material used to slow down the particles. One of the earliest and most direct methods of measuring the range of charged particles was to photograph their tracks in an expansion chamber and thus obtain a direct measurement of the range in the gas in the chamber. This method was not very satisfactory in the case of nuclear disintegration experiments because

of the various technical difficulties involved. More recently, photographic plates with specially prepared thick emulsions have been used to measure the range of particles directly in the emulsion of the plate. Ionisation chambers and proportional counters have also been widely used to measure the range of particles by interposing absorbing material between the source of particles and the counter. The first quantitative measurements on artificial disintegrations were made by Cockroft and Walton by this method and the technique was developed to a higher degree of precision by Lewis, Wynn Williams and many other workers, both in the field of artificial disintegrations and in the study of radio-active decay. A detailed discussion of these techniques is outside the range of this thesis but we must note two fundamental limitations of the range method of energy measurement. First, its resolution even with the best technique is limited by the effect of straggling. This means that it is not possible to resolve particle groups whose energy differs by less than a few percent and this may cause difficulty if a nucleus with closely spaced energy levels is being investigated. Second, and more important, is that it is not possible to observe particles which have a range comparable with that of the incident particles which have been scattered from the target material and its backing material. The energy of these

scattered particles will depend upon the mass of the target nuclei and upon the angle of observation relative to the direction of the incident beam, but, since the target nuclei will generally be of considerably greater mass than the incident particles, the energy of the elastically scattered particles will usually be only slightly smaller than that of the incident particles. The cross-section for elastic scattering is several orders of magnitude larger than the disintegration cross-section for nuclear reactions in the energy range we are considering and hence it is quite impossible to observe the disintegration particles if their range is less than that of the incident particles. The effect of this limitation is particularly serious in the case of (p,α) reactions because of the smaller range of alpha-particles compared to that of protons of the same energy. The range-energy curves for alpha-particles and protons are shown in Fig.I (iii). It will be seen, for example, that a 500 KeV proton has the same range as a 1.7 MeV alpha-particle and hence it would not be possible to observe by the range method alpha-particles of energy less than 1.7 MeV from a nuclear reaction induced by 500 KeV protons. In practice the limit would probably be somewhat higher on account of the effects of straggling.

A second method of measuring the energy of charged particles is to measure their radius of curvature in a magnetic field. This method has also been used for a

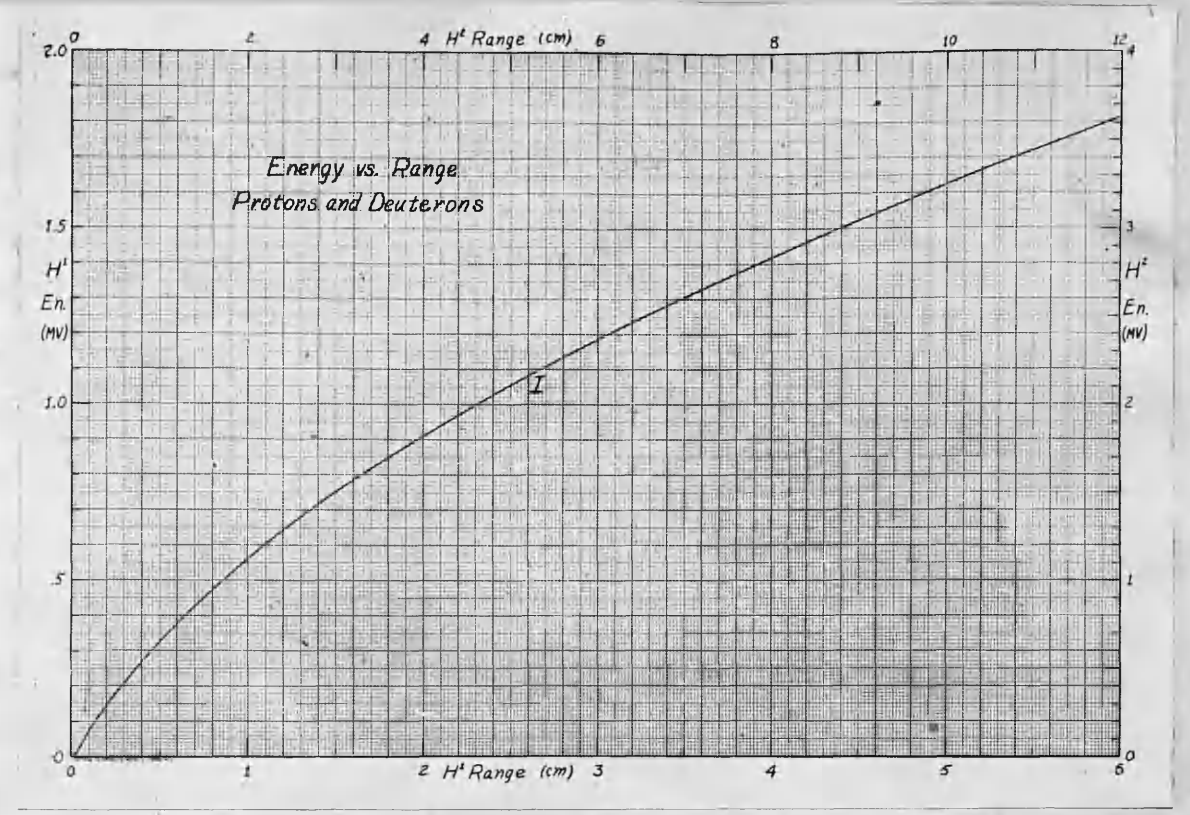
Energy vs. Range
Protons and Deuterons
H¹ Range (cm)
H² Range (cm)
H¹ En. (MV)
H² En. (MV)
I

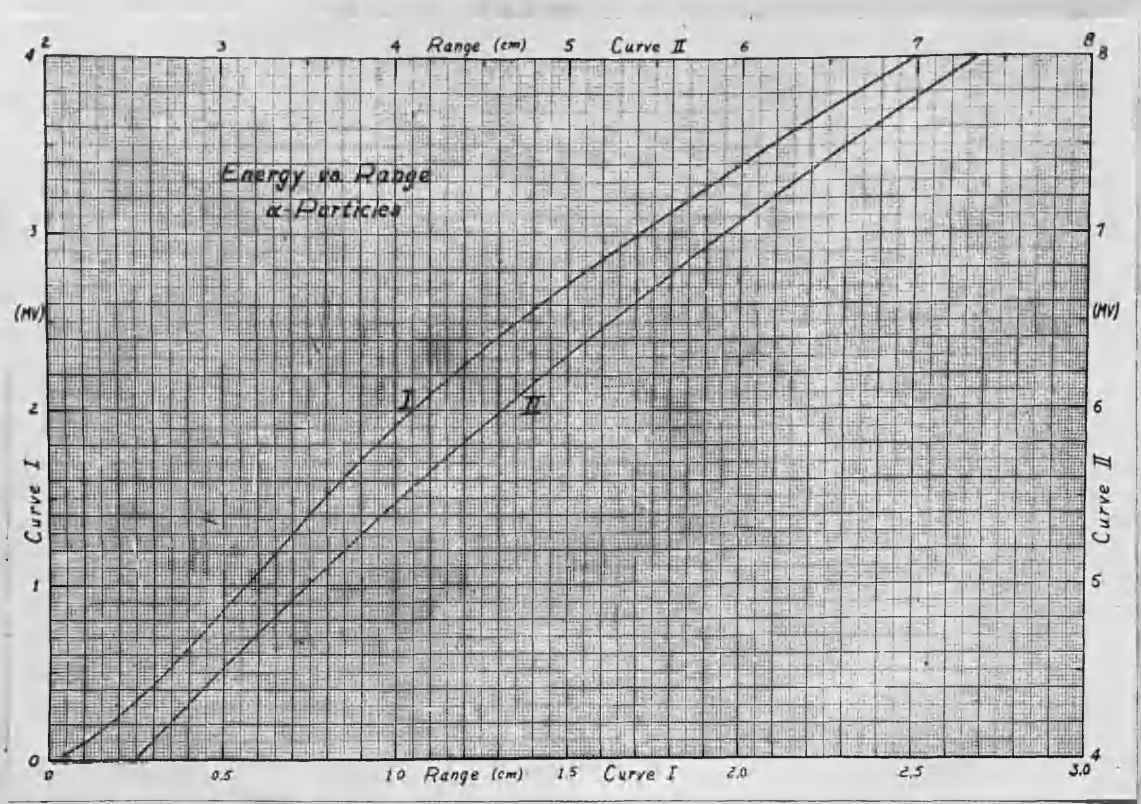
Energy vs. Range
α-Particles
Range (cm)
Curve I
Curve II
(MV)
I
II

Fig. I (iii).

considerable time in measurements on the particles from radioactive disintegrations but it is only comparitively recently that magnetic spectrometers suitable for making measurements on particles from nuclear reactions have been developed. The particular problems involved in the design of such spectrometers will be discussed in section III.1. and we shall only discuss the basic properties of the method. It can easily be shown that the radius of curvature ρ of a charged particle of mass M, charge Ze, and energy E electron volts in a uniform magnetic field H is given by the relation:

$$H\rho = \sqrt{\frac{2EM}{Z^2e}}$$

We note that the quantity M/Z^2 is the same for both a proton and an alpha-particle and that consequently they will have the same $H\rho$ value if their energies are the same. Thus in the case of a (p, α) reaction it will be possible to resolve alpha particle groups from the elastically scattered protons if their energy is greater than that of the protons. This represents a considerable improvement on the lower limit imposed by the range method. The case of (d, p) and (d, α) reactions is not so favourable because the quantity M/Z^2 is twice as large for deuterons and hence it will only be possible to resolve protons or alpha-particles from the scattered deuterons by magnetic analysis alone if their energy is more than twice

that of the deuterons. However, in the case of (d,p) reactions it is always possible to prevent the scattered deuterons from reaching the detector of the spectrometer by placing an absorber of suitable thickness in front of the detector, because the range of the protons arriving at the detector will always be greater than that of the deuterons at a given value of the magnetic field, since the deuterons will have only half the energy of the protons. It will, of course, be necessary to change the thickness of the absorber to cover a large range of energies. This technique is not suitable for (d,α) reactions because of the smaller range of alpha particles. The method of magnetic analysis for the energy measurement of charged particles is also capable of much greater precision and resolution than is possible with the range method.

5 (b) Gamma-Rays.

We shall now consider the detection and measurement of the gamma-radiation emitted in nuclear reactions. The interaction of gamma-radiation with matter produces high energy electrons by three separate processes and it is by means of these electrons that we are able to detect the presence and measure the energy of the radiation. The three processes involved are (a) the Compton effect, (b) the photo-electric effect and (c) the pair production process. The Compton effect results in the production of electrons of

all energies from zero up to an energy slightly less than that of the original gamma-rays. The photo-electric effect produces homogeneous groups of electrons of energy equal to that of the original gamma-rays minus the binding energy of the atomic electron shell from which the electron has been ejected. The pair production process gives rise to electron-position pairs whose total energy is equal to the original gamma-ray energy minus the rest energy, $2mc^2$, of the electron-position pair, but the energy is not necessarily divided equally between the electron and positron, so that the spectrum of either is a continuous function of energy. The cross-sections for these three processes are all functions of the energy k of the gamma-rays and of the atomic number Z of the nuclei with which the gamma-rays interact. These cross-sections are shown as a function of energy for lead in Fig.I (iv), which is taken from Heitler's "Quantum Theory of Radiation". It will be seen that the cross-sections for the Compton and photo-electric effects decrease with increasing energy, whilst the cross-section for pair production increases continuously with energy from the threshold at $k = 2mc^2$.

We can now consider the basic methods of gamma-ray energy measurement based on these three processes.

The only precise methods are those in which a magnetic spectrometer is used to measure the energy of the electrons or positions produced by one or other of the above processes.

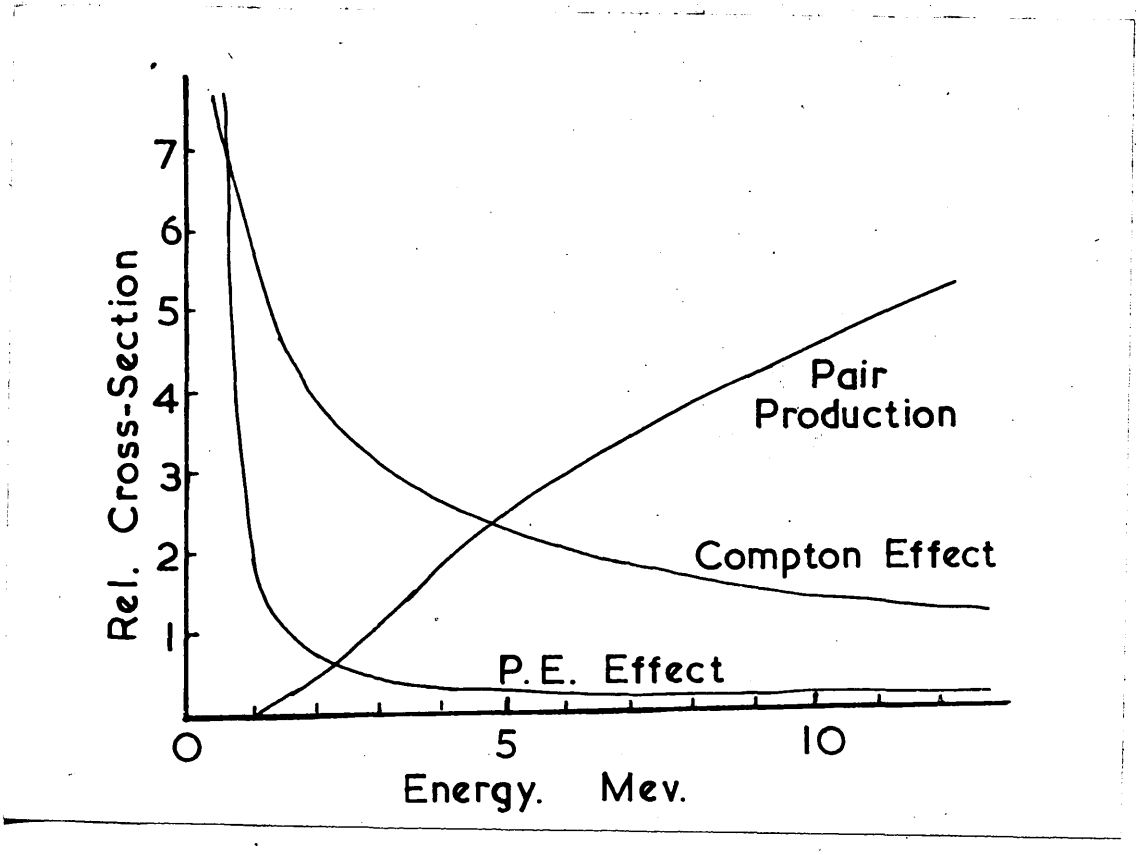

Fig.I(iv) . Cross-Sections for Radiation Processes.

Methods involving the measurement of the total absorption coefficient of the gamma radiation or the absorption coefficient of the secondary electrons are not capable of high accuracy and are particularly unsatisfactory if the spectrum of the gamma radiation is complex. In the energy range below about 3 Mev it is possible to measure the energy of the photo-electrons ejected from a thin foil with a magnetic spectrometer and hence to calculate the gamma-ray energy with high precision. A measurement of the end-point of the Compton electron distribution can also be made to yield an accurate value for the gamma-ray energy, but because of the continuous distribution this method is subject to difficulty in the case of a complex gamma-ray spectrum. These methods have had very wide application in the measurement of the gamma-rays emitted in radio-active decay processes, where the gamma-ray energy is seldom greater than 2·5 Mev. However, in the case of nuclear reactions, gamma-ray energies of up to 18 Mev are observed and energies in the region of 10 Mev are quite common. We see from Fig.I (iv) that the cross-section for the photo-electric effect is very small in this region and hence it is not practical to make use of the effect to measure gamma-ray energies. The Compton cross-section is also much reduced, but it still provides a possible method of measurement if the spectrum is fairly simple. The most satisfactory measurements in this high

energy region, however, have been those based on the pair production process. The first application of this process to the measurement of gamma ray energies was made in conjunction with an expansion chamber placed in a uniform magnetic field. The gamma rays were allowed to fall on a thin lead foil placed in the expansion chamber and the energies of the electron-positron pairs were calculated from a measurement of their radii of curvature in the magnetic field. This technique was applied to the measurement of gamma-rays from nuclear reactions in light elements by Fowler et al (1939) and Halpern and Crane (1939). Although this method was much superior to any other available at the time it has certain disadvantages. The principal disadvantage is the time involved in taking the large number of expansion chamber photographs which are necessary to obtain reasonable statistical accuracy. The accuracy of the method is also limited by the effect of multiple scattering of the electron and positron tracks in the gas of the cloud chamber. However, in 1948 Walker and McDaniel developed a coincidence magnetic spectrometer, based on the pair production process, which overcame the difficulties inherent in the expansion chamber technique. The development of this spectrometer made it possible to make precision measurements of the energy and intensity of high energy nuclear gamma-rays in a reasonable time with the source strengths available from nuclear reactions. A

spectrometer of this type has been developed in this laboratory and a more detailed description of its construction and operation will be given later in this thesis, together with the experimental measurements made with it.

* * * * * * *

Part II. The Acceleration of Charged Particles.

II.1. Summary of General Methods.

We may divide the methods used for the acceleration of charged particles to high energies into two basic categories: (a) the 'direct' method and (b) the multiple acceleration method.

The first method uses a high tension D.C. generator to accelerate the charged particles down an evacuated tube and is only capable of accelerating the particles up to the maximum voltage provided by the generator. This was the method used by Cockroft and Walton (1932) in their pioneer experiments on the artificial disintegration of nuclei. Their high tension generator consisted of a cascade rectifier circuit of the type which will be described later in this thesis. Electrostatic generators of the type developed by Van der Graaff (1931) have also been widely used to accelerate particles by the direct method. The maximum particle energy which can be obtained by this method is limited by corona and spark discharge from the high voltage terminal of the generator to ground. In practise this limits the voltage to about 2×10^6 volts in air at atmospheric pressure, even in very large enclosures. Some improvement can be obtained by placing the generator and accelerator tube in a chamber containing gas at high

pressure, but the mechanical difficulties involved are very considerable. So far, this technique has only been applied to electrostatic generators and the maximum voltage which has been attained is of the order of 4 Mv.

The multiple acceleration method uses a comparatively low alternating voltage to accelerate the particles many times until they attain a high energy. The first successful accelerator of this type was the cyclotron developed by Lawrence et al (1932). This type of machine has been developed to give particle energies as high as 400 Mev and machines to give energies in excess of 1000 Mev are under construction.

However in the energy range up to a few Mev, the direct method has many advantages over the multiple acceleration method. In particular it gives a beam of particles with a much greater degree of homogeneity in energy than is possible with multiple accelerators. It also gives a much larger beam current, which is an important factor at low energies because of the comparatively small yield of nuclear reactions at these energies. It is also very much more simple to construct and operate.

The high tension set which has been constructed and used to perform the nuclear physics experiments described in this thesis is of the direct type. The details of the construction and operation of this set will be described

in the following parts of this section. The research work which was performed in the design of this equipment will also be described in detail, where the work involved is new and was performed by the author. This work is mainly concerned with the development of a new type of ion source.

A general view of the high tension equipment, which is housed in a large laboratory on the first floor of the building, is shown in the photograph of Fig.II (1). It consists of three principal pieces of equipment, the 800 kv D.C. generator, the accelerator tube and the power column. The accelerated beam of particles passes through a tube through the floor of this room into the 'beam room' on the ground floor, where it is used for disintegration experiments. The control equipment for the H.T. set and a large part of the electronic equipment necessary for the experimental work is situated in a small room adjacent to the beam room.

We shall now describe the design and development of the various parts of this equipment in detail.

* * * * * * *

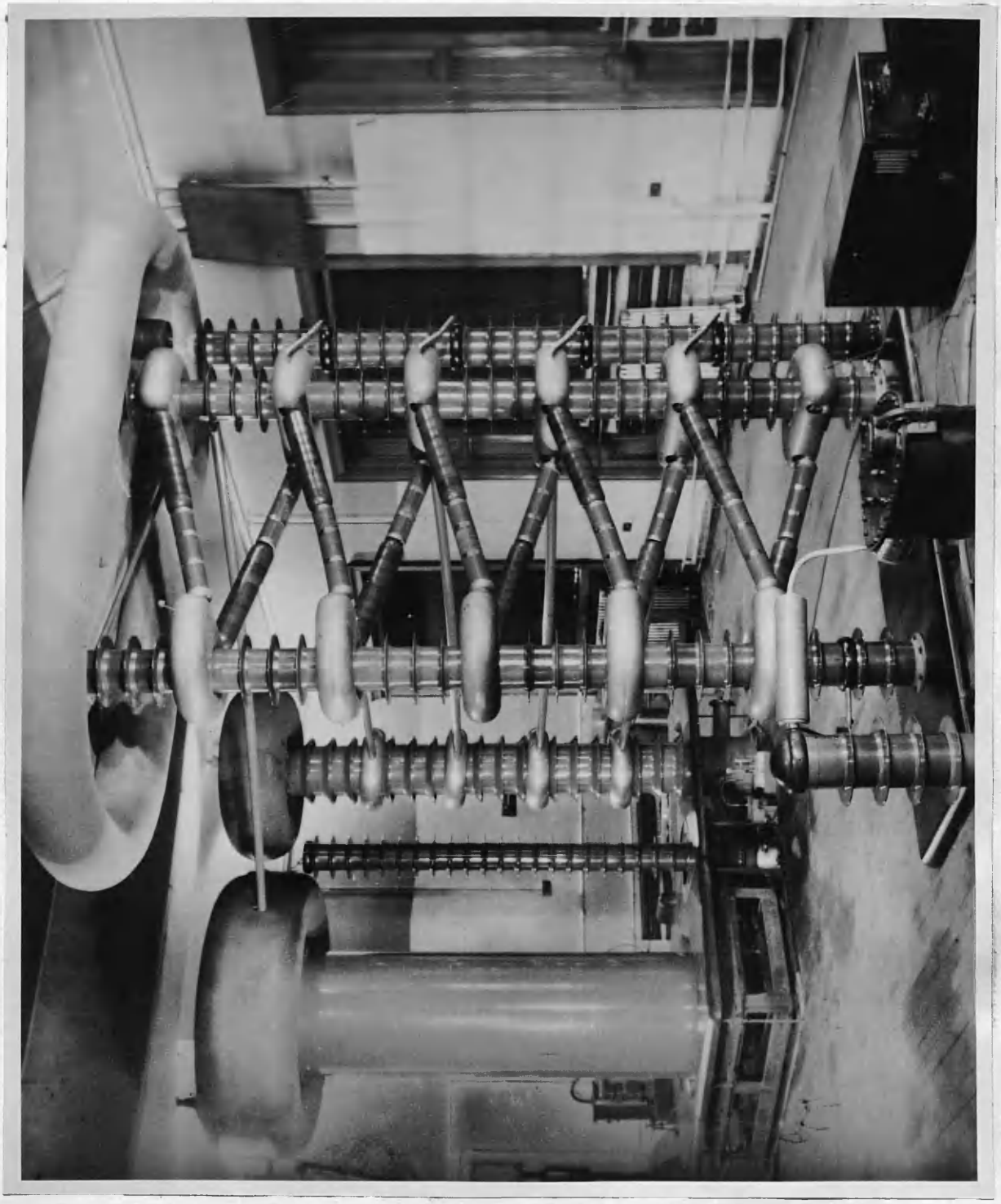

Fig. II (i). The Glasgow H.T. Set.

II.2. The High Tension Generator.

(a) Principle of Operation.

The generator used for supplying the high voltage for the Glasgow accelerator set was constructed by Messrs. Philips of Eindhoven. It consists of a five stage cascade generator, similar in principle to the original design of Cockroft and Walton. The essential details of the operation of the generator may be seen from the schematic circuit diagram of Fig.II (ii)a, and the voltage wave-forms at various points in the circuit which are shown in Fig.II (ii)b. The transformer T_1 is supplied with a controlled variable A.C. voltage with a frequency of 400 cycles per second. This voltage is supplied by a 250 volt generator and can be varied from 0 to 250 volts by means of a variac. The secondary of T_1 develops a voltage with a peak amplitude of up to 80 k V. The condenser C_1 and the mercury vapour rectifying valve V_1 act as a simple half-wave rectifier circuit so that C_1 becomes charged to the peak voltage V_o of the transformer. The condenser C_6 is then charged to the peak voltage $2V_o$ reached by the point B, through the rectifier V_2. By an exactly similar process the condensers C_7, C_8, C_9 and C_{10} also become charged to a voltage of $2V_o$ and since they are all connected in series, the high potential terminal K reaches a voltage of $10V_o$ with respect to ground.

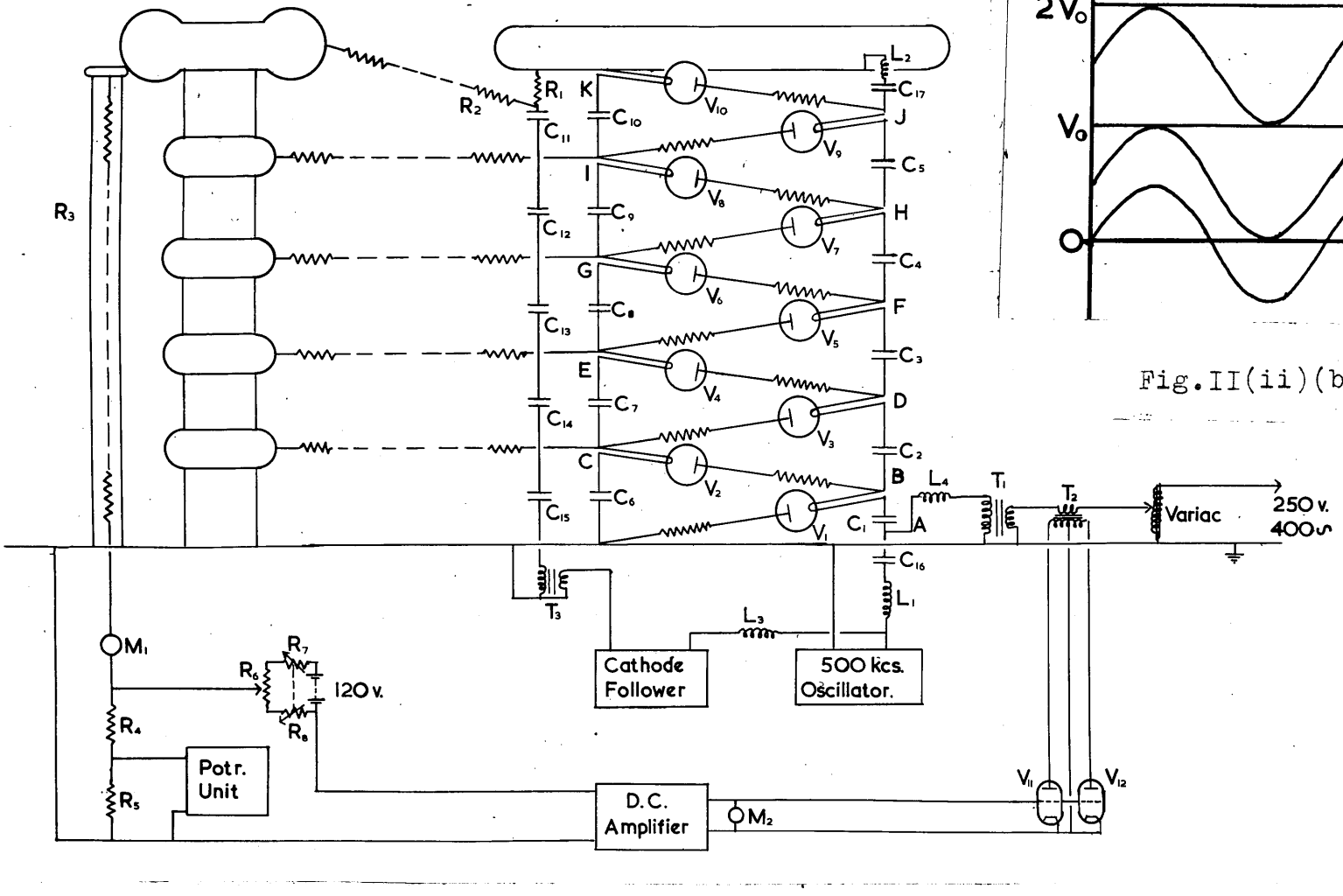

Fig.II(ii)(a). Schematic Diagram of H.T. Generator.

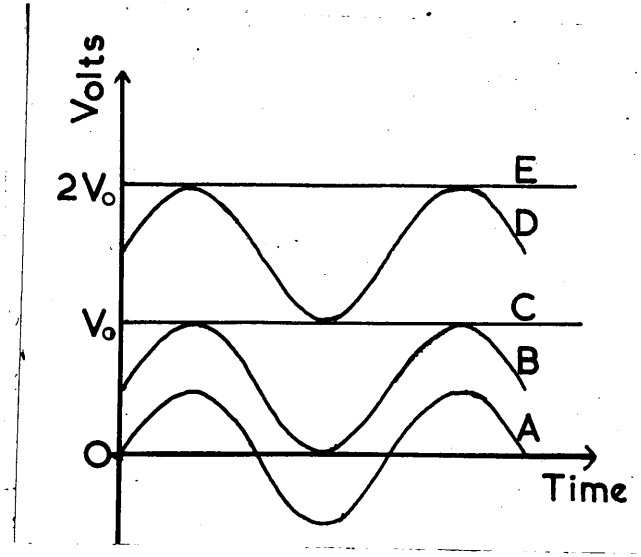

Fig.II(ii)(b).

Thus a voltage of 800 k V is obtained with a peak voltage of 80 k V from the secondary of the transformer T_1 . The filaments of the rectifying valves are heated by means of a radio-frequency current supplied by the 500 kc oscillator. This current is fed to the point A through a series tuned circuit C_{16} , L_1 tuned to 500 kc , the condenser C_{16} serving to insulate the oscillator output from the point A. The current then flows through the condensers C_1 to C_5 through another series tuned circuit C_{17} , L_2 , and finally through the condensers C_{10} to C_6 to ground.. Small dust-core transformers, not shown in Fig.II (ii)a have their primary windings connected between the condensers. The radio-frequency voltages developed across their secondary windings are then used to heat the rectifier filaments.

(b) Ripple Voltage.

The high voltage terminal of the generator is connected to the top terminal of the accelerator column through the 10 MΩ smoothing resistance R_1 and the 1.5 MΩ surge prevention resistance R_2 . The smoothing condensers C_{11} to C_{15} are connected in series between the junction of R_1 and R_2 and ground, via the secondary of a transformer T_3 whose function will be described later. Thus any ripple which is present on the high voltage terminal of the generator is reduced by a factor $k = R_1 C\omega$, where C is the

effective series capacity of the condensers C_1 to C_{15} and $\omega/2\pi$ is the frequency of the ripple voltage. The value of C is .003 μfd and if we assume that the ripple frequency is 400 c.p.s. then k = 75. The maximum ripple voltage on the generator is of the order of 10 kV at 500 kv, and hence the smoothing circuit should reduce this ripple to about 130 volts. It was found, however, that the ripple on the high voltage terminal of the accelerator tube was still of the order of 1500 volts. After some investigation it was found that the majority of this ripple was due to direct capacity pick-up from the A.C. side of the generator to the spinnings on top of the accelerator column and power stack. This component of the ripple was measured directly by switching off the filament heating of the rectifying valves to remove the D.C. voltage and observing the ripple voltag on an oscillograph connected via a cathode follower to the top terminal of the accelerator column. The estimated capacity of 3 $\mu\mu fd$ between the A.C. side of the generator and the spinnings is quite sufficient to account for the observed ripple voltage because of the very high A.C. voltage, of the order of 160 kV peak to peak, on the AC. side of the generator. In order to reduce this capacity pick-up it would be necessary to reduce the capacity itself or to reduce the value of the surge prevention resistance R_2, since the latter is the effective impedance across

which the ripple voltage is developed. There was no practical method of reducing the capacity and it was felt to be undesirable to reduce the value of R_2 because of the possible damage to the accelerator tube electrodes and the generator itself when a discharge takes place in the accelerator tube. The method finally adopted was to 'back-off' the ripple voltage by means of a suitable anti-phase voltage fed through the smoothing condensers from the transformer T_3. For this purpose it is necessary to have a voltage which is proportional to the A.C. voltage on the generator. A convenient source of such a voltage was found to be the output terminal of the radio-frequency oscillator, since it is connected to the high voltage terminal A of the transformer via the .0001 $\mu fd.$ condenser C_{16} and is effectively connected to ground in the oscillator via a .03μfd condenser. Thus a voltage of about 1/300 of the transformer secondary voltage appears at this point. The R.F. choke L_3 is used to remove the 500 kcs/sec R.F. voltage and the remaining 400 c.p.s. voltage is fed to a cathode follower via circuits which control its phase and amplitude. The output of the cathode follower is fed to the transformer T_3, which has a step-up ratio of 10/1. The system was set up by observing the ripple voltage on the top of the accelerator column by the method previously described and adjusting the phase and amplitude controls until the ripple

was reduced to a minimum. It was not possible to reduce the ripple to zero because of the different components of higher harmonics in the two waveforms, but a reduction by a factor of 10/1 was achieved and this was felt to be sufficient in view of other unavoidable sources of voltage fluctuation.

* * * * * * *

(c) Voltage Measurement and Stabilisation.

The voltage on the accelerator tube is measured by means of the oil cooled resistance R_3. This resistance has a value of about 1200 MΩ and consists of 1200 1 MΩ carbon resistances wound in a spiral on a perspex former. The whole assembly is placed in a cylindrical container through which the transformer oil is circulated. The current through this resistance flows to earth through the meter M_1 and the resistances R_4 and R_5. The meter M_1 is used for direct reading of the set voltage, its scale being marked in intervals of 10 kv from 0 to 1000 kv. A pre-set shunt across the meter is provided and was set after measurements had been made on the excitation curve of the well-known 440 KcV resonance in the reaction $Li^7(p,\gamma)Be^8$. For more accurate measurement of the voltage the potential developed across the resistance R_5 is measured by means of a standard potentiometer unit. The resistance R_5 consists of a number of high stability wire wound resistances connected in series, with a total value of about 1200Ω. The potentiometer unit uses a standard cell as a reference voltage. The potential across R_5 can thus be measured to an accuracy of 100 microvolts. The value of R_5 was adjusted by measurements on several accurately known nuclear resonances so that it was almost exactly one millionth of the value of $R_3 + R_4 + R_5$.

The readings of the potentiometer unit in milli-volts therefore give directly the voltage on the set in kilo-volts to a relative accuracy of about 100 volts. The absolute accuracy of this measurement is not better than about 1% at present because of the rather large temperature and voltage coefficients of the main resistance R_3, but it is hoped to improve this in the near future when better quality resistances are provided by Messrs. Philips. However, it is possible to make accurate measurements of the position of unknown resonances by comparison with measurements made immediately before or after on the position of known resonances in the same voltage region. The large number of sharp resonances in the reaction $Al^{27}(p,\gamma)Si^{28}$ which have been accurately measured by Brostrom et al (1948) are particularly useful for such comparisons.

In order to hold the set voltage constant against long period fluctuations due to changes in supply voltage, load current, etc., a stabiliser has been constructed. The resistances R_4 and R_5 are used to develop a voltage of about 10^{-4} of that on the set. This voltage is then backed off by means of a controllable voltage from a 120 volt reference battery. The ganged decade resistances R_7 and R_8 and the potentiometer R_6 serve to control the reference voltage. The difference voltage is then fed to the input of a D.C. amplifier with a voltage gain of

about 1000. The circuit of this amplifier is shown in Fig.II (iii). It will be seen to consist of a conventional type of 'chopper' amplifier and is free from D.C. drifts corresponding to changes in input of voltage of more than 50 micro-volts, which is a considerably higher degree of stability than is necessary in this application. The output of the amplifier is used to control the grid-cathode potential of two large power triodes V_{11} and V_{12}. These valves are connected across the two halves of the split secondary winding of the transformer T_2, whose primary is connected in series with the primary of the main H.T. transformer T_1. The transformer T_2 has a step-up ratio of 240/1. The impedance presented by the primary of T_2 is therefore controlled by the grid-cathode voltage of the control valves V_{11} and V_{12}. The range of control is limited by the maximum allowed power dissipation of the valves V_{11} and V_{12} and this corresponds to a change of about 15% in the voltage on the primary of the main transformer T_1 with the circuit used. It is therefore necessary to adjust the main control variac to approximately the desired voltage before the stabiliser can operate. A voltmeter M_2 is used to monitor the output of the D.C. amplifier and the variac is set so that the system stabilises with this meter approximately in the middle of its range. The performance of this stabiliser has been

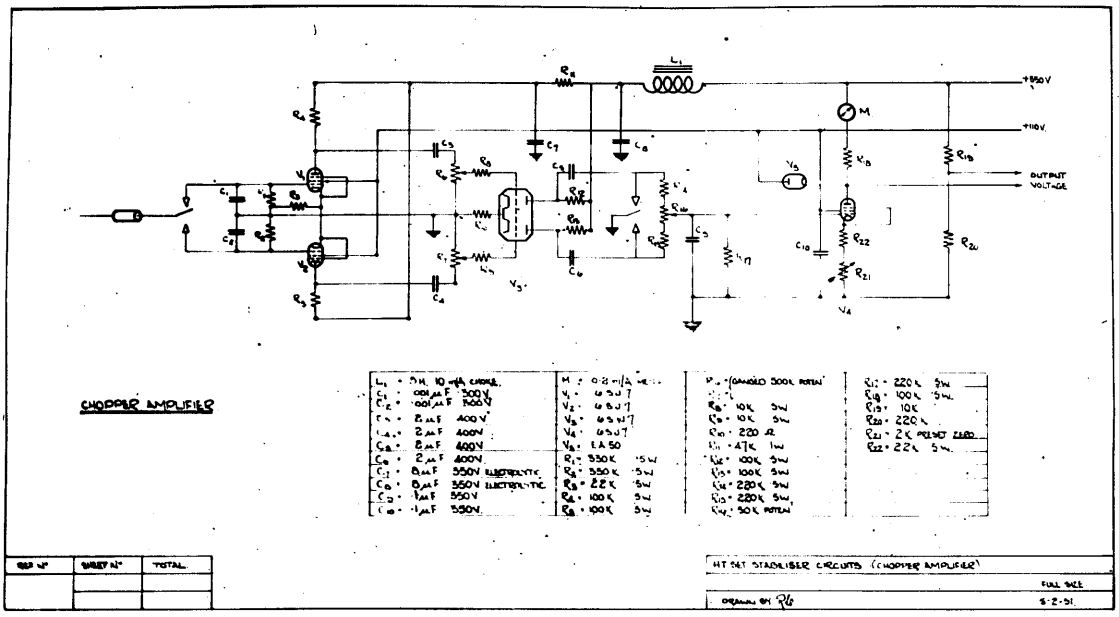

Fig.II(ii)(c). Circuit Diagram of D.C. Amplifier.

very satisfactory. It has a response time of 1/10 sec. and reduces any fluctuations of lower frequency than this by a factor of 100. The principle remaining voltage fluctuations on the set are due to irregular striking of the rectifier valves, which has been a frequent source of trouble. These fluctuations are too fast to be completely removed by the stabiliser and can only be removed by careful selection of the rectifier valves - a process which has not always been possible because of shortage of supply. It may be mentioned that the room temperature must be maintained at at least 22° C. to obtain satisfactory operation of these valves.

* * * * * * *

II.3. The Ion Source and Initial Beam Focussing.

(a) General Requirements.

The particles which are most frequently required for disintegration experiments are the proton and the deutron. These are normally produced in an ion source by running some form of discharge in hydrogen or deuterium. For conciseness we shall discuss the problem in terms of hydrogen, although almost everything that will be said applies equally to deuterium.

We note at this stage that three types of ion will be produced in a discharge in hydrogen, protons (H_1^+), molecular ions (H_2^+) and triatomic ions (H_3^+). The factors affecting their relative abundance will be described later. Now all these ions will be accelerated in the high voltage tube to equal kinetic energies, but the individual protons in the H_2^+ and H_3^+ ions will only have respectively one half and one third of that kinetic energy and are therefore of little use. It is usually desirable to separate the protons from the other ions by magnetic analysis before using them for disintegration experiments.

Thus in order to obtain a large proton beam current we require an ion source which will deliver a large ion current containing a high percentage of protons to the accelerator tube. It is further desirable that the

initial energy inhomogeneity of the ion source beam should be less than the normal variations in voltage on the H.T. set in order that it should not contribute to the final energy spread of the beam at the target.

It is also desirable that the ion source and its associated equipment should be reasonably compact and use as little power as possible, since the whole assembly, including the generator supplying the power, must be contained inside the high voltage terminals of the accelerator column and power stack.

* * * * * * *

(b) Previous Work.

A great deal of work has been done between 1933 and the present day to produce an ion source satisfying all these requirements and it is convenient first to summarise very briefly the work which had been published up to the commencement of the present work in 1946.

The source used by Cockroft and Walton in their early experiments was designed by Oliphant and employed a high voltage (30 kV) cold cathode discharge. Such sources are still used today and have the advantages of simplicity and reasonably good ion current and proton percentage. Unfortunately, they have a large energy spread, of the order of magnitude of the voltage used to maintain the discharge. They also require a rather large power input, of the order of 3 kW.

A second type of source which became very popular, particularly with workers on Van der Graaf generators, was the hot cathode, low voltage arc, type of source developed particularly by Tuve et al. and Lamar et al. This gave a rather smaller output than the Oliphant source, but the energy spread was very small, probably less than 100 volts. The hot filament which was required to maintain the arc was a source of trouble, as it required frequent replacement.

The first suggestion for the use of radio frequency

voltages for maintaining an ion source discharge was made by Getting (1941). During the war great advances were made in radio-frequency technique and it was natural that workers in the field of ion sources should consider the application of these techniques to their particular problems after the war. The first report of work on these lines was published by Thoneman (1946) just prior to the commencement of this work. His apparatus Fig.II (iii) consisted of a 2-litre Pyrex flask containing H_2 at low pressure, in which a discharge was maintained by a 60 mcs/sec R.F. voltage applied between ring electrodes round the bulb. D.C. potentials of up to 20 KV. were applied between a tungsten probe in the top of the bulb and a cylindrical electrode in the neck of the flask, the probe being made positive. Because of the high mobility of the electrons as compared with the positive ions the main plasma of the discharge takes up the same potential as the positive probe and leaves a short 'dark space' above the negative electrode, across which almost all the D.C. potential is developed. It was found that the boundary of this dark space was sharply defined and approximately spherical in shape. Thus positive ions which diffused across it from the main plasma were accelerated by the potential gradient and focused into a narrow beam which passed through the cylinder and was collected by an electrode at the bottom of the neck of

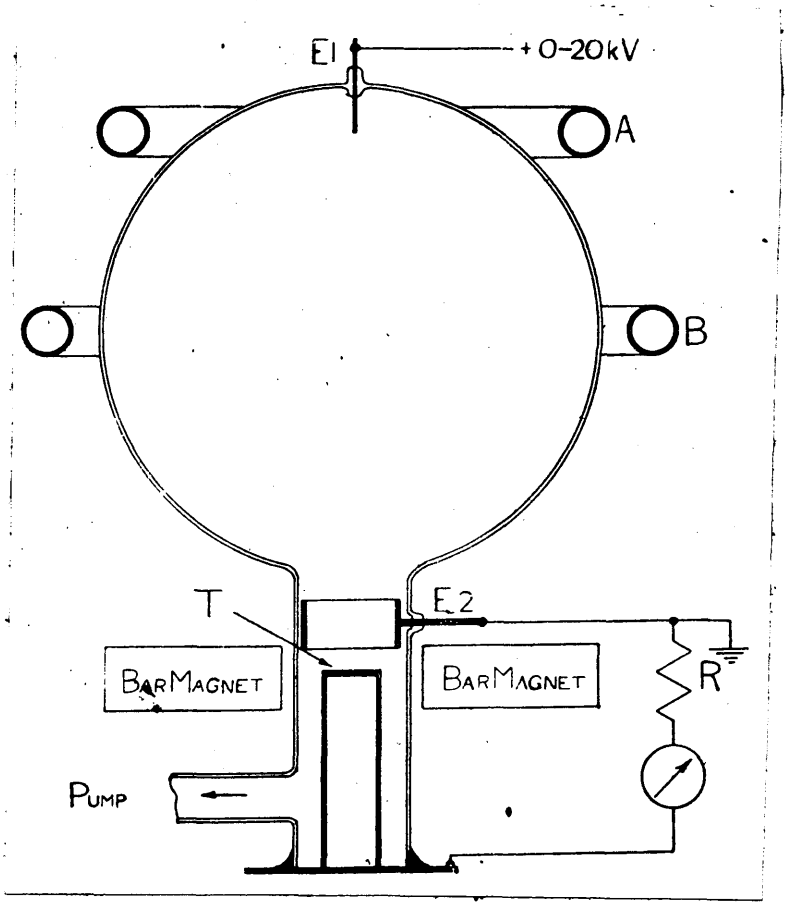

Fig.II(iii). R.F. Source (Thoneman).

the flask. Thoneman was able to obtain currents of up to 10 m.a. to the collector electrode, though it is possible that some of this current was due to secondary electrons leaving the collector. Thoneman did not attempt to take the ion beam through a small aperture or canal, as would be necessary in the case of an ion source supplying a high vacuum accelerator tube, nor did he measure the proportion of protons in the ion beam. However, it was clear that there was a good probability that an ion source of high performance could be designed on these lines.

* * * * * *

(c) Present Work.

It was therefore decided to build an apparatus rather similar to that of Thoneman to obtain some experience of this technique and to proceed from that to a measurement of the proton percentage at an early stage. This apparatus is shown in Fig.II (iv). A 200 mcs/sec. oscillator designed for pulse operation as a radar transmitter was available from Government surplus disposals and was modified to give a continuous output of about 30 watts. This was used to supply ring electrodes S S′ surrounding the bulb of a 1-litre Pyrex flask. A tungsten probe was first used for the positive D.C. electrode, but it was soon found that during operation a fairly well focussed beam of electrons was projected up the centre of the flask and caused intense local heating of the probe and its seal, which frequently cracked the glass. These electrons originated as secondary electrons, produced when the ion beam struck the collector and guard electrodes in the neck of the flask. Consequently this probe was replaced by the air cooled block of aluminium A shown in the diagram. The collector electrode T measured the ion current passing through a $\frac{1}{8}$" diamter hole in the guard plate C. Pumping speed calculations showed than an aperture of this size could well be tolerated between the ion source and the

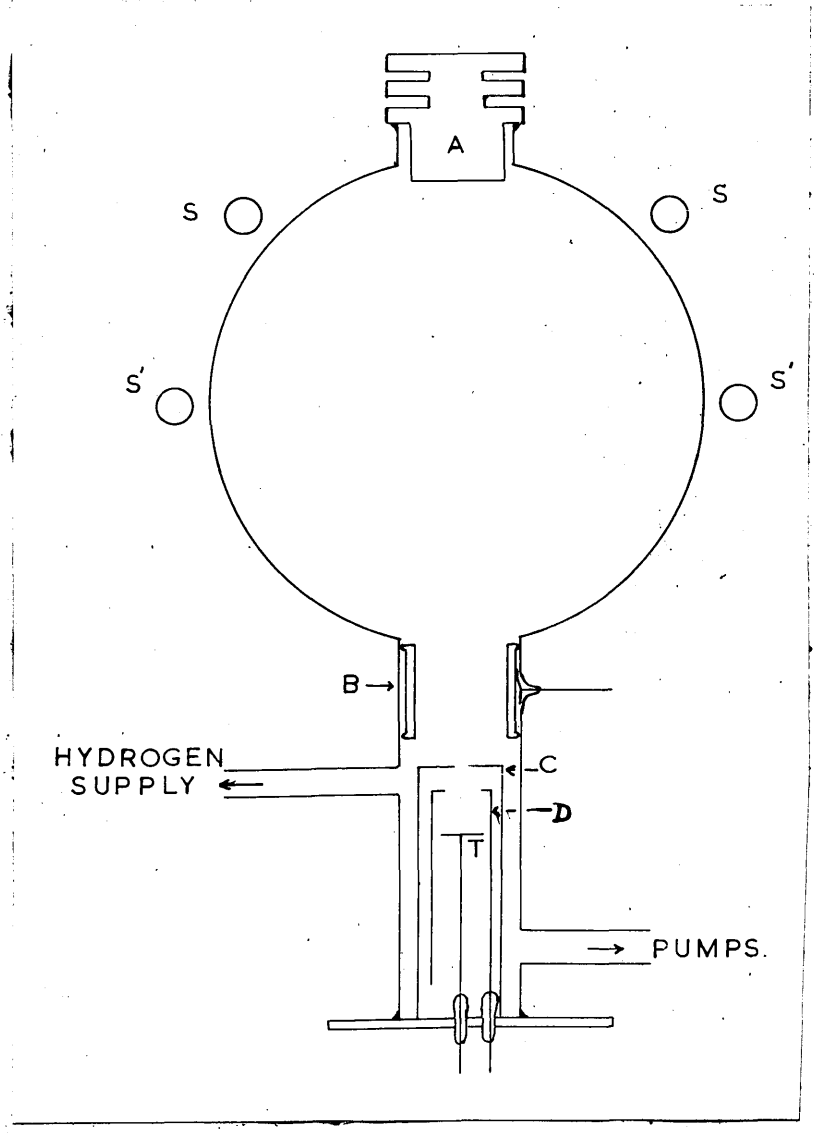

Fig. II(iv). Modified Version of Thoneman Source.

accelerator tube on the H.T. set. Secondary electrons were prevented from leaving the collector by the electrode D which could be made up to 400 volts negative with respect to T and C, but could not itself be bombarded by the beam. A potential of 300 volts was necessary to suppress secondary electrons completely and with no suppression voltage the target current was exaggerated by a factor of five by secondary electrons. The ion current was measured as a function of the extraction voltage and the results are shown in Fig.II (v). It will be seen that an ion current of 700 μa. was obtained at the maximum voltage of 6 Kv produced by the main power pack and that the current appeared to have reached saturation at this voltage.

In view of the promising results obtained in these preliminary experiments it was decided to proceed at once to measure the constitution of the ion beam by magnetic analysis. The apparatus shown in Fig.II (vi) was constructed. The ion beam passed through a $\frac{1}{8}$" diameter hole into a flat 'pill-box' shaped vacuum chamber placed between the 3" diameter poles of an electro-magnet. A collector plate was situated in a side post soldered to the chamber at a point on the circumference 90° from the entrance aperture. A 1/16" slit in the chamber wall in front of the collector allowed particles which had been deflected through 90° by the magnetic field to reach the collector.

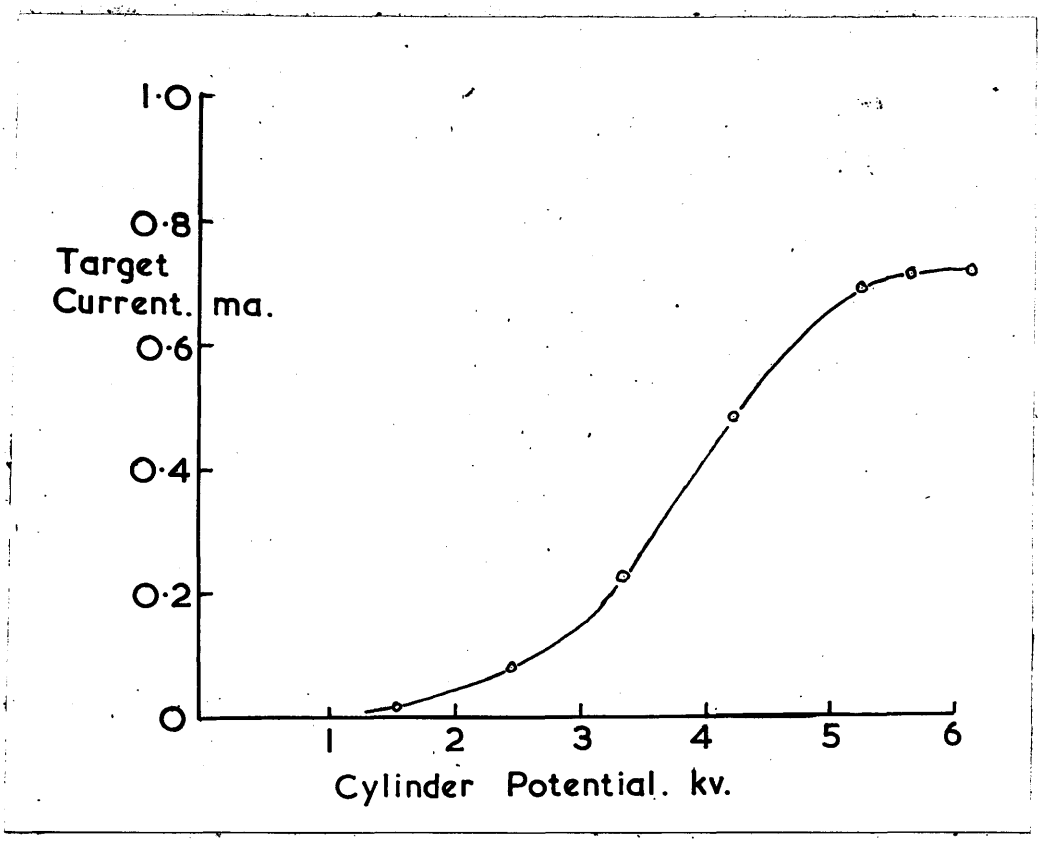

Fig.II(v). Ion Current from R.F. Source.

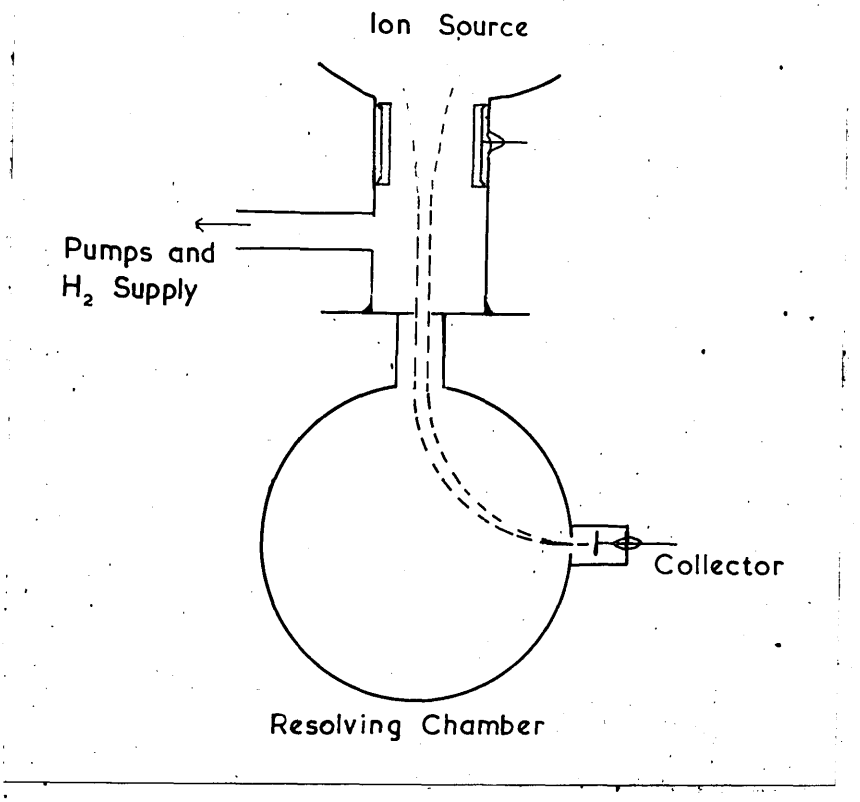

Fig.II(vi). Magnetic Analyser for R.F. Source.

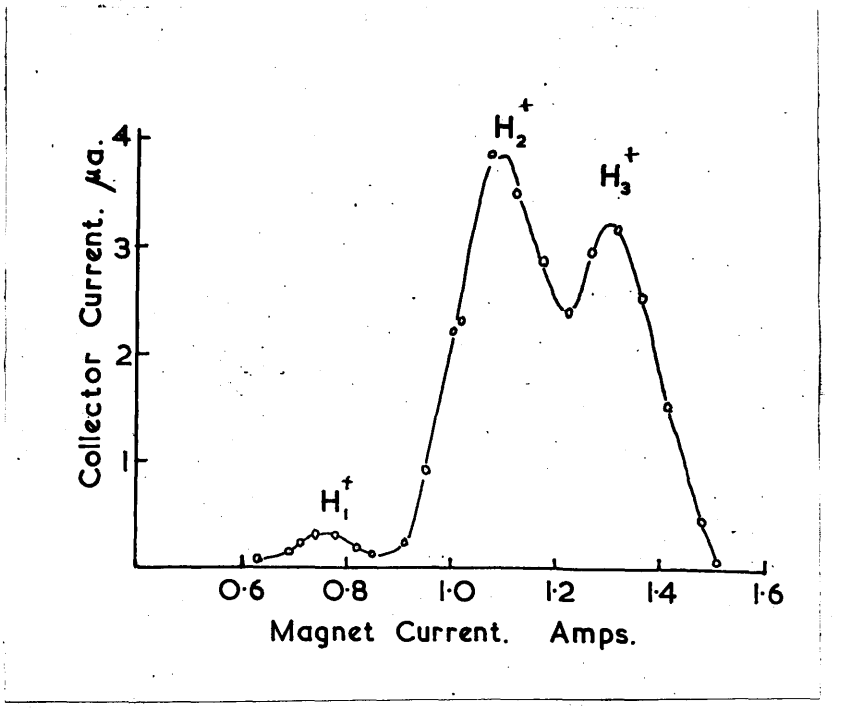

Fig.II(vii). Ion Mass Spectrum of R.F. Source.

Thus, by measuring the collector current as a function of the magnetic field the mass spectrum of the particle could be measured. A typical graph obtained with this apparatus is shown in Fig.II (vii). It will be seen that the beam consists mainly of H_2^+ and H_3^+ ions and only 4% of the ions are protons. No improvement in proton percentage could be obtained by varying the pressure through the range from 2 to 10 microns over which the source would operate satisfactorily. It was clear that an investigation into the reasons for the small proton percentage was required.

Before describing further experimental work it is convenient to discuss the factors influencing the proportions of the various types of ions produced in a discharge of this type. First, it is clear that almost all the ionisation produced will be due to electrons which have gained energy from the R.F. field, since the large mass of the positive ions only allows them to acquire a very small amount of energy. Let us consider a particle of charge e and mass m situated in an electric field E given by:

$$E = E_o \sin \omega t. \qquad (1)$$

Let x be the distance of the particle from a fixed point, measured in the direction of E. Then the equation of motion of the particle will be:

$$m \frac{d^2x}{dt^2} = E e \qquad (2)$$

We shall assume first that the pressure is sufficiently low that the frequency of collisions of the particle with gas molecules is very small compared with the frequency, $\omega/2\pi$, of the electric field. We can then find the steady state solution of equation (2) to determine the energy of the particle. Substituting for (1) in (2) we obtain:

$$\frac{d^2x}{dt^2} = \frac{e}{m} E_o \sin \omega t. \qquad (3)$$

This has the steady state solution:

$$\frac{dx}{dt} = - \frac{e E_o}{m \omega} \cos \omega t. \qquad (4)$$

$$x = - \frac{e E_o}{m \omega^2} \sin \omega t. \qquad (5)$$

Assuming that the particle has no drift velocity ($\frac{dx}{dt} = 0$ at $\omega t = \pi/2$) and that the origin is chosen at the centre of oscillation ($x = o$ at $t = 0$), the kinetic energy T of the particle is then given by:

$$T = \tfrac{1}{2} m \left(\frac{dx}{dt}\right)^2$$

$$T = \tfrac{1}{2} \frac{e^2 E_o^2}{m \omega^2} \cos^2 \omega t. \qquad (6)$$

or, if V is the kinetic energy in electron volts:

$$V = \frac{T}{e} = \tfrac{1}{2} \frac{e}{m} \frac{E_o^2}{\omega^2} \cos^2 \omega t. \qquad (7)$$

The maximum energy V_o at t = 0 is:

$$V = \tfrac{1}{2} \frac{e}{m} \frac{E_o^2}{\omega^2} \qquad (8)$$

Thus we see that the energy acquired by a particle in the field is inversely proportional to its mass and hence a proton will only acquire 1/2000 of the energy of an electron in the same field. If, for example, we take $\omega/2\pi$ = 200 mcs/sec and Eo = 200 volts/cm then $V_o \sim 40$ electron volts for electrons and $V_o \sim .02$ electron volts for protons. It is therefore clear that the electrons will be the primary agents in producing ionisation. It is also satisfactory to observe that the R.F. field will not contribute to any energy inhomogeneity of the proton beam.

Let us now consider the processes which will occur in an R.F. discharge in hydrogen. First we may define the primary processes as those caused by collisions of electrons with H_2 molecules, and the secondary processes as those in which the products of the primary processes are involved. The primary processes are:-

$$H_2 + e^- \rightarrow H_2^+ + 2e^- \qquad (A)$$

$$H_2 + e^- \rightarrow H_1 + H_1^+ + 2e^- \qquad (B)$$

$$H_2 + e^- \rightarrow H_1 + H_1 + e^- \qquad (C)$$

Reaction (A) is the normal ionising process, forming a molecular ion, reaction (B) produces ionisation and dissociation and reaction (C) produces dissociation into neutral atomic hydrogen. It is known from experiments with electron beams passing through H_2 at low pressure

(Smyth 1931) that the cross section for reaction (A) is about 20 times that for reaction (B) for electrons of energies of the order of 100 volts or less. Thus only 5% of the ions produced in these processes will be protons and the remaining 95% will be molecular ions. Now let us consider the secondary processes which will occur. Firstly, those concerning the H_2^+ ions will be:

$$H_2^+ + e_0^- \rightarrow H_2 \qquad (D)$$

$$H_2^+ + H_2 \rightarrow H_3^+ + H_1 \quad (E)$$

$$H_2^+ + e^- \rightarrow H_1 + H_1^+ + e^- \quad (F)$$

Reaction (D) consists of simple recombination with a low energy electron (e_0^-) and is most likely to occur when the H_2^+ ion collides with the walls of the vessel. Reaction (E) can occur when the ion collides with a neutral gas molecule and seems to have a high probability, since it is the only reaction which can explain the high proportion of H_3^+ ions observed under conditions where the proportion of H_1^+ ions (and hence of H atoms) is very small. Reaction (F) consists of dissociation of the H_2^+ ion by a fast electron and will clearly not be a serious competitor to (D) and (E) under any normal conditions of ionisation density. The H_3^+ ions formed by reaction (E) will finally recombine with a free electron and will immediately dissociate, since H_3 is not stable.

$$H_3^+ + e_0^- \rightarrow H_2 + H_1 \qquad (G)$$

Thus we see that the primary process (C) and the secondary processes (E) and (G) result in the formation of atomic hydrogen. Now these atoms of hydrogen will finally recombine with each other to form normal molecular hydrogen. However, it is known that the probability of such recombination taking place in the volume of the gas itself is very small and that almost all the recombination takes place on the walls of the vessel enclosing the gas. It is clear than an equilibrium concentration of atomic hydrogen will be built up, such that the rate of production of atomic hydrogen by the discharge processes is equal to the rate of recombination. If a high concentration of atomic hydrogen is produced, then a high proportion of protons will be produced by direct ionisation.

$$H_1 + e^- \rightarrow H_1^+ + 2e^- \qquad (H)$$

It is clear from these general considerations that the factors which will be important in producing a high concentration of atomic hydrogen will be (i) a high rate of ionisation (ii) a low rate of recombination of atomic hydrogen on the walls of the vessel. The former can be obtained by using as much R.F. power as possible and we shall later see that some improvement can be obtained by the use of a suitable magnetic field. There is very little quantitative information available on the rate of recombination on different materials. However, it is clear from the work of Wood on the spectra emitted from

hydrogen discharge tubes that a clean glass surface gives a much lower recombination rate than any other common material.

With these considerations in mind it was decided to experiment with an 'R.F.capillary' source shown in Fig. II (viii). The discharge was maintained in a Pyrex tube A of 5 mm bore connected between two cylindrical bulbs BB surrounded by the R.F. electrodes CC. The ions were extracted through the canal E by applying a potential between it and the probe F. It was thus hoped to obtain a high ionisation density with only a small surface area of metal exposed to the discharge. At the same time a more convenient form of magnetic analyser was built and this is shown below the source in Fig.II. (viii). The ions emerging from the canal were accelerated and focussed by the electrostatic lens G. The voltage across this gap could be adjusted from 0-15 kv and was normally set so that the beam was focussed onto the slit S placed in front of the Faraday collecting cylinder H. An analyser, consisting of crossed electric and magnetic fields, was placed between the focussing system and the collector. The electric field was provided by the two parallel plates I I. The magnetic field in a plane at 90° to the electric field was provided by a small permanent magnet with 1" diameter poles, which gave a field of about 400 gauss. Now if a particle of charge e, mass M and velocity v passes through the analyser

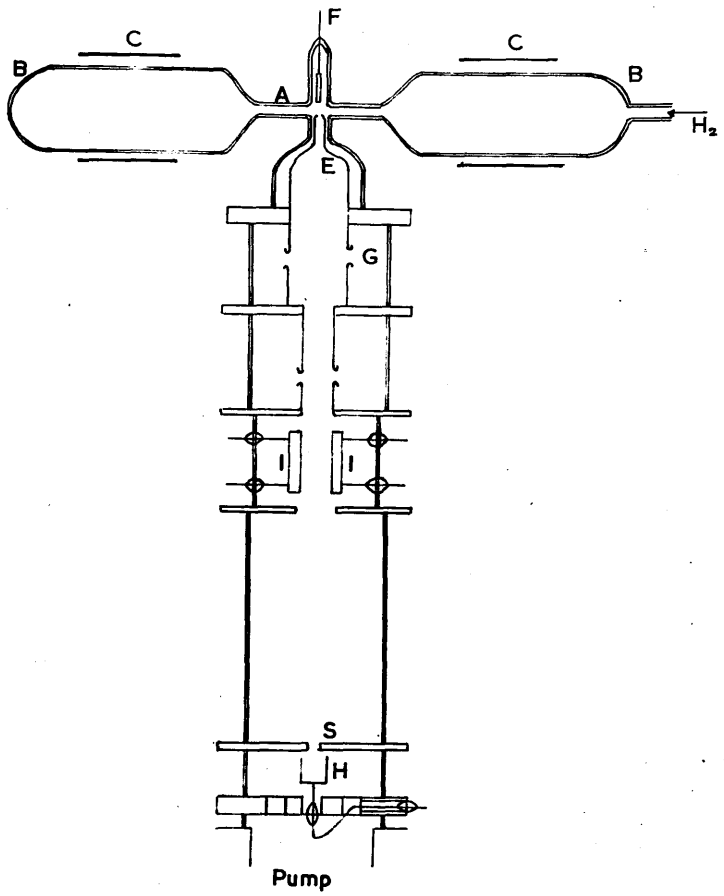

Fig.II(viii). R.F. Capillary Source and Crossed Field Analyser.

it will be deflected along a path of radius of curvature ρ given by:

$$\frac{Mv^2}{\rho} = (Hev - Xe) \qquad (9)$$

Where X is the electric field and H the magnetic field, both being assumed to act over the same length of path. If V is the energy of the particle in electron volts:

$$Ve = \tfrac{1}{2} Mv^2 \qquad (10)$$

Hence:
$$\frac{2V}{\rho} = H\sqrt{\frac{2Ve}{M}} - X \qquad (11)$$

For particles which remain undeflected and pass through the slit S we have $\rho = \infty$ and hence:

$$X = H\sqrt{\frac{2Ve}{M}} \qquad (12)$$

Thus by measuring the collector current as a function of X we obtain the mass spectrum of the ions in the beam. This method of analysis was found to be very convenient and simple to use for the following reasons. (i) Since the whole apparatus was in a vertical line it was easily assembled and supported directly on top of the flange of the vacuum pump. (ii) Only a comparatively small and light permanent magnet was required, instead of a large electro-magnet. (iii) The total focused beam current could be measured quickly and directly by removing the magnet and reducing the deflector voltage to zero. (iv) The ion source and focusing electrodes could be changed without disturbing the analysing system. The resolution was

sufficient to give almost complete separation of the H_1^+ peak from the H_2^+ peak, but the H_3^+ peak was not completely resolved from the H_2^+ peak, although its magnitude could usually be estimated fairly accurately. A typical spectrum obtained with this analyser of the beam from the capillary source described above is shown in Fig.II (ix).

After careful cleaning and outgassing, the capillary source was found to give a yield of about 25% protons. Although this was not as high as was desired, it was considerably better than that which had been obtained with the original Thoneman type of source and confirmed that development was proceeding along the right lines. In respect of total ion output the performance was poor, the maximum ion current being 100 μa. with a probe voltage of about 1600 volts. At higher probe voltages the discharge in the capillary was completely 'blown out' in the region of the electrodes and the output dropped almost to zero. When the source was giving 25% protons the colour of the discharge was pink instead of the characteristic blue which had been observed with the Thoneman source, and, indeed, with the capillary source when it was first used before it had been outgassed. This change in colour was due to the increased strength of the Balmer lines emitted by excited hydrogen atoms, relative to the band spectrum emitted by the hydrogen molecules, the red colour being due to the strong H_α line of the Balmer series. This

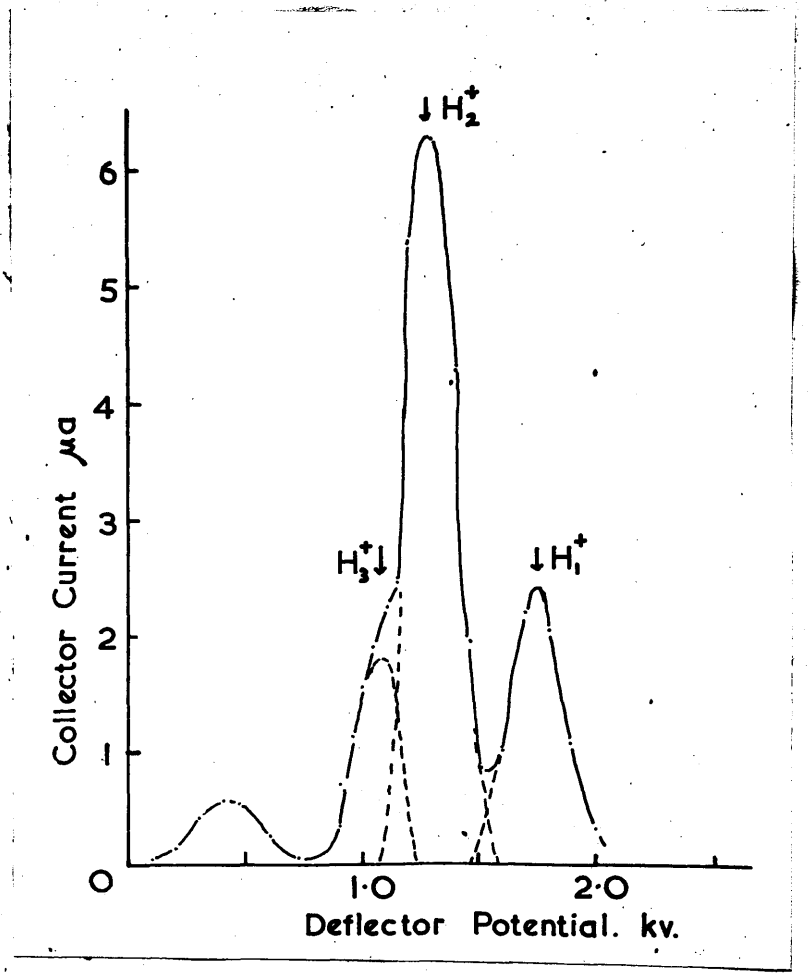

Fig.II(ix). Ion Spectrum of Capillary Source.

colour change gave a very useful quick visual indication of the order of magnitude of the proton percentage. A photograph of the spectrum emitted by a later type of source when giving about 60% protons is shown in Fig.II (x). It was observed that the colour of the discharge in the capillary source did not change from the bulbs to the capillary, and it seemed probable that the concentration of atomic hydrogen was more or less constant throughout the apparatus.

In view of the results obtained with the capillary source a new source of the type shown in Fig.II (xi) was constructed. This source retained the essential feature of exposing only a small area of metal to the discharge, which had been found necessary for forming a high concentration of atomic hydrogen. But it was hoped that, by reverting to a type of extraction similar to that used in the Thoneman source, an increased beam current would be obtained. The discharge was maintained in the Pyrex tube A by the R.F. voltage applied between the cylindrical electrodes B B. The ions were extracted through the exit canal C, $\frac{1}{8}$" diameter by $\frac{1}{2}$" long, in the aluminium block D by applying a potential between it and the probe P. The tungsten probe was set back in the side tube through which the hydrogen entered the discharge tube in order to minimise its effect as a surface for recombination of atomic hydrogen. As in the Thoneman source, the extraction

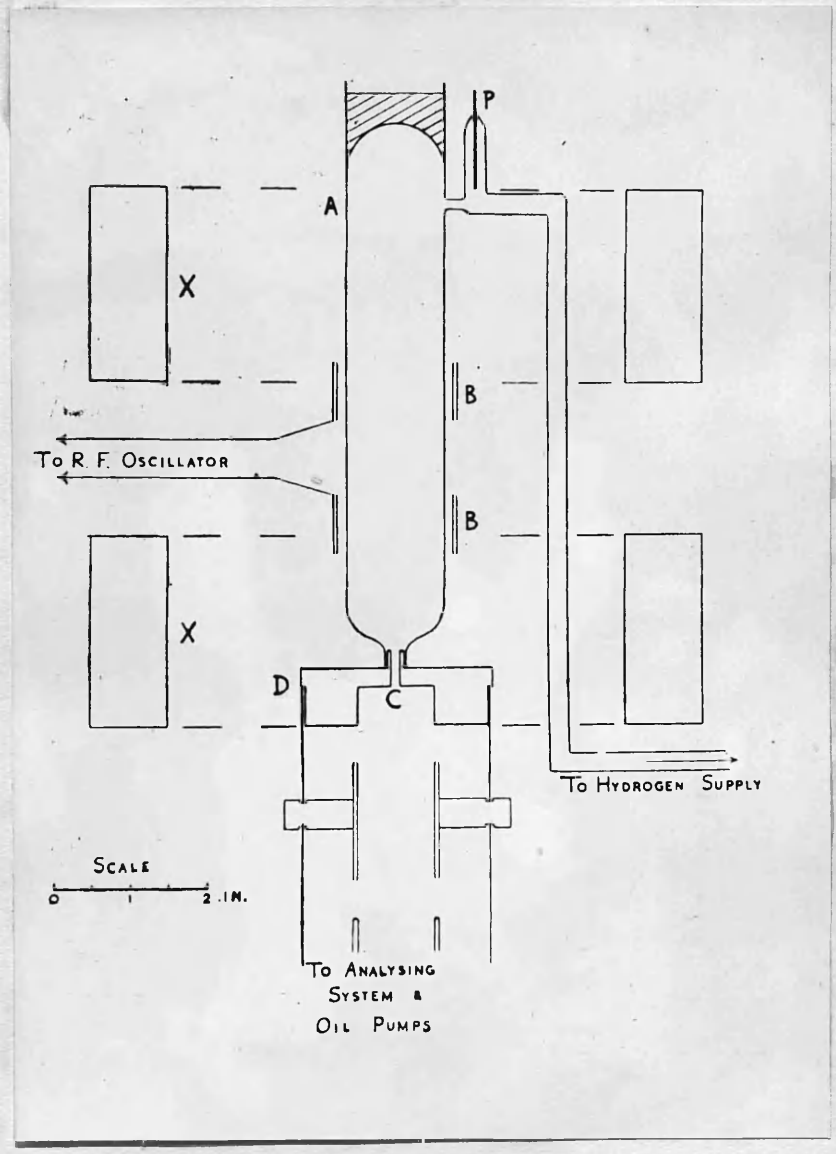

Fig.II(xi). New Source (Mark I).

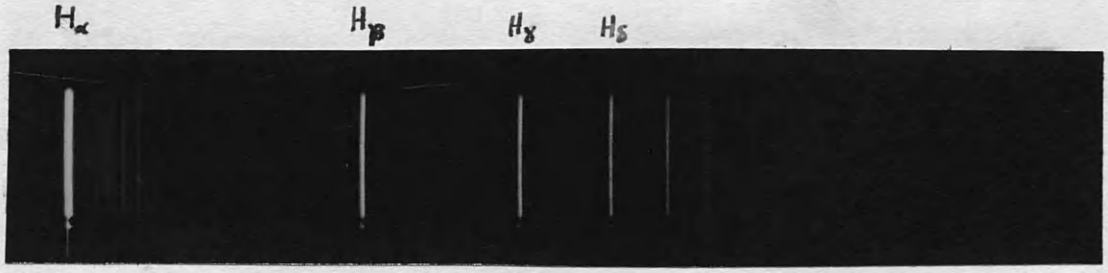

Fig. II (x) Optical Spectrum from R.F. Source.

voltage produced a small 'dark space' above the canal, whose boundary with the bright plasma of the discharge was roughly spherical in shape. This boundary moved upwards as the extraction voltage was raised. The secondary electron beam accelerated up the tube from the canal was again a source of trouble and a small oil bath was fitted to the top of the tube to conduct the heat away from the bombarded area. Before the bath was fitted the glass was frequently cracked or melted and even afterwards this effect limited the maximum probe voltage which could be applied. Provision was also made for a magnetic field parallel to the axis of the discharge tube. This was provided by the Helmholtz coils xx, which produced a field of up to 300 gauss in the region of the tube.The purpose of this field was as follows. We have already observed that the concentration of atomic hydrogen should depend on the rate of ionisation, now an electron which is oscillating under the influence of the R.F. field will, in general, have a drift velocity super-imposed on its motion. This drift velocity will finally cause it to collide with the walls, if it does not collide with a gas molecule first. Now if there is an axial magnetic field, the component of velocity perpendicular to the field direction will cause the electron to move in a circular path in this plane. The component of velocity parallel to the field direction

will be unaffected and the electron will therefore spiral along the lines of force. This means that the electron will spend a longer time in the gas before it is lost by collision with the wall and hence a larger fraction of the R.F. power will be expended in ionising the gas relative to that expended in collisions with the walls. It was found that when a magnetic field of about 100 gauss or more was applied, the brightness of the discharge increased considerably and the colour showed a marked reddening. The quantitative effect on the proton percentage can be seen from the graphs of Fig.II (xii). It will be seen that the proton percentage increased from 30% to 54% when the field was switched on. The effect of the gas pressure on the proton percentage was also investigated and is shown in Fig.II (xiii). It will be seen that the proton percentage was almost constant at pressures above about 10 microns (10^{-3} mm Hg) but began to fall at lower pressures. Having thus attained the necessary conditions for a good proton percentage, the total ion current was measured as a function of the probe voltage and the pressure. The current was not found to be critically dependant on the pressure at pressures above about 10 microns, provided that the output matching controls on the R.F. oscillator were adjusted for maximum power at each pressure. At pressures below 10 microns the discharge became rather unstable and it became difficult to match the

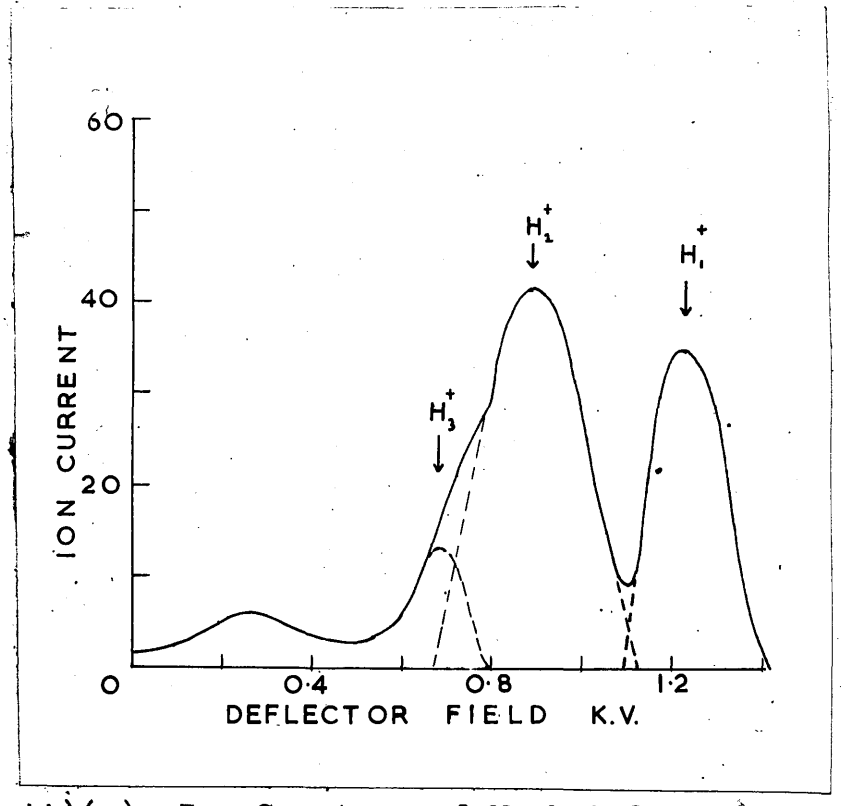

Fig.II(xii)(a). Ion Spectrum of Mark I Source Without Magnetic Field.

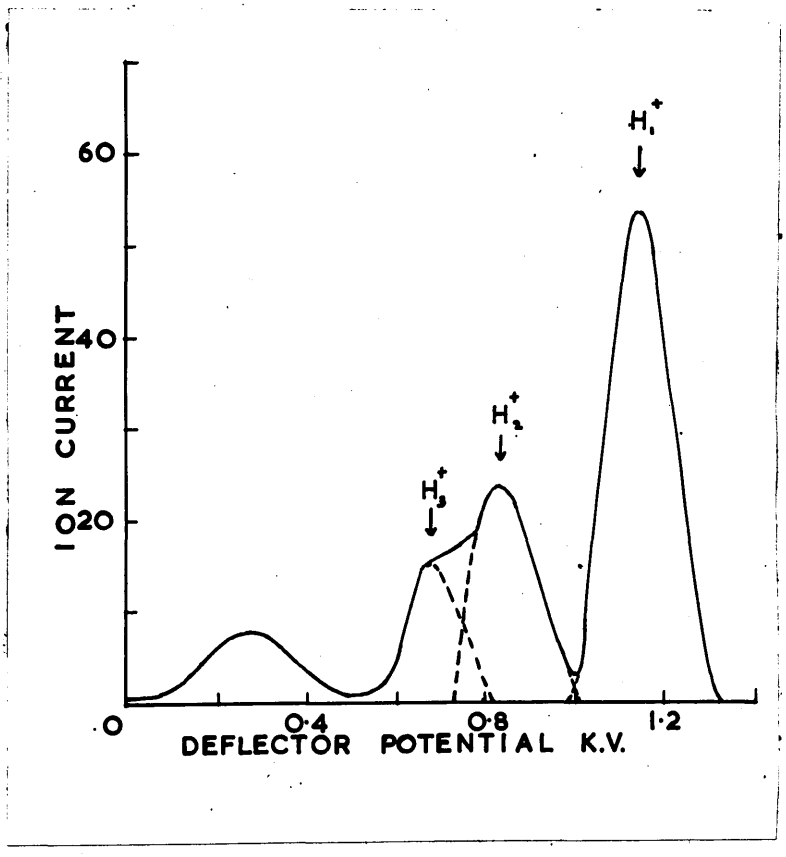

Fig.II(xix)(b). Ion Spectrum of Mark I Source With Magnetic Field.

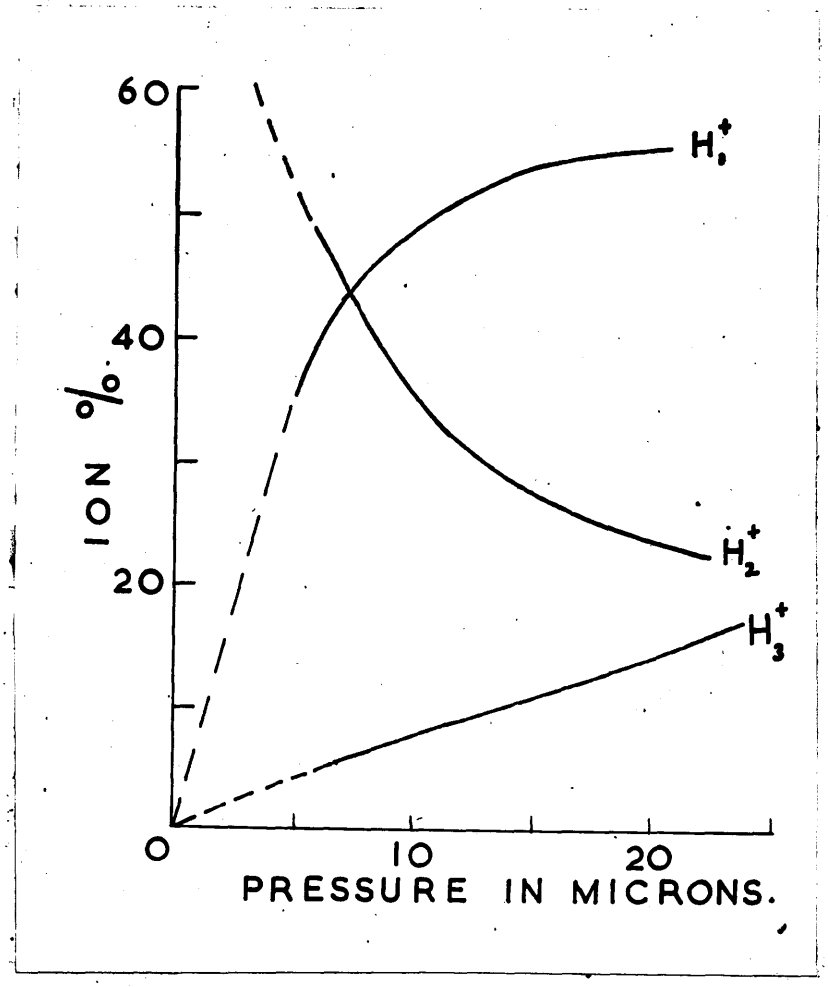

Fig.II(xiii). Ion Percentages Versus Gas Pressure, Mark I Source.

oscillator properly. A graph of the total ion current as a function of the probe voltage at a pressure of 15 microns is shown in Fig. II (xiv). For this measurement the analysing chamber and the collecting system were connected together and used as a deep Faraday cage. It will be seen that the ion current rose rapidly to 500 μa. at a probe voltage of 2.5 Kv and then tended to level off at higher voltages. With the maximum focusing voltage of 15 Kv which was available it was only possible to focus the beam through the slit into the final collecting cylinder H at probe voltages up to 2.8 Kv. Under these conditions the current to the cylinder was 400 μa. without magnetic analysis and 240 μa. with the analyser magnet in position and the electrostatic deflecting field set for the proton maximum.

As the construction of the H.T. set was proceeding it was felt that the time had come to design a source and focusing arrangements which could be put on the accelerator tube, even if modifications had to be made later. For this purpose the source shown in Fig.II (xv) was constructed. It will be seen that some small modifications had been made. In order to save space, which would be at a premium in the spinning on top of the accelerator column, the size of the magnet coils had been considerably reduced. The brass formers of these coils were insulated from each other and from ground, so that they could be used as the

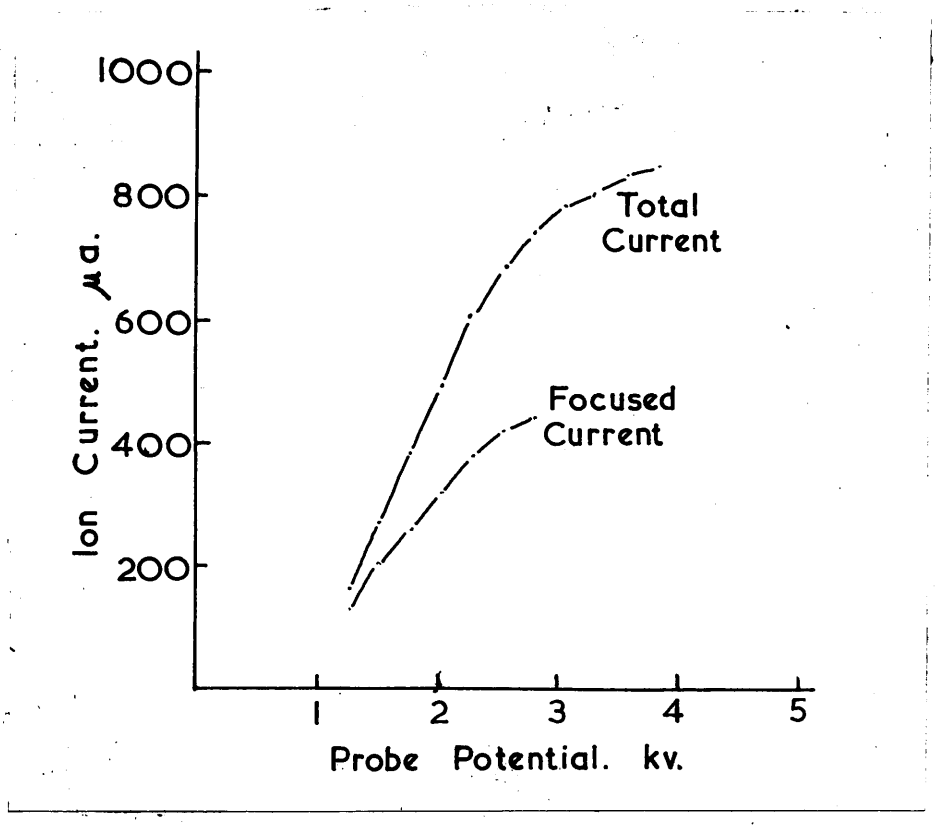

Fig.II(xiv). Ion Current From Mark I Source.

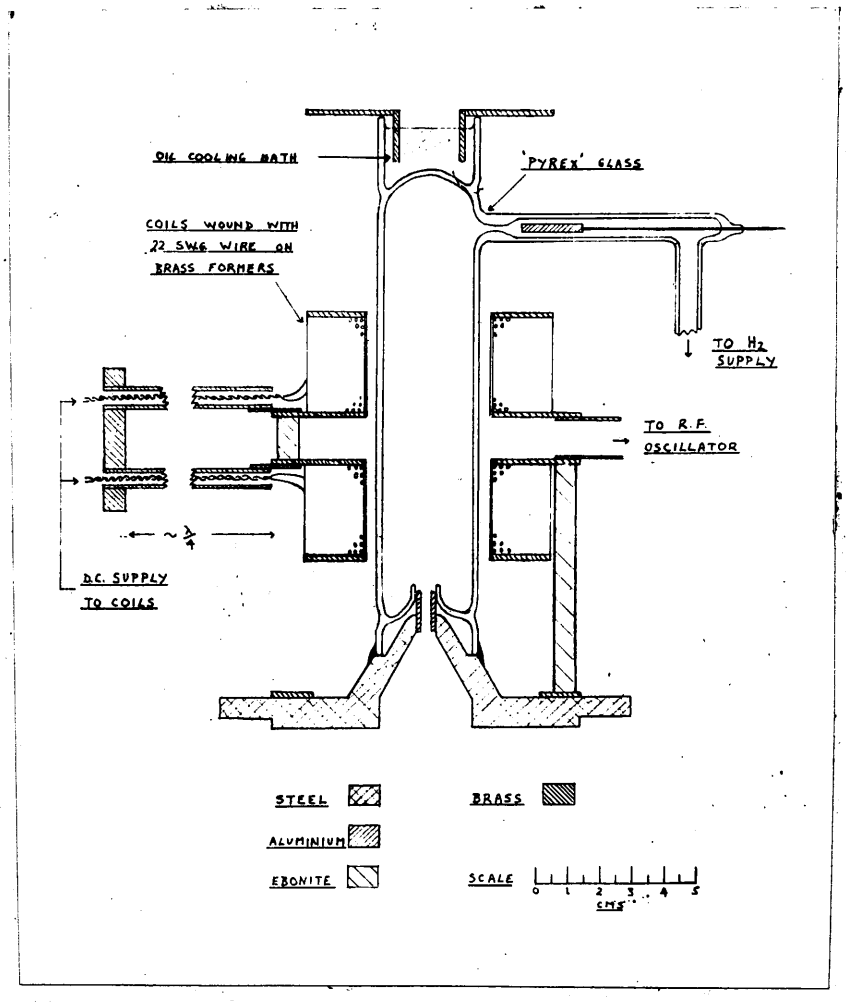

Fig.II(xv). New Source (Mark II).

R.F. electrodes. Two pieces of copper tube, slightly less than a quarter of a wavelength long, were fixed to the coil formers and soldered into a brass shorting bar at their far ends. A sliding shorting bar (not shown in Fig.II (xv)) was also fitted so that the whole formed a 'stub' of variable inductance which could be used to match out the self-capacity of the electrodes. The twin concentric cables from the oscillator were tapped onto this stub at a point which was found by experiment to give the best match to the characteristic impedance of the cables. The D.C. connections to the magnet coils were brought out down the centre of the copper tubes forming the matching stub and emerged at the rear of the shorting bar so that they did not affect the R.F. circuit. The source tube itself was similar to the previous ones except for the inverted glass 'skirt' round the canal. The purpose of this was to reduce the effect of sputtering of the aluminium canal onto the glass of the source, which had previously been found to cause erratic operation of the source after a few hours running. We may say here that although this modification increased the useful life of a source to about 30 hours, it was still a major source of trouble and later necessitated a complete re-design of the extraction arrangements. The total ion current from this source was measured, using a collector a short distance below the exit

canal. As usual, an electrode was placed above the collector to prevent secondary emission electrons from leaving the collector. A number of measurements, made with differnet bias voltages on the collector and the electrode showed that, with the correct bias voltages, the collector current was a true measure of the ion current. A graph of the ion current and probe current as a function of the probe voltage is shown in Fig.II (xvi). It will be seen that the performance of this source was quite satisfactory.

This source was installed on the accelerator tube and was used in preliminary tests of the focusing and alignment of the accelerator electrodes.

The original focusing system which had been constructed to focus the ion beam from the source to the first main accelerator tube was found to be rather unsatisfactory. The design of the accelerator tube had been taken, with only minor modifications, from a tube which had been operated successfully by the Philips Company in Eindhoven in conjunction with an Oliphant type of ion source. The first accelerator gap was at a distance of about 50 cms. below the top plate of the accelerator tube, on which our ion source had to be mounted, and hence the beam had to travel this distance with only the comparitively small voltages, of the order of 10 kv, which were available from the ion source power

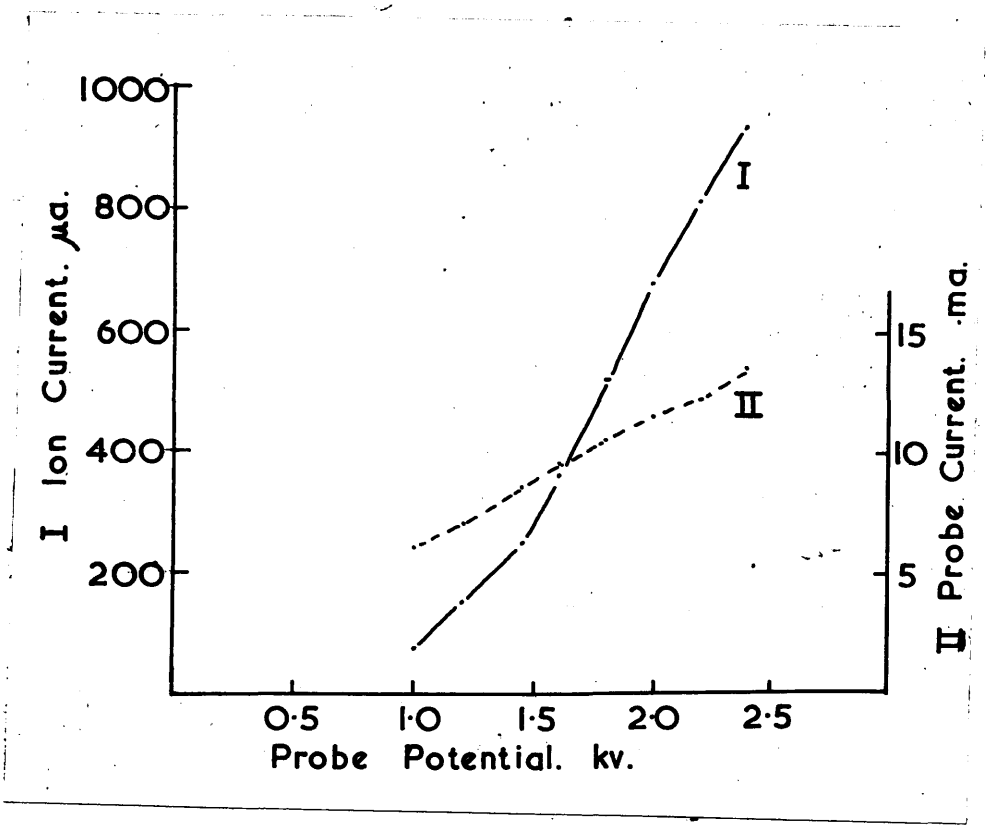

Fig.II(xvi). Ion and Probe Currents from Mark II Source.

supplies. It was found that this was a difficult problem, mainly because of the space charge repulsion effects in a low voltage, high current beam. These space charge effects prevented the formation of a finely focused beam at high current densities and caused a large part of the beam to strike the accelerator electrodes.

In view of these focusing difficulties a completely new system was developed for the initial focusing of the beam. At the same time a new method of extracting the ions from the ion source was developed in order to overcome the sputtering troubles which were responsible for the short useful life-time of the source.

The final system which was developed and installed on the accelerator tube is shown in Fig.II (xvii). The principal change in the design of the ion source itself is in the method of extracting the ions. This method is based on that described by Bayly and Ward (1948). The discharge tube A is made almost flat on its lower end and rests on the aluminium electrode C. The vacuum seal between A and C is made with a rubber ring round the outside of the tube. A circular hole is ground in the flat end of A and a circular lip, turned on the electrode C, projects through this hole. The aluminium canal E is fixed to the main steel supporting plate D and projects into the central hole in the electrode C. The electrode

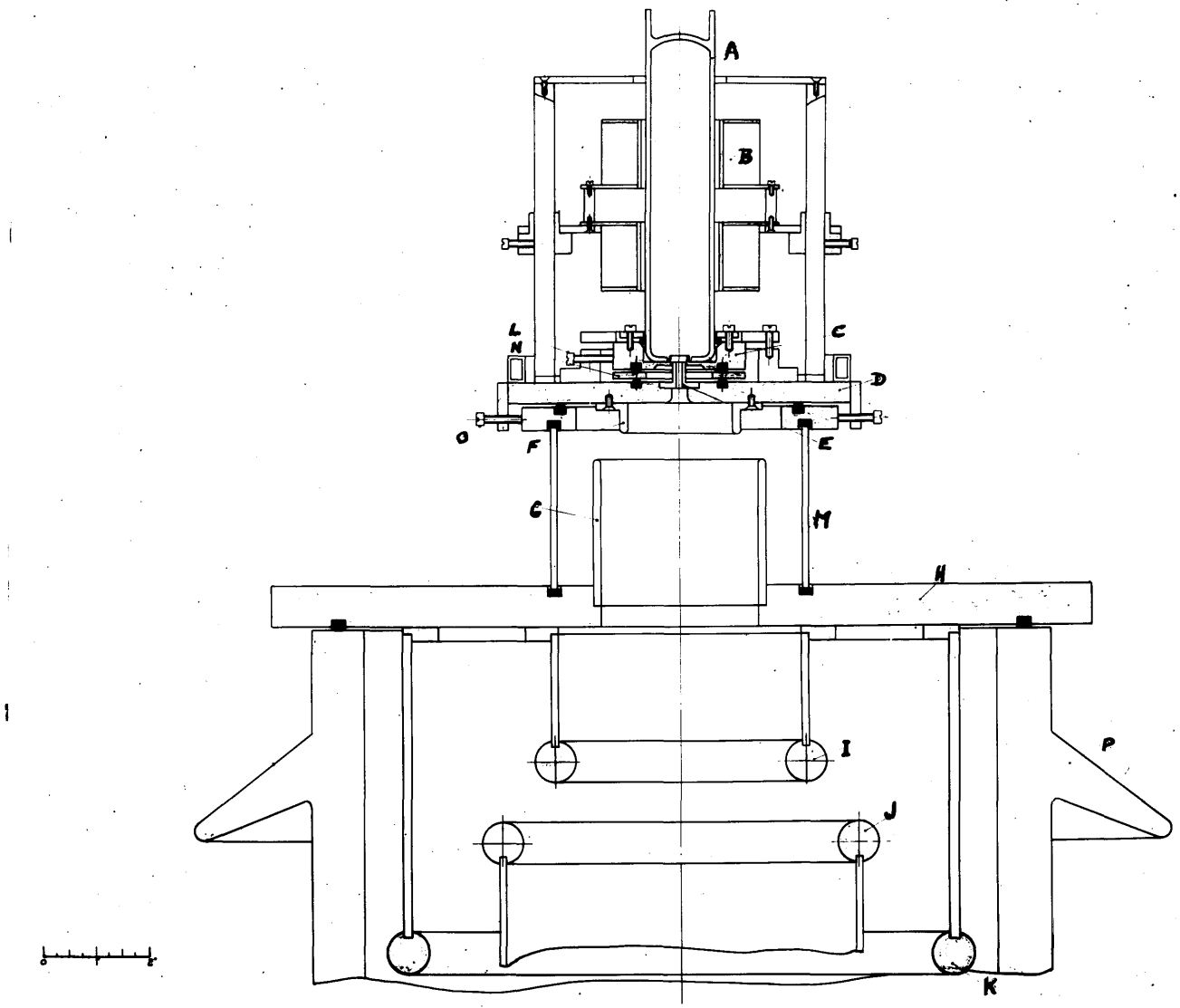

Fig.II(xvii). Final Ion Source (Mark III) and Focusing Arrangements.

C is insulated from the plate D by means of a glass plate N, which is in the form of an annular ring. The vacuum seals between C, N and D are made with rubber rings. The extraction voltage is applied between the electrode C and the canal E. The projecting lip on C effectively replaces the probe used in the previous type of source. When the extraction voltage is applied, a dark space is formed above the canal, its boundary with the bright plasma of the discharge being approximately hemispherical and bounded by the upper edge of the projecting lip on C. Thus the ions are accelerated and focused through the canal as before. However, with this arrangement the extracting field is determined solely by the metal electrodes and it is therefore quite unaffected by sputtering. It is, of course, still possible for sputtered aluminium to reach the upper parts of the inside walls of the discharge tube A and after a long time this causes a reduction of the proton percentage because it increases the recombination coefficient for atomic hydrogen to molecular hydrogen. However, the useful life of the source under these conditions is found to be at least 100 hours, after which time it is necessary to remove the source tube and remove the aluminium deposit with caustic soda solution. The construction of the source mounting makes the removal and replacement of the tube a comparatively simple matter and the alignment of

the extraction electrodes is not disturbed in the process. It was found during initial experiments with this system that the exit current was very sensitive to the alignment of the canal in the hole in the electrode C. In the final arrangement this alignment is made adjustable by means of four screws tapped into an ebonite ring and bearing on the periphery of the electrode C, which is otherwise free to slide relative to the glass plate N. For simplicity only one of these screws L is shown in Fig. II (xvii). After the source had been installed these screws were adjusted until the exit current through the canal was a maximum. During this adjustment the exit current was measured by connecting all the accelerator tube electrodes together and connecting a meter between them and ground. The top terminal of the accelerator column was, of course, also connected to ground during this measurement.

The hydrogen or deuterium enters the ion source through a small tube let in through the plate D, which leads into the space between D and C. For simplicity this tube is not shown in Fig. II (xvii).

Before this source assembly was mounted on the accelerator tube its performance was tested in the usual way. Typical curves of the total ion current emerging from the canal and of the current flowing to the canal are shown in Fig. II (xviii). It will be seen that an

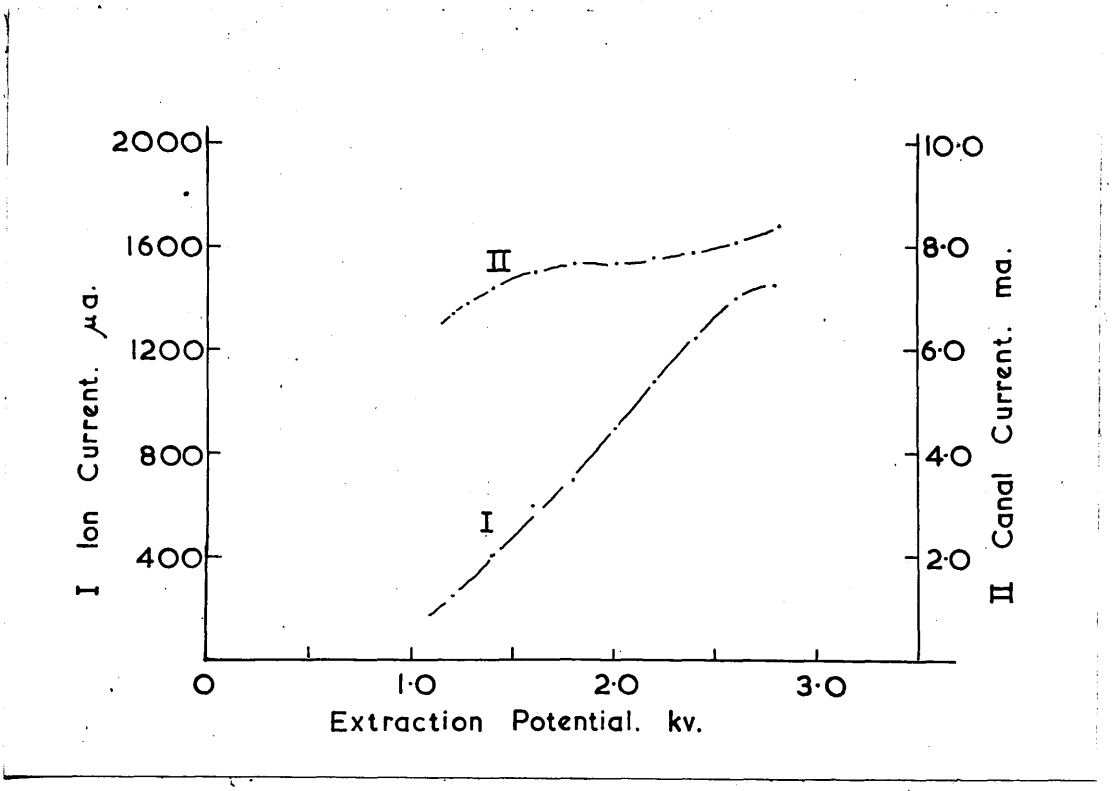

Fig.II(xviii). Ion and Probe Currents from Mark III Source.

ion current of 1300 micro-amps is obtained with an extraction voltage of 2.6 Kv and that the canal current is of the order of 8 m a. A large part of the canal current is, of course, due to secondary electrons.

The whole of the ion source assembly is insulated from the main steel top plate H of the accelerator column and is supported from it by the glass cylinder M. The 'focus' power pack, which supplies a potential of up to 14 kV, is connected between the plate D and the plate H. Thus the ions are accelerated by this potential as they pass across the gap between the cylindrical electrodes F and G. It will be seen that this gap is only a short distance below the exit canal E and this distance is very much smaller than the focal length of the lens formed by F and G. Thus this lens has very little effect on the divergence of the ion beam leaving the canal and serves merely to accelerate it. The beam continues to diverge until it reaches the first main accelerating gap formed by the cylindrical electrodes I and J. The electrode J is supported from the plate which is at the first junction of the accelerator column below the top. Thus a potential equal to that produced by one stage of the H.T. generator is applied between I and J. This potential is, of course, one-fifth of the total potential produced by the generator and therefore varies from 0 to 160 kv as the generator voltage varies from 0

to 800 kv. Now the focal length of a given electrostatic lens is a function of the voltage ratio V_2/V_1 where V_1 is the voltage of the ions before passing through the lens and V_2 is their voltage afterwards. It is independent of the actual values of V_1 and V_2 provided that space charge effects are negligible. The focal lengths of such lenses as a function of the voltage ratio and the electrode diameters are known from work on electron optics. (Epstein 1936).

In this application it is necessary that the lens formed by the electrodes I and J should have a focal length such that it forms a real image of the exit canal E at the next accelerating gap of the accelerator tube, which is at a distance of about 1 metre below the top plate of the tube. Thus, to a first approximation, the focal length of this lens must be equal to its distance from the canal. Further, this focal length must be maintained at this value over the full range of voltage over which the H.T. set is required to operate. Now the useful range of the H.T. set is considered to be from 150 kv to 800 kv, which corresponds to a range of from 30 kv to 160 kv for the voltage between the electrodes I and J. We denote this voltage by V_5, the extraction voltage of the source by V_3 and the accelerating voltage between F and G by V_4. Then the voltage ratio across the lens I J is given by:

$$R = \frac{V_5 + V_4 + V_3}{V_4 + V_3} \qquad (9)$$

To a first approximation we can neglect $V_4 + V_3$ in comparison with V_5 and obtain:

$$R = \frac{V_5}{V_4 + V_3} \qquad (10)$$

Now the normal maximum extraction voltage applied to the source is about 2 kv. The dimensions of the electrodes I and J were chosen so that the calculated focal length of the lens formed by them was equal to its distance from the canal E when the voltage ratio, R, was equal to 15. If the H.T. set is at its minimum useful voltage of 150 kv, so that V_5 = 30 kv, then R will be equal to 15 when V_3 = 2 kv and V_4 = 0. As V_5 is increased, V_4 may be increased at the same time to maintain R at the required value of 15. When V_5 reaches its maximum value of 160 kv, $V_4 + V_3$ will require to be approximately 11 kv and hence V_4 will be 9 kv. During this process the voltage ratio across the accelerating gap formed by F and G will vary from 1 to 4.5 as V_4 is varied from 0 to 9 kv. Over this range the focal length of the lens formed by this accelerating gap is considerably greater than its distance from the canal and hence its only effect will be to form a virtual image of the canal which will be very slightly above the actual position of the canal and this will have a

negligible effect on the focusing properties of the main lens I J. In practice the 'focus' voltage V_4 is remotely controlled from the beam room and is manually adjusted for optimum focus of the beam which finally reaches the target. It must be mentioned that the voltage ratios across all the subsequent accelerating gaps down the tube remain constant as the H.T. set voltage is varied. This system is found to work in a very satisfactory manner and gives a well focused beam over the full required range of H.T. set voltage for total beam currents up to about 300 micro amps. At higher beam currents the beam becomes more diffuse and part of it is lost by collision with the walls of the resolving chamber. This effect is almost certainly due to the effects of space charge repulsion in the first stage of the accelerator tube. However a resolved proton beam of between 150 and 200 micro-amps can be obtained at the target, which is considerably more than that obtained by previous workers on similar installations.

* * * * * * *

II (4). The Accelerator Tube and Associated Equipment.

(a) Tube and Electrode Design.

A diagram of the accelerator tube is shown in Fig. II (xix). The acceleration of the particles takes place in five separate stages. This number of stages was chosen because the H.T. generator provides five equally spaced voltage points between ground and its high voltage terminal. The main body of the tube consists of five sections of porcelain tube 12" inside diameter, 14" outside diameter and 20" long. The accelerating electrodes are supported from steel plates mounted between the junctions of the porcelain tubes. The vacuum seals between the steel plates and the porcelain tubes are made with rubber gaskets located in grooves in the plates. A lateral movement of the porcelain tubes relative to the steel plates is provided by the adjusting screws which bear onto small brass shoes on the outside of the tubes. It was found to be possible to make small adjustments of these screws even when the accelerator tube was evacuated, provided that the rubber gaskets had been well greased before assembly. This facility proved to be of great value in aligning the electrodes. The external parts of the plates and the adjusting screws are normally enclosed in smooth aluminium spinnings to reduce the electric field gradients

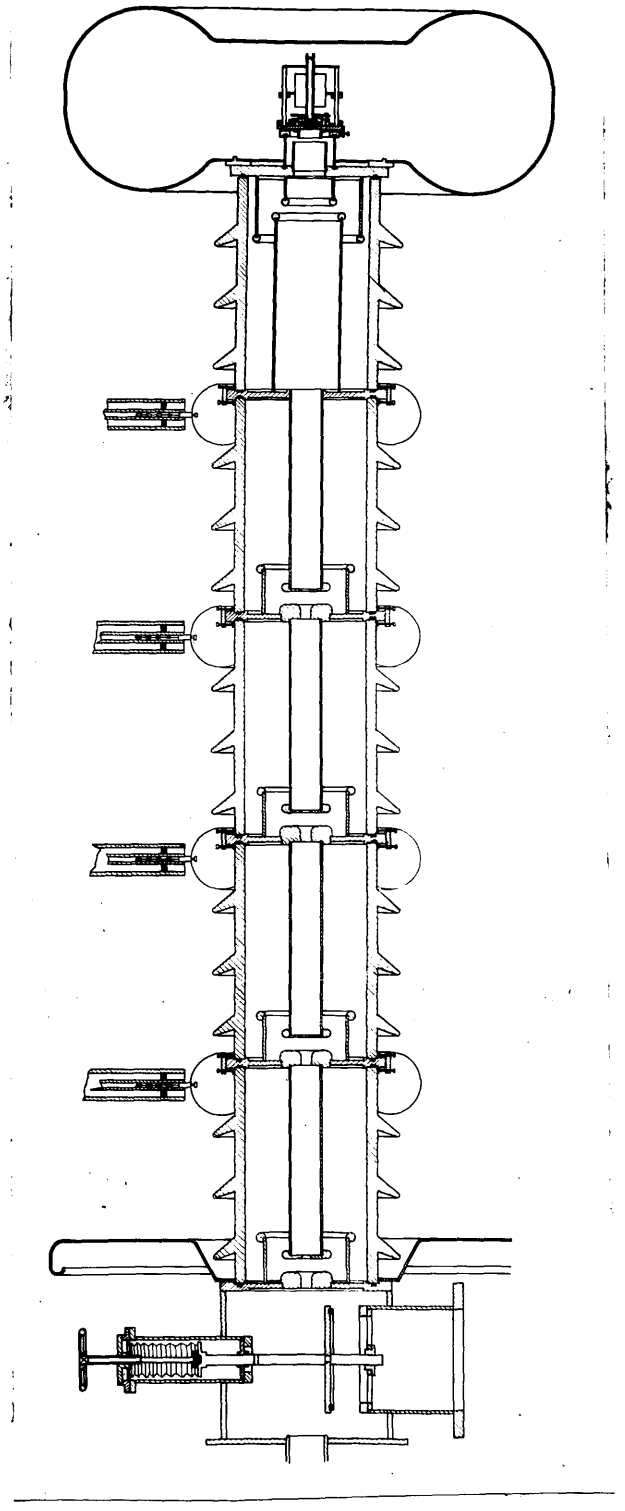

Fig.II(xix). Section Through Accelerator Tube.

at the surface. These spinnings are connected across to the appropriate spinnings on the generator through 10 MΩ resistances. These resistances consist of 200, 50 kΩ, carbon resistances connected in series and placed inside 2" diameter paxolin tubes.

The accelerating electrodes themselves are made to a standard design which had been successfully used by Messrs. Philips. It will be noted that each accelerator gap is surrounded by a shielding electrode, whose purpose is to prevent any surface charges which may become built up on the walls of the porcelain tubes from causing small random deflections of the beam. The first accelerating gap, which is different from the other four, has already been described in the preceding section. The remaining accelerating gaps have much smaller apertures, the upper electrode of each gap having a $\frac{3}{4}$" diameter hole and the lower one a $1\frac{1}{2}$" diameter hole. This is done in order to reduce the secondary electron current, caused by bombardment of the electrodes by stray ions, to as small a value as possible.

During the process of alignment of the tube electrodes the current to each electrode was measured by means of meters inserted in the resistances connecting the electrodes to the H.T. generator. For the safety of the observer, these meters were observed through a telescope! The adjusting screws on the steel plates

carrying the electrodes were adjusted for minimum current to each electrode in turn, starting from the top of the column. It was found to be possible to reduce the current to each electrode, except the first, to less than 20 microamps, with a beam current of several hundred microamps. The current to the first electrode is usually of the order of 300 microamps, but a considerable part of this current is probably due to secondary electrons, which are able to traverse this section more easily than the subsequent ones because of the larger diameter of the electrodes.

After traversing the last accelerator gap the ion beam passes down a 4" diameter tube through the floor of the room in which the H.T. set is housed and into the beam room below. The magnetic analyser and target arrangements will be described in the following section.

The whole system is continuously evacuated by means of a 16" diameter oil diffusion pump of standard design, which is backed by a 4" diameter diffusion pump and a Kinney mechanical pump. Penning ionisation gauges and Pirani gauges are fitted at the base of the accelerator column and the top of the main diffusion pump and their associated meters are mounted in the control room beside the control desk of the H.T. generator.

* * * * * *

(b) The Power Column.

The ion source power supplies are provided from a separate power column. This column consists of a large paxolin tube 32" in diameter and 9' high. A generator is mounted in the spinning at the top of this column and is driven from an induction motor at the bottom by means of a leather belt. The generator provides 1.5 Kw of A.C. power at 80 volts 2000 cycles and 500 watts of D.C. power at 24 volts. This generator was available from ex-Government disposals and the D.C. power is not really required, it is only used for supplying the magnet coils on the ion source. The 200 mcs. oscillator for the ion source, the power packs for the probe and focus voltages and the current for the palladium leaks, which control the supply of hydrogen or deuterium to the ion source, are supplied from the A.C. output of the generator. It is necessary to control the probe and focus voltages and the palladium leak current from the beam room when the H.T. set is operating. These voltages and currents are controlled by variacs situated in the spinning on top of the power column, which are driven by nylon strings from pulleys at the base of the column. These pulleys are, in turn, remotely driven from control knobs in the beam room by means of Selsyn motors.

* * * * * * *

(c) Magnetic Analyser and Target Arrangements.

We have already seen that the beam of charged particles from the ion source contains a number of unwanted ions as well as the protons or deuterons which are required for disintegration experiments. In order to separate the protons or deuterons from the other types of ion we use a magnetic analyser.

Using the nomenclature of section I 5(a), we have seen that:

$$H\rho = \sqrt{\frac{2EM}{Z^2 e}}$$

Now if a particle of charge Ze is accelerated through a potential difference V volts it acquires a kinetic energy E electron volts, where: $E = VZ$

$$\text{Thus} \quad H\rho = \sqrt{\frac{2VM}{Ze}}$$

Thus we see that if a beam of particles is accelerated through a fixed potential difference V, we can separate out, by magnetic deflection, particles having different values of M/Z. This enables us to separate the atomic ions from the associated molecular and triatomic ions of the same gas. However it must be noted that the deuteron has the same value of M/Z as the hydrogen molecular ion and hence these particles are not separated by magnetic analysis.

The principles involved in the design of a magnetic

analyser for this purpose are very similar to those discussed later in this thesis (Section III (1)) in connection with the design of a magnetic spectrometer for energy measurements on charged particles. The beam of particles is initially parallel in this case and hence we can obtain focusing of the beam by employing the type of deflection shown in Fig. III (1). The choice of the value of the angle of deflection, θ, is determined by a number of factors. The value of 90° has been used in a number of installations of this type. It has the advantage that, with a vertical accelerator tube, the emergent beam is horizontal, which is convenient for many experimental arrangements. However, the beam is then focused at the point where it emerges from the magnet poles and diverges after that, with consequent loss of beam current per unit area if the target must be placed some distance away. Also, this type of deflection involves the use of a rather large magnet.

After a careful consideration of all the factors involved we finally decided to use a deflection angle of 30°. A schematic diagram of the resolving chamber is shown in Fig.II (xx). It will be seen that circular magnet pole pieces are used and the whole system is made symmetrical about the axis of the beam. Thus the proton beam can be deflected to the left or right hand

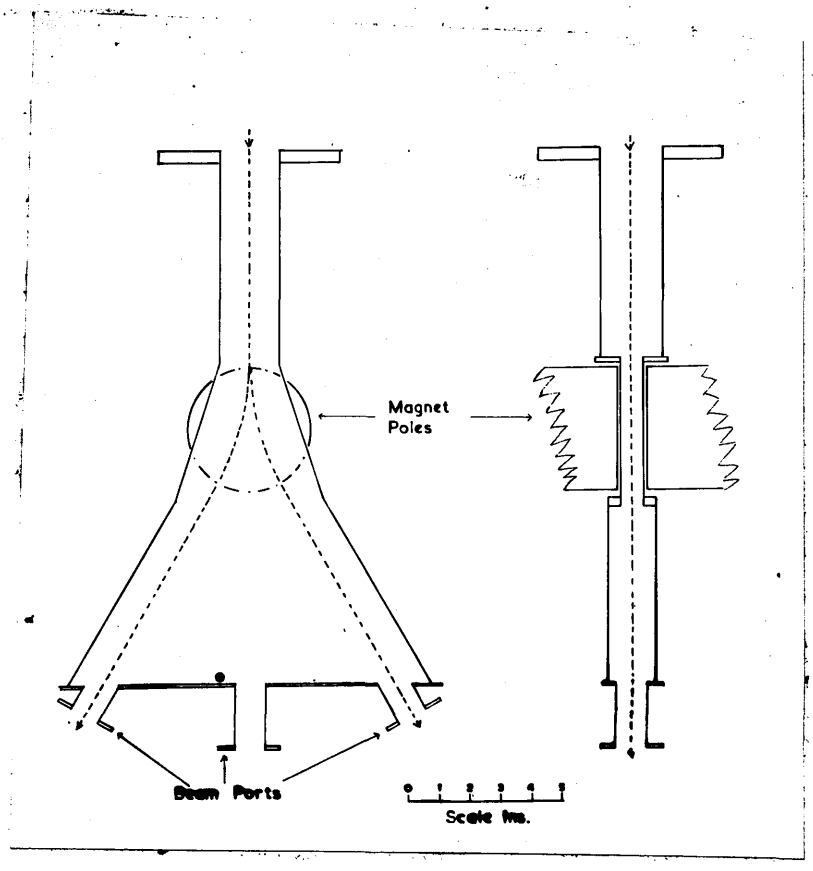

Fig. II(xx). Schematic Diagram of Resolving Chamber.

target ports by simply changing the direction of the current through the magnet coils. This allows a rapid change-over to be made between two separate experiments without the necessity of changing the target and the associated experimental equipment. A flap-type vacuum valve is placed in the beam tube immediately above the resolving chamber so that the chamber can be filled with air when it is necessary to change a target, without letting air into the accelerator tube. The chamber can be roughly re-evacuated via a by-pass tube from the backing pump before opening the flap valve.

The current for the deflecting magnet is supplied from a small 80 volt 2000 cycle generator via a rectifier and stabiliser system essentially similar to that designed for the H.T. generator. This system was originally designed to work from the 50 cycle mains, but it was found to be difficult to reduce the ripple voltage to a sufficiently low level.

* * * * * * *

Part III. Instruments for Measurements on Reaction Products.

III.1. The Heavy Particle Spectrometer.

(a) Fundamental Considerations.

We have already noted that the method of magnetic analysis has many advantages for the detection and precise measurement of the energy of the heavy charged particles emitted in nuclear reactions. We now consider the design of a spectrometer for this purpose.

The principle requirements of such a spectrometer are (a) a high degree of resolution in energy and (b) a large solid angle for collection of particles leaving the target. It is also desirable that these requirements should be achieved with a magnet of reasonable dimensions.

In order to achieve the maximum resolution and solid angle with a magnet of given size it is necessary to utilise the focusing properties which are inherent in the deflection of charged particles in a magnetic field. We consider first the property of first order focusing in the plane of deflection of particles moving in a uniform magnetic field. The well-known case of 180° focusing, with the source and collector both in the region of the field, is a special case of this general property. Let us consider the case illustrated in Fig.III.(1). Here the magnetic field has the uniform value H over the region

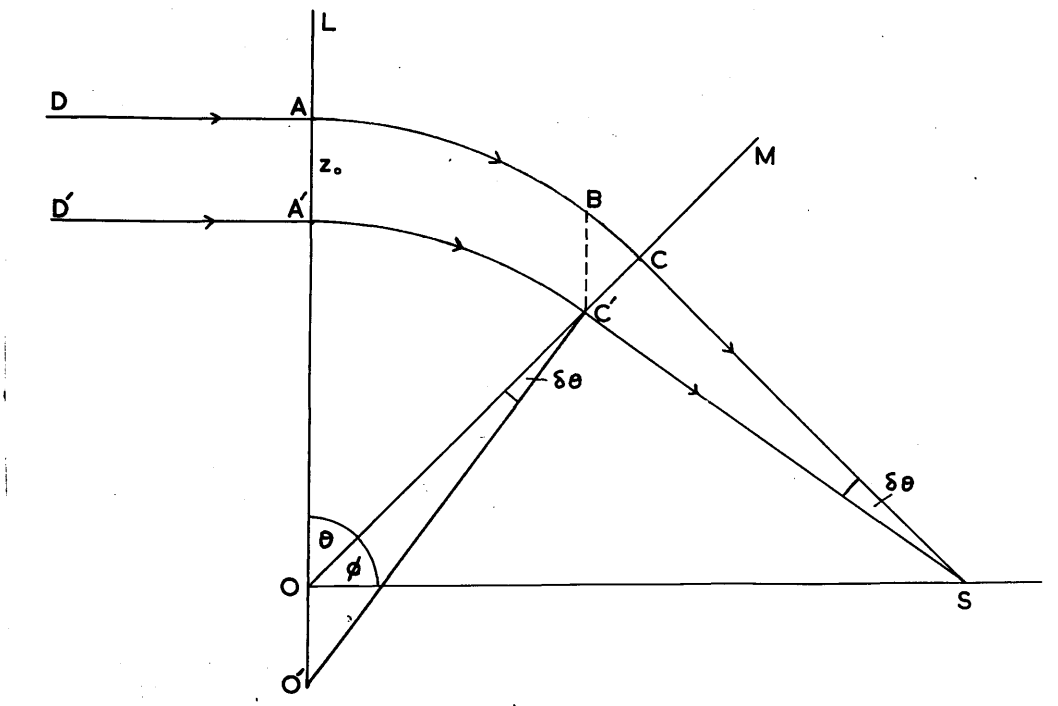

Fig.III(i). Focusing of Parallel Beam by Wedge-Shaped Poles.

enclosed by the lines OL and OM and has the value zero over the region outside these boundaries. Suppose that a parallel beam of charged particles is incident normally on the boundary OL and that DA and D′A′ are the paths of two such particles, where $AA' = z_0$. After entering the field region the particles will travel in circular paths of radius ρ, given by the relation defined in section I.5:-

$$H\rho = \sqrt{\frac{2EM}{Z^2e}}$$

Now let H be adjusted so that ρ = OA. The particles will then travel along the circular arcs AC and A′C′ centred on O and O′ respectively, where $OO' = AA' = z_0$. After leaving the field region the particles will travel along the straight lines CS and C′S, which are tangents to the arcs AC and AC′ respectively. We assume that $z_0 \ll \rho$ and consider the triangle BC′C, where B is the intersection of a line through C′ parallel to OL with the arc AC.

Let: $\hat{LOM} = \theta$

then: $\hat{BC'C} = \hat{LOM} = \theta$

Also: $BC' = OO' = z_0$

and since: $\hat{BCC'} = 90^\circ$

$$CC' = z_0 \cos\theta \qquad (1)$$

$$\therefore \hat{CSC'} = \delta\theta = \frac{CC'}{SC} = \frac{z_0 \cos\theta}{SC} \qquad (2)$$

Now since SC and SC′ are tangents at C and C′,

$$\hat{OC'O'} = \hat{CSC'} = \delta\theta$$

Now in the triangle $CC'O'$, since $O'\hat{O}C' = 180^\circ - \theta$ and $\delta\theta$ is small,

$$\frac{CC'}{\delta\theta} = \frac{O'C'}{\sin\theta}$$

Hence: $$\delta\theta = \frac{z_0 \sin\theta}{\rho} \qquad (3)$$

Thus from (1) and (2)

$$\frac{z\cos\theta}{SC} = \frac{z_0 \sin\theta}{\rho}$$

or $$SC = \rho \cot\theta \qquad (4)$$

Now let $S\hat{O}C = \phi$ and consider the triangle SOC in which $S\hat{C}O = 90^\circ$.

Then $$\tan\phi = \frac{SC}{OC}$$

$$\therefore \tan\phi = \frac{\rho\cot\theta}{\rho} \qquad \text{from (4)}$$

$$\tan\phi = \cot\theta$$

Hence $$\theta + \phi = 90^\circ \qquad (5)$$

Thus we see that, since the relations (4) and (5) are independant of z_0, all the particles which are initially incident in directions parallel to DA will be focused at a point S which lies on the normal to OL through the point O, provided that $z_0 \ll \rho$.

Now it is clear that the paths of the particles are reversible, and hence if we have a point source of particles at S then the particles leaving S in directions making small angles with SC will emerge as a parallel beam after passing through the region of the magnetic field.

We can now apply this treatment to the case shown in Fig. III (2). Here we have the magnetic field contained in the wedge shaped region defined by the lines ON and OM, each of which make an angle θ with respect to OL. Then it is clear that the particles from a point source S will be focused at the point S′, where SOS′ is the line through O normal to OL. We are again only considering particles which leave S in directions near to SD, where $\hat{SDO} = 90^{\circ}$.

We can now consider the design of spectrometers based on this focusing principle. The special case when $2\theta = 180^{\circ}$ is the case of '180° focusing' which has been widely used in spectrometers for both β-rays and heavy charged particles. This type of spectrometer is not particularly convenient for measurements on nuclear reactions because of the difficulties involved in getting the incident proton or deuteron beam onto the target, which is inside the magnetic field of the spectrometer. However, these difficulties are not insurmountable and can be overcome by bringing the incident proton beam onto the target through a hole in the magnet pole, so that it travels parallel to the direction of the magnetic field and is not deflected by it. This technique has been used by Buechner et al (1948) in the design of a spectrometer of high precision. Such a spectrometer has the advantage that it is possible to make absolute measurements of the particle energies by measurement of the magnetic field and the distance between

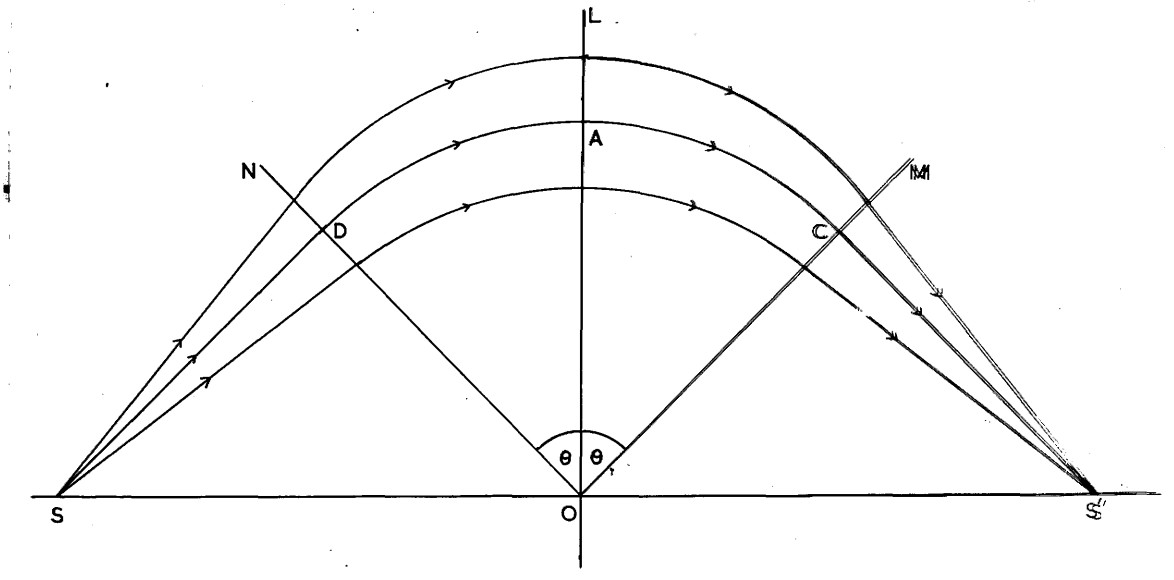

Fig.III(ii). Slit to Slit Focusing by Wedge-Shaped Poles.

the source and the collector. In the case of a spectrometer of smaller deflection angle, with the source and collector outside the magnetic field, the effects of the fringing field make a precise absolute calibration very difficult. With this type of spectrometer it is usual to calibrate the instrument by the use of particles of known energy. A spectrometer of this type with a deflection angle of 90° has been described by Burcham (1949).

The spectrometer which has been used for the experimental work described in this thesis was constructed to suit a magnet which was available in the laboratory. This magnet had circular poles 4" in diameter and was capable of producing a field of up to 11,000 gauss with a gap of 2 cms. For the experiments planned at the time it was necessary to measure the energy of alpha-particles up to at least 2 MeV. This meant that the spectrometer had to be designed so that the radius of curvature ρ of the paths of the particles was not less than 15 cms. With this radius of curvature the maximum deflection angle allowed by the size of the magnet poles was of the order of 45°. If we consider a spectrometer of the type shown in Fig.III (ii) with $\rho = 15$ cms. and $2\theta = 45^{\circ}$ we find that SD = S'C = 34 cms. Now we can see from the geometry of Fig.III (ii) that the solid angle of acceptance of the spectrometer will be given by:

$$\Omega_1 = \frac{z_0 \cos\theta}{SD} \cdot \frac{l}{2SD + 2\rho\theta}$$

where l is the length of the collector slit normal to the plane of the diagram. If we assume that z_0 and l are both made equal to 2 cms, which are of the order of magnitude of the values allowed by the dimensions of the magnet poles, then we find that $\Omega_1 = 1/500$ steradians.

We now consider a spectrometer of the type shown in Fig.III (1), where S is now the source of particles and a collimator is placed in the region DA in front of the collector to select only those particles travelling in directions parallel to AD. Then with $\rho = 15$ cms. and $\theta = 45^\circ$ we see that SC = 15 cms. The solid angle Ω_2 is given by:

$$\Omega_2 = \frac{z_0 \cos\theta}{SC} \times \frac{l}{SC + \rho\theta + d}$$

where l is the width of the collector normal to the plane of the diagram and d is the distance of the collector from the point A. If we put $z_0 = l = 2$cms as before and make d = 12 cms, which is a reasonable practical length for the collimator, we find that $\Omega_2 = 1/100$ steradians. Thus this type of spectrometer should give a solid angle approximately five times as large as that given by a conventional wedge spectrometer with the same magnet poles. It must be noted that in order to obtain this result it is necessary to use a collector which is sensitive over the full area of 2 cms. square. Furthermore it has been assumed that the collimator will be 100% transparent to

particles travelling parallel to the selected direction and that the focusing is perfect, so that mono-energetic particles from the source will emerge in a parallel beam. However it was felt to be worthwhile to construct such a spectrometer since it was different from any previous design and should be at least as good as the conventional wedge type.

The spectrometer which was actually constructed is shown in Fig.III (iii). The beam of bombarding particles from the accelerator tube passes through the slit S and strikes the target T. The target is water cooled and insulated from ground so that the target current can be measured. The target is surrounded by an insulated tube A which is normally maintained at a potential of about -100 volts with respect to ground in order to prevent secondary electrons from leaving the target. The incident particles pass through a circular hole in the upper side of this tube and the reaction particles emerge through wide slits at the end of it. The main body of the spectrometer consists of an iron tube B, which is soldered to a tube C of rectangular cross section fabricated from sheet brass. This rectangular tube fits between the magnet poles and is bent in a radius of curvature of 15 cms. A second iron tube D is soldered to C and contains the collimator E. This collimator consists of thin sheets of mica 10 cms long with a spacing of .36 cms. The mica is sufficiently thick

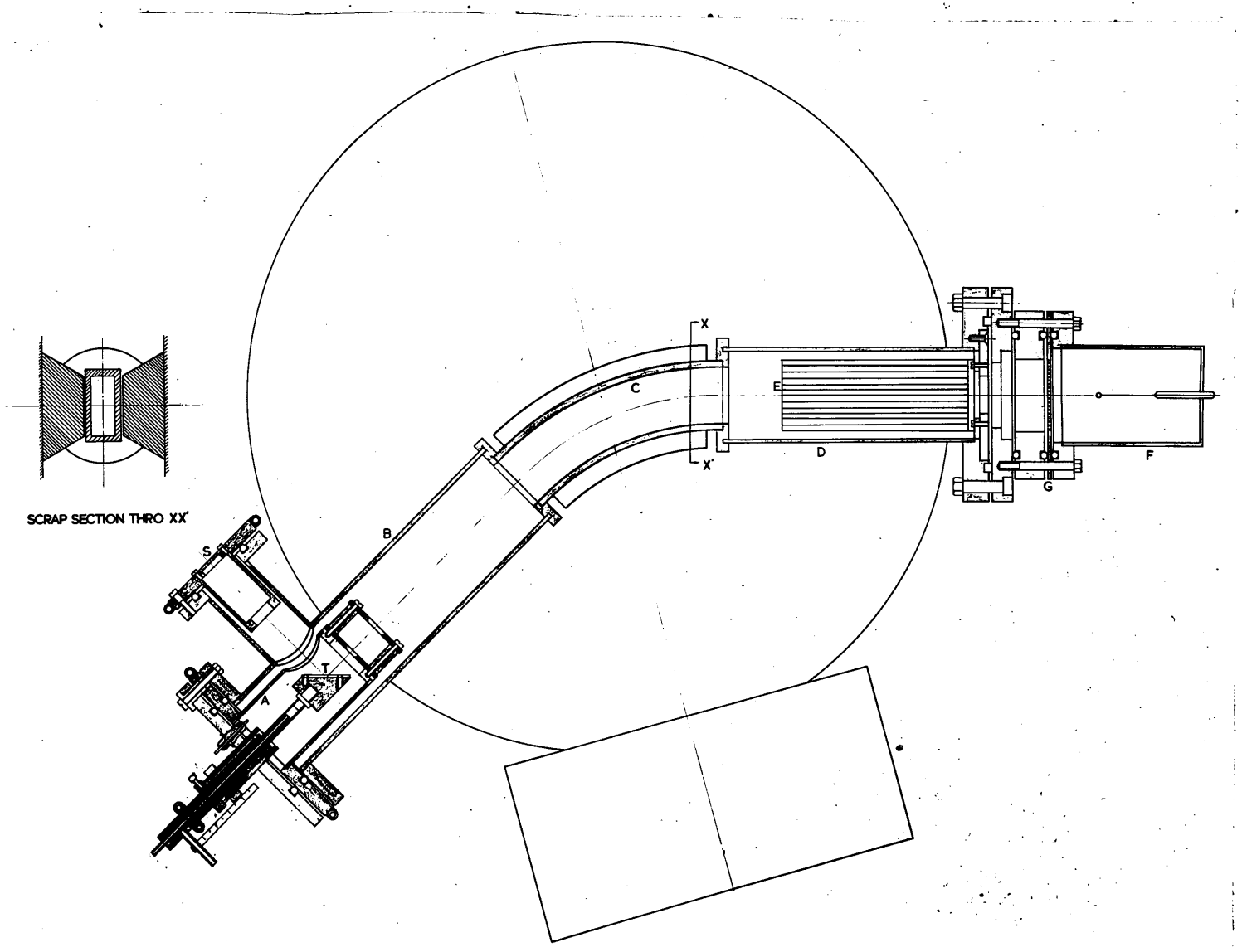

Fig.III(iii). Construction of Spectrometer.

to stop protons or alpha particles of the energies with which the spectrometer can be used, but its thickness is negligible in comparison with the spacing between the sheets. The cut-off angle of the collimator is $\pm 2°$. Two types of collector have been used for detecting the particles after they emerge from the collimator. The original detector consists of a zinc-sulphide screen with a photo-multiplier placed behind it to detect the light pulses emitted when the particles impinge on the screen. The electrical pulses from the multiplier are then amplified and counted in the usual way. The second type of collector consists of a proportional counter and is shown in Fig.III (iii). The window between the counter and the spectrometer consists of a thin collodion film of about 3 mms. air equivalent thickness. This film is supported on a grid which was made by drilling 1 mm. diameter holes as closely spaced as possible in the brass plate. This grid has a transparency of 45%. The counter is filled differentially in situ.with pure methane to a pressure of about 5 cms. of mercury. It operates with a potential of about 1200 volts on the central wire and the pulses are passed through a linear amplifier and amplitude discriminator to a scaler.

It was found that a considerable number of scattered protons were able to reach the collector even when the magnetic field was very much higher than the value appropriate

to the energy of these protons. This effect is presumably due to multiple scattering of the protons at the walls of the spectrometer. The number of protons elastically scattered from the target is, of course, many orders of magnitude larger than the number of reaction particles produced. In the case of (p,α) reactions, it is possible to discriminate against the background of scattered protons by means of the pulse amplitude discriminator. The proportional counter was found to give a very much better uniformity of pulse size for mono-energetic alpha-particles than the scintillation counter and for this reason it was used in most of the work described in this thesis.

In the proportional counter the pulse size due to alpha particles of the order of 1.5 MeV is about three times the maximum pulse size due to scattered protons and is constant to better than 20%. It is therefore possible to set the discriminator so that the effect of the scattered protons is completely eliminated, whilst maintaining 100% efficiency for counting the alpha particles. Typical curves of counting rate against discriminator setting are shown in Fig.III (iv) for both types of collector and clearly indicate the superiority of the proportional counter in this respect. It must be emphasised that this result is only achieved at the expense of a reduction of the effective solid angle of the spectrometer by a factor of 45% due to

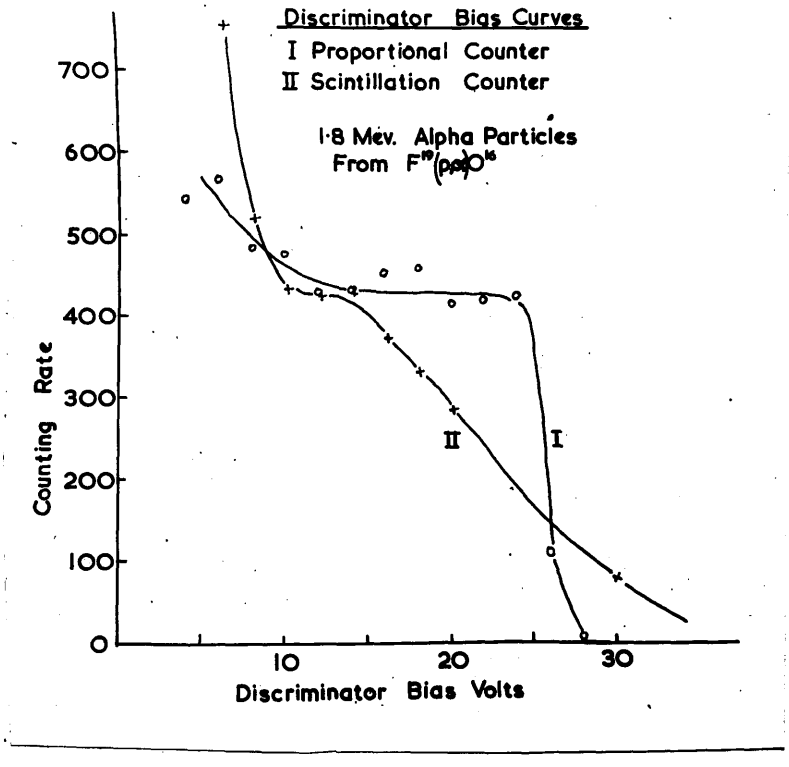

Fig.III(iv). Discriminator Bias Curves.

the presence of the grid supporting the counter window.

In order to attain the maximum possible field over the required area with the magnet available, special pole pieces were constructed. A cross section through these pole pieces is shown in Fig.III (iii). They were constructed by turning a ring of low carbon steel to the cross-section shown, with a mean radius of 15 cms., and then milling two 45° sectors from this ring. Shims were fitted to the edges of the poles to improve the constancy of the field over the central region and were adjusted experimentally until the field was constant to better than 1% over radial distance of ± 1 cm. from the central radius.

The magnet current is supplied from a generator and is stabilised and controlled to an accuracy of about 0.1%. The current is measured by means of a 15 amp. meter and can be measured to an accuracy of about 0.2%. A careful calibration was made of the magnetic field against the magnet current by means of a fluxmeter and this calibration has been used in all subsequent work to convert magnet current readings to equivalent fluxmeter readings. In order to reduce hysteresis effects the magnet current is always raised to its maximum value and then reduced to the required value before taking a reading. In order to make an absolute calibration of the spectrometer the alpha particles from the reaction $F^{19}(p,\alpha)O^{16}$ were used. This reaction proceeds to a number of excited states of O^{16} as

well as to the ground state. The alpha particles used in this calibration were those which lead to an excited state of O^{16} at 6.13 MeV. The Q-value for this transition has been measured by a number of workers and the best mean value is 1.977 MeV. A narrow resonance with a comparitively high yield for this reaction occurs at a proton energy of 340 keV. A thick target of calcium fluoride was bombarded with protons whose energy was just sufficient to produce the full thick target yield of the reaction. The spectrum of the resulting alpha particles is shown in Fig.III (v). The value of the flux at the maximum of this spectrum was 89.2 and the calculated energy of the alpha particles was 1.837 MeV. Now we have seen that the $H\rho$ value is proportional to the square root of the energy of the particles and if we assume that the fluxmeter readings F are proportional to $H\rho$ and that ρ is constant we have $F = K\sqrt{E}$ where K is constant. From the above measurement the value of K was calculated. The value of E for a group of particles of unknown energy can then be calculated from a measurement of F, the fluxmeter reading at the peak of the spectrum. For convenience a graph of F against E was plotted, from which the values of E could read off directly.

The spectrum of Fig.III (v) illustrates the resolving power of the instrument. It will be seen that the width of the peak at half amplitude is 6.1%. This is in good agreement with the value of 6% calculated from the geometry

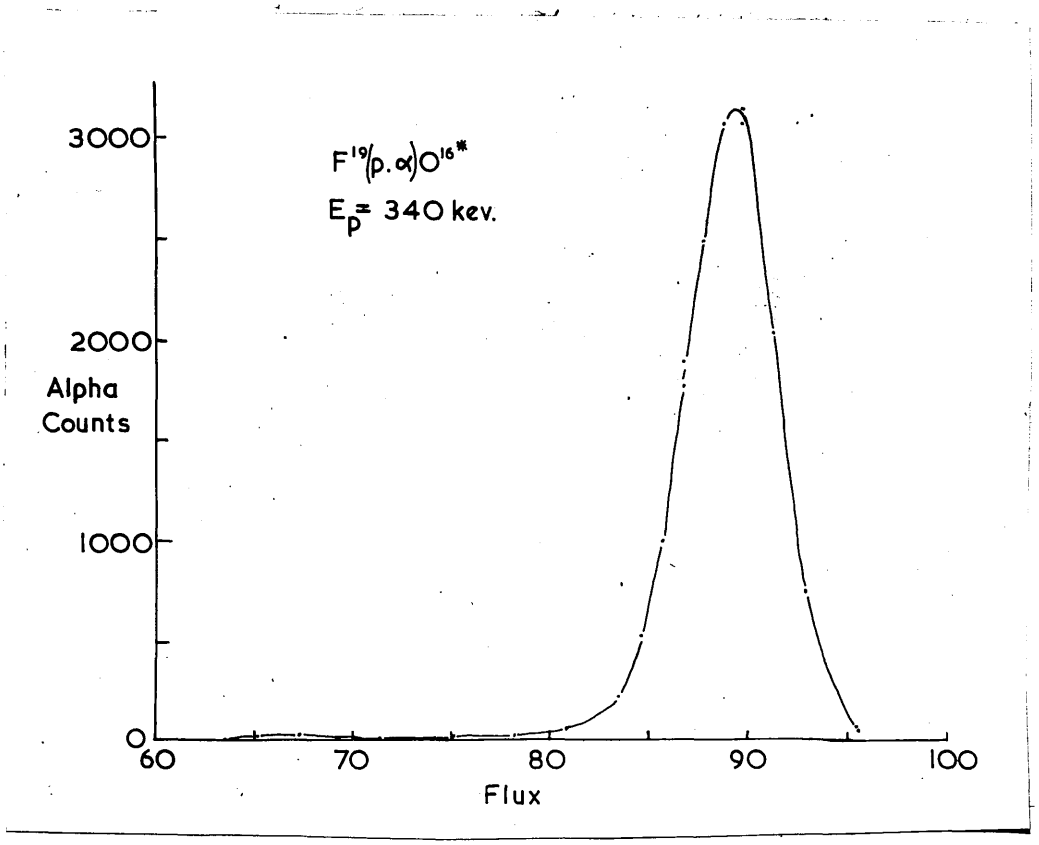

Fig. III(v). Spectrum of Alpha-Particles From $F^{19}(p,\alpha)O^{16}$.

of the collimator and the width of the target. It is estimated that the centre of the peak can be measured to an accuracy of $\pm$ 0.5% in flux, which corresponds to $\pm$ 1% in energy.

* * * * * * *

III.2. The Gamma-Ray Spectrometer.

The basic principles involved in the measurement of the energy of gamma-rays have already been discussed in section I.5. The spectrometer which was used in the experimental measurements described in part IV of this thesis was designed and tested by Dr.E.R.Rae. However, for the sake of completeness, we shall give a brief description of the spectrometer and the way in which it was used in the present work.

The general arrangement of the target and pair spectrometer is shown in Fig.III (vi). The resolved beam from the accelerator tube emerges from the resolving chamber down the axis of a glass tube inclined at 30° to the vertical. A shallow water-cooled brass cup is sealed by a demountable rubber gasket joint to the end of this tube. Targets are normally prepared on thin brass or copper discs, which are clamped to the inside of the cup. The cup is insulated from ground and is connected to the input of the current integrator.

A Geiger counter with thick aluminium walls is mounted at a fixed distance from the target and was used to monitor the gamma-ray intensity. All runs were made for a fixed number of counts in this counter. The current integrator readings were used mainly to check target deterioration.

The vacuum chamber of the spectrometer consists of a

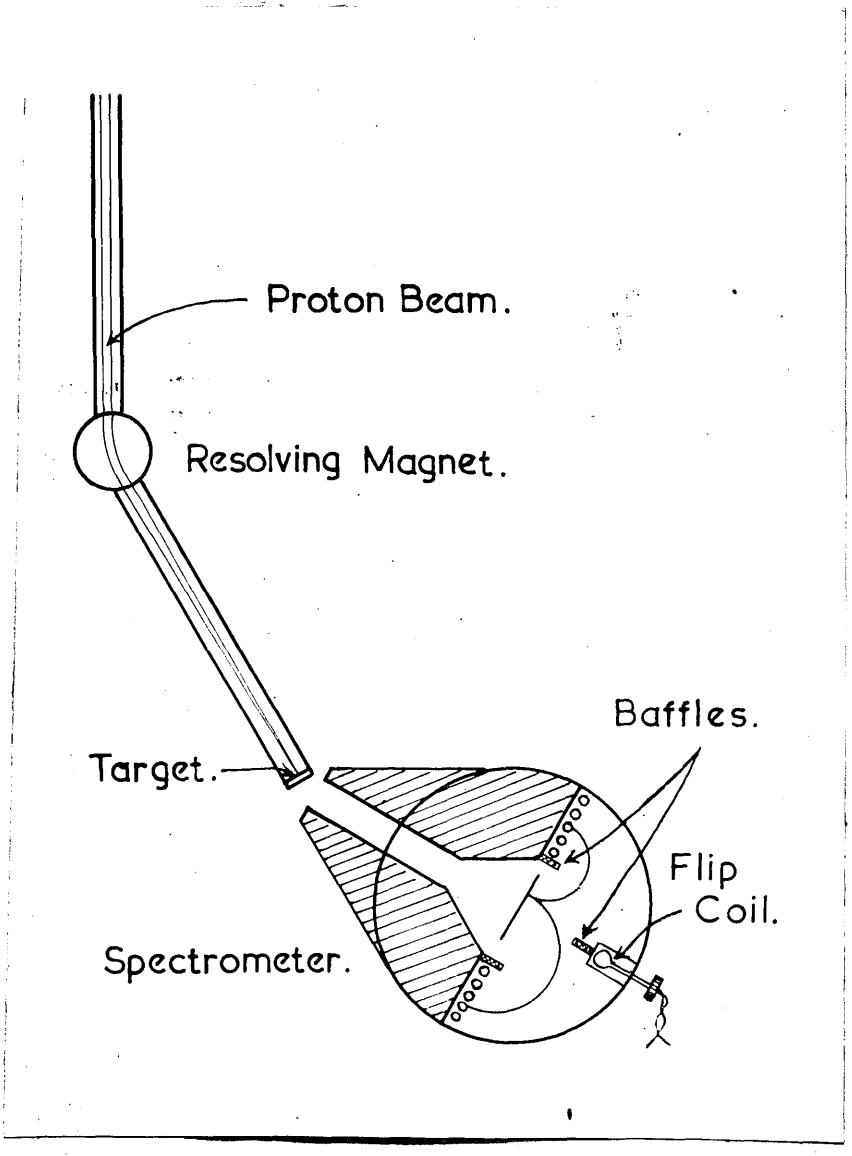

Fig.III(vi). Pair Spectrometer and Target Arrangements.

circular copper cylinder 12" in diameter and 2¼" long, with circular steel end plates 14" in diameter and ½" thick sealed to the cylinder on one side with a soldered joint and on the other with a rubber gasket. The gamma-rays from the target are collimated by the lead shielding blocks and allowed to fall on a thin lead foil placed at the centre of the vacuum chamber. This foil is mounted on a light frame which can be rotated about an axis through one edge by means of a rod passing through a rotary vacuum seal. Thus it is possible to take measurements of the background coincidence counting rates by rotating the foil through 90°, so that it lies against the vertical end plates of the vacuum chamber. These background rates were negligible when measurements were made on proton induced reactions, but were often serious in deuteron induced reactions because of the difficulty of providing adequate screening of the counter from the gamma rays produced by the accompanying neutrons.

The chamber is placed between the 12" diameter poles of an electro-magnet of conventional design, which provides a field of up to 7000 gauss. This field is sufficient to measure gamma-ray energies up to 30 MeV. The field is measured by means of a flip coil and fluxmeter. The relative accuracy of this measurement is estimated to be of the order of 0.3%. An absolute calibration of the instrument was made by measuring the spectra of the gamma

rays from Fluorine and Lithium under proton bombardment and will be described later. A magnet current of 50 amps at 50 volts is required and this is supplied by a D.C. generator. The current is stabilised and controlled to an accuracy of 0.1% by a feed-back circuit operating on the field current of the generator.

The electron-positron pairs, which are ejected predominantly normal to the lead foil by the gamma-rays, are deflected through 180° by the magnetic field and detected by two sets of five Geiger counters placed in the plane of the foil, but screened from direct gamma-radiation by the lead blocks. These counters have windows of 0.001" copper foil to allow the electrons and positrons to enter them with a minimum of scattering. Baffles are placed in the vacuum chamber to reduce the background due to electrons produced by gamma-rays from (n, γ) reactions in the counter walls and the lead shielding behind them, which could otherwise traverse the spectrometer and cause spurious coincidences.

The output pulses from the counters are fed via cathode cathode followers and shaping circuits to twenty-five coincidence circuits, each with a resolving time of about 2 μ secs. The arrangement of these circuits is shown in the schematic diagram of Fig.III (vii). The output pulses from the coincidence circuits are grouped into nine different energy channels, as shown in Fig.III (vii),

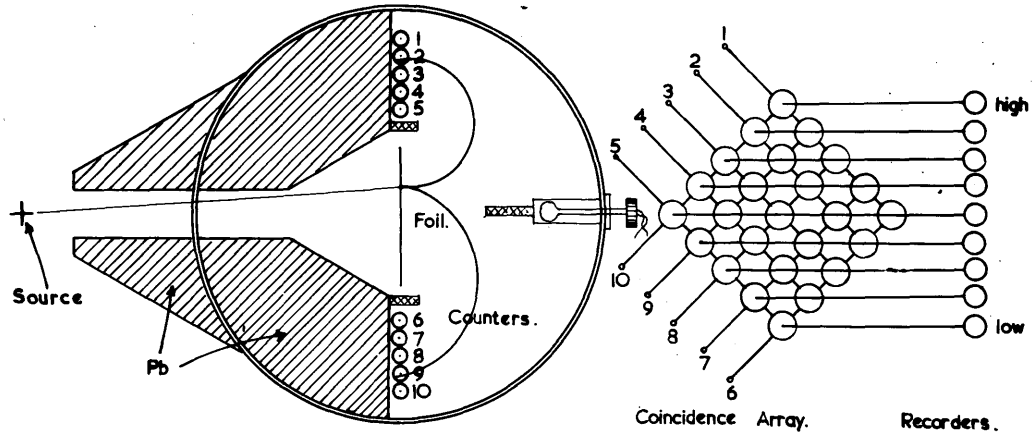

Fig.III(vii). Pair Spectrometer and Counting Circuits.

and the output of each channel is recorded on a mechanical counter. These counters are switched on and off by a master control unit. The output pulses from the monitor Geiger counter are recorded on a scale of 100 and the output of this scaler is used to operate the master control unit. Thus all runs can be made for a fixed number of monitor counts.

In measuring a particular gamma-ray spectrum a series of runs are usually made at a sequence of values of the magnetic field to cover the desired energy range. Each magnetic field setting gives counts in nine different energy channels, the spacing between channels corresponding to 5.8% of the $H\rho$ value of the centre channel. The interval between successive values of the magnetic field is usually of the order of 10% or less, so that there is considerable overlap between the runs. The results are then normalised for channel number and flux and plotted as a function of the mean $H\rho$ value of a single particle. The precise energy of a particular gamma ray is determined from the value of the half amplitude point on the high energy side of the peak, as this point can be measured more accurately than the $H\rho$ value of the peak itself and also should be less dependent upon the effects of scattering and energy loss in the foil. An analysis similar to that of Walker and McDaniel (1948) shows that a relation of the form:

$$k = 600\ H\rho\,(1 + 2.5\,\mu^2/k^2)$$

should be accurate to within 0.5% over the energy range from 3.5 MeV upwards, where k is the energy of the gamma-rays and μ the rest energy of an electron. No absolute calibration of the fluxmeter coil was made. It was assumed that the fluxmeter readings were proportional to the magnet field. The spectra of the 6.13 MeV gamma rays from the 340 keV resonance of the reaction $F^{19}(p, \alpha, \gamma)O^{16}$ and of the 17.6 MeV gamma ray from the 440 keV resonance of the reaction $Li^{7}(p, \gamma)Be^{8}$ were measured and used to calculate the conversion factor between fluxmeter readings and $H\rho$ values. The values of the conversion factor obtained from the two measurements differed by only 0.5% and the mean value was used in the calculation of subsequent results.

The spectrum of the 6.13 MeV gamma rays from $F^{19}(p,\alpha,\gamma)O^{16}$ is shown in Fig.III (viii) to illustrate the resolution of the spectrometer.

* * * * * * *

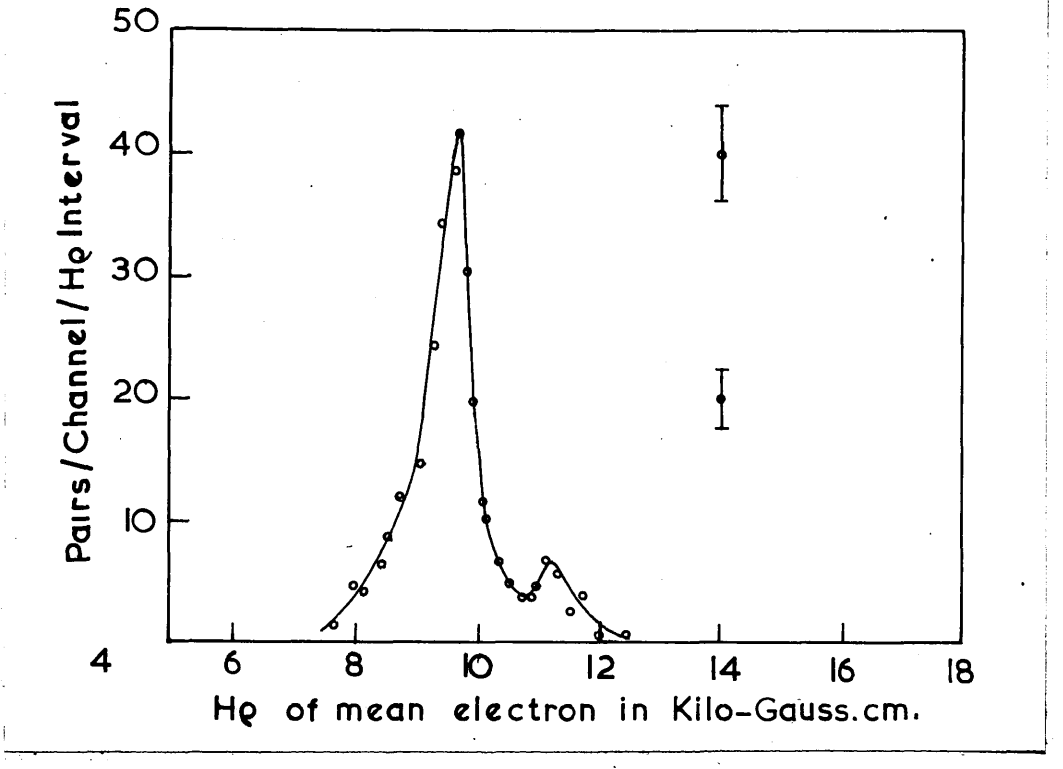

Fig.III(viii). Spectrum of Gamma-Rays from F^{19}+p at 340 kv.

Part IV. Experimental Measurements on Nuclear Reactions.

IV.1. The Reaction $Li^7 + p$.

The capture of protons by Li^7 results in the formation of the compound nucleus Be^8. The excited Be^8 nucleus can then decay by the emission of two alpha-particles or by the emission of gamma-radiation to the ground state or to lower excited states of Be^8. An energy level diagram which illustrates these processes is shown in Fig.IV (1). If the excited Be^8 nucleus is formed in a state having angular momentum and parity values such that the emission of two alpha-particles is allowed, then this process will take place, since the life time for alpha-emission of such high energy will be many orders of magnitude shorter than that for the emission of gamma quanta. However if, for example, an excited state of Be^8 is formed with an odd number of units of angular momentum, so that alpha-particle emission is completely forbidden, then the state can only decay by the emission of gamma-radiation. The re-emission of a proton is, of course, always allowed, but this will simply be observed as elastic or inelastic scattering. The emission of gamma-radiation with energy of the order of 17 MeV from the bombardment of Li^7 with protons has been observed and measured by a number of workers. This radiation has been found to show a strong resonant excitation at a proton energy of 440 kev, the width of the resonance being about 11 kev. This radiation is assumed

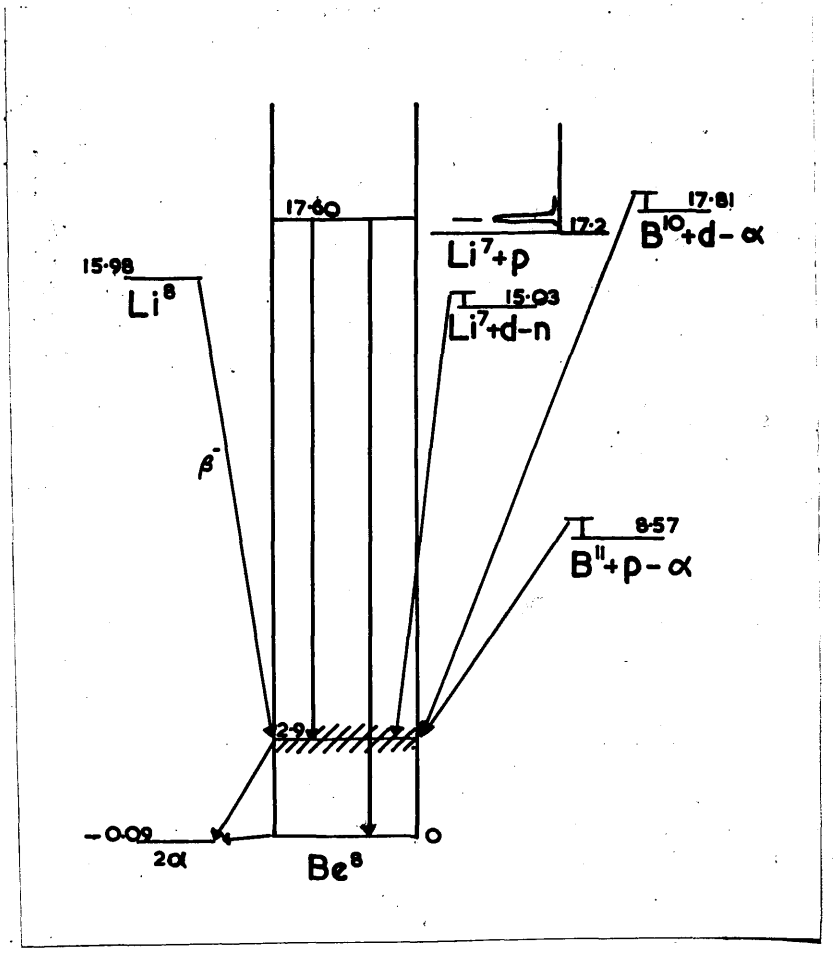

Fig.IV(i). Energy Level Diagram for Be^8.

to come from a level in Be^{8} at about 17 Mev above the ground state, which has angular momentum and parity values which forbid the emission of two alpha-particles. Early measurements of the gamma-ray spectrum (Delsasso et al 1937) showed a strong line at about 17 MeV and indicated the presence of radiation in the region of 14 MeV, but the resolution of the methods used were not sufficient to definitely establish the presence of this lower energy radiation. However, in 1948 Walker and McDaniel made a precision measurement with their newly-developed pair spectrometer and established that the radiation consisted of a sharp line at 17.6 MeV and a broad line centred at 14.8 Mev with an energy width of about 2.1 Mev. The most reasonable assumption for the presence of the 14 MeV radiation is that it is due to a transition to a broad level in Be^{8} at about 2.8 MeV above the ground state. The presence of such a state had already been suggested by the measurements of Dee and Gilbert (1936) on the reaction $B^{11}(p,\alpha)Be^{8}$. This level must decay either by the emission of two alpha-particles or by the emission of a gamma-ray. The width of the level suggests very strongly that the former process takes place. The emission of alpha particles of the order of 1.5 Mev was searched for by Rumbaugh et al (1938) following the gamma-ray measurements of Delsasso et al (1937). However, these workers used the range method of measurement and the presence of the scattered

protons, whose maximum range is almost equal to that of 1.5 Mev alpha-particles, prevented observation of the alpha-particles.

After the publication of the results of Walker and McDaniel we decided to search for these alpha-particles with the magnetic spectrometer described in section III (1). Preliminary measurements were made with a target of normal lithium but the presence of the intense group of alpha-particles from the reaction $Li^6(p,\alpha)He^3$ prevented observation of the particles from Li^7. A separated isotopic target of Li^7 was therefore obtained from A.E.R.E. Harwell. With this target alpha-particles were observed with an energy of the order of 1.5 Mev which showed a resonant excitation very similar to that for the gamma-rays. The final results are shown in Fig. IV (ii) and Fig. IV (iii). These measurements were made with a lithium hydroxide target of thickness equivalent to about 15 kev for protons of 500 kev. Fig.IV (ii) shows the excitation curve of the alpha particles and the gamma-rays as a function of proton energy. For this measurement the magnet current of the spectrometer was set to the value corresponding to the maximum of the alpha-particle spectrum. It will be seen that the excitation curve of the alpha-particles is almost identical in shape with that of the gamma-rays, providing strong confirmation that the same highly excited level in Be^8 is involved in both processes. The spectrum of the

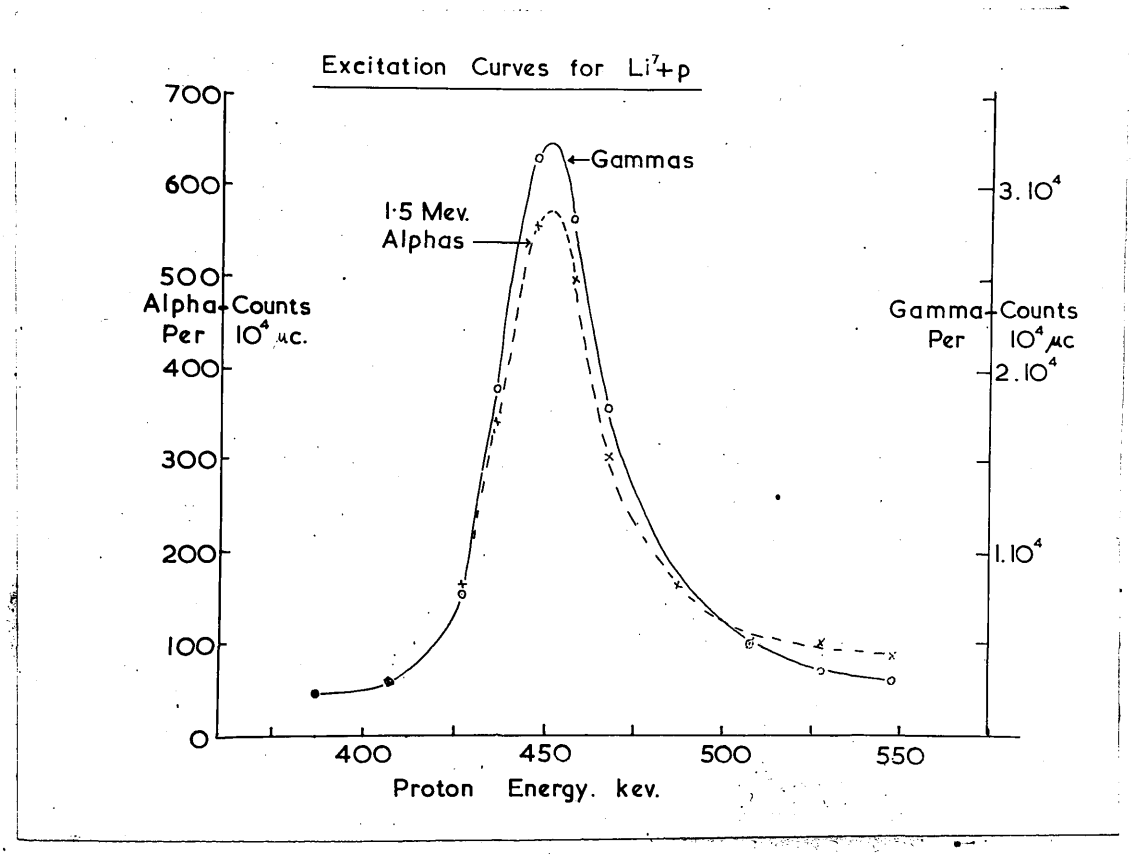
Excitation Curves for Li^7+p
700
600
500
400
300
200
100
0
Alpha-Counts Per 10^4 μc.
Gammas
1·5 Mev. Alphas
3.10^4
2.10^4
1.10^4
Gamma-Counts Per 10^4 μc
400
450
500
550
Proton Energy. kev.

Fig.IV(ii).

alpha-particles, taken at a proton energy corresponding to the maximum of the excitation curve, is shown in Fig. IV (iii). It will be seen that the spectrum shows a broad group with a maximum at an energy of 1.5 Mev and an experimental width at half amplitude of 1.2 Mev. The energy width after allowance has been made for the finite resolution of the spectrometer is 1.05 Mev.

In order to calculate the position and width of the energy level in Be^8 from this data it is necessary to make allowance for the momentum of the incoming proton and of the outgoing 14.8 Mev gamma ray. The effect of the momentum recoil due to the gamma ray is negligible on the position of the maximum energy but has an appreciable effect on the energy width. If we assume that the angular distribution of the gamma-ray is isotropic (Devons and Hine 1949) then we can calculate that it would contribute an energy width of about 400 keV to a homogeneous group of alpha-particles of the energy observed in this experiment. If we call this width γ and the true width of the Be^8 level $2\Gamma_0$, then the observed width Γ of the spectrum of single alpha-particles should be given by:

$$\Gamma^2 = \Gamma_0^2 + \gamma^2 \qquad (1)$$

Taking the observed value of Γ to be 1.05 Mev we obtain a value of 0.97 Mev for Γ_0 and hence a value of 1.94 Mev for $2\Gamma_0$, the true width of the Be^8 level. This is in good

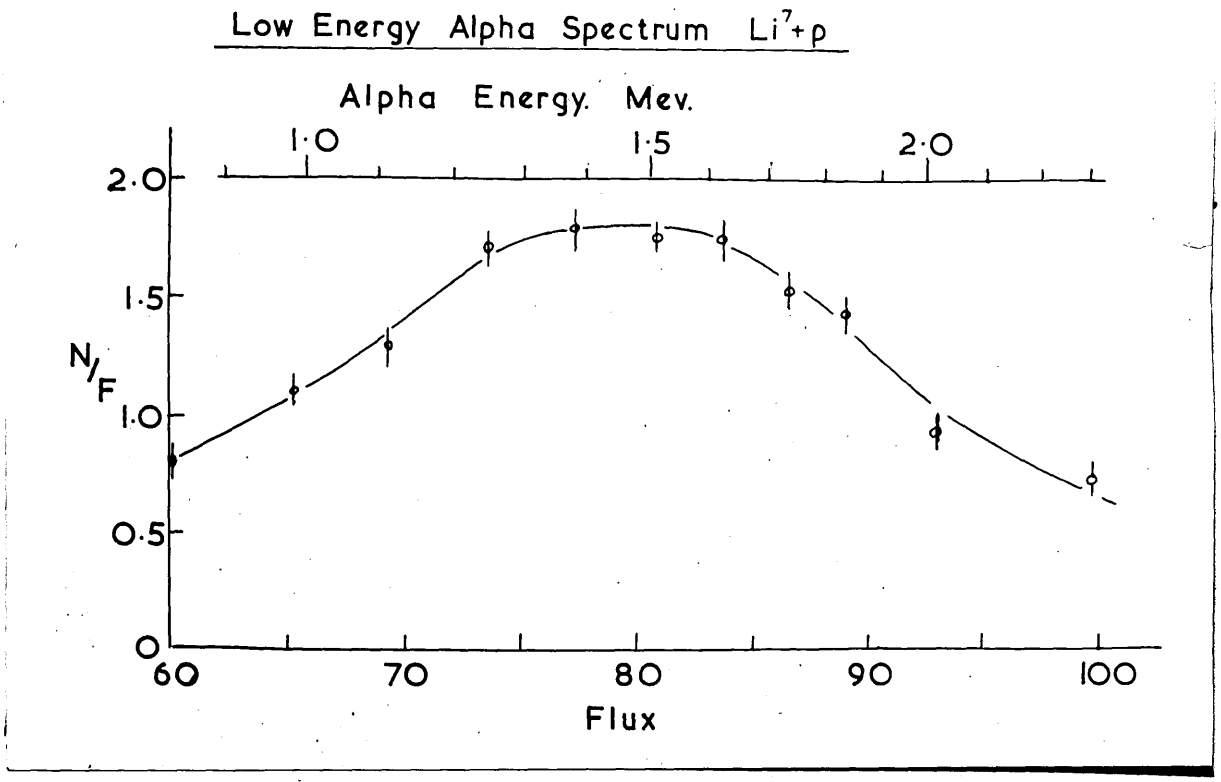
Low Energy Alpha Spectrum Li^7+p
Alpha Energy. Mev.
1·0
1·5
2·0
2·0
1·5
N/F
1·0
0·5
0
60
70
80
90
100
Flux

Fig.IV(iii).

agreement with the value of 2.1 Mev obtained by Walker and MacDaniel (1948) from the gamma-rays. From the energy of 1.5 Mev for the maximum of the group and the proton bombarding energy of 450 kev we calculate the position of the centre of the level in Be^8 to be 2.7 Mev above the state of two free alpha-particles. The best value for the energy release in the disintegration of the ground state of Be^8 into two alpha-particles is 0.09 Mev (Tollestrup et al 1949). Taking this value, we obtain an energy of 2.6 Mev for the position of this level above the ground state of Be^8, which is in reasonable agreement with the value of 2.8 Mev found by Walker and MacDaniel.

A similar investigation of this reaction has been made by Burcham and Freeman (1950) and their results are in satisfactory agreement with those presented here.

* * * * * * *

IV. 2. The Reactions B^{10} + d and B^{11} + d.

(a) The Gamma-Rays and their assignment.

The reactions induced in the two isotopes of boron by deuteron bombardment have been studied by a variety of methods and have yielded a considerable amount of information on the energy levels of the various residual nuclei involved, namely Be^{8}, Be^{9}, B^{11}, B^{12}, C^{11} and C^{12}. The gamma-ray spectrum from the bombardment of natural boron, which consists of 80% B^{11} and 20% B^{10}, has been studied by Gaerttner et al (1939) and Halpern and Crane (1939) by the cloud chamber technique discussed in section I.5. However, because of the complication of the spectrum and the comparitively poor resolution and statistical accuracy inherent in the experimental method, it was difficult to assign the observed gamma rays to particular reactions with any degree of certainty. It was therefore decided to investigate these gamma-rays with the spectrometer described in section III 2. and to use separated isotopic targets of B^{10} and B^{11} to assist in the interpretation of the results.

Measurements were first made with a target of natural boron in order to obtain a direct comparison with the earlier work. The target was prepared by making a paste of finely powdered amorphous boron in alcohol and allowing it to evaporate on a brass plate. The target was

bombarded with 600 keV deuterons in the manner described in Section III 2. and the measured gamma-ray spectrum is shown in Fig.IV (iv).At the time of this measurement the spectrometer had not been fitted with the baffles mentioned in Section III 2. and the background coincidence rate due to neutrons was of the same order of magnitude as that due to pairs produced by gamma-rays in the foil. This background was subtracted to obtain the true spectrum shown in Fig.IV (iv), but, as a result, the statistical errors were rather large.

A target of B^{10}, prepared in the Harwell electromagnetic separator, was then bombarded with 600 keV deuterons and the measured gamma ray spectrum is shown in Fig.IV (v). The background was considerably smaller on this run, partly because of the very much smaller neutron flux from the $B^{10}(d,n)C^{11}$ reaction as compared with that from $B^{11}(d,n)C^{12}$, and partly because of the baffles which had been fitted to the spectrometer. The gamma-ray yield was also greater because of the use of an isotopic target. The statistical accuracy was, therefore, very much better on this run than on the previous one.

A third run was made with a target of separated B^{11} under similar conditions and the gamma-ray spectrum is shown in Fig.IV (vi). The background on this run was of the order of one third of the true coincidence rate at the peak of the spectrum and has been subtracted to give the

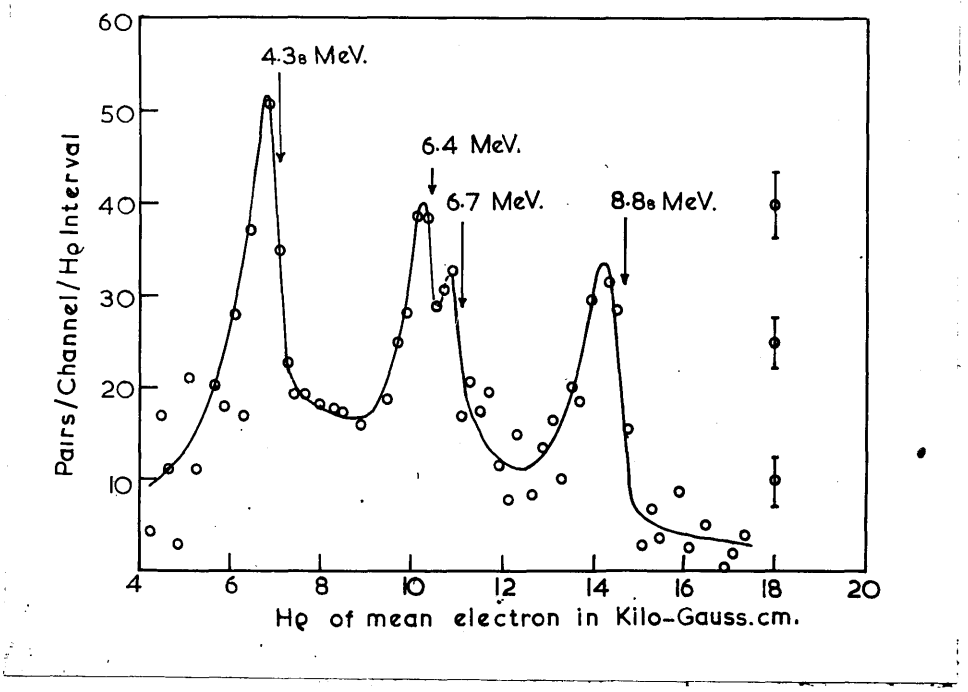

Fig.IV(iv). Gamma-Rays from B+d at 600 kv.

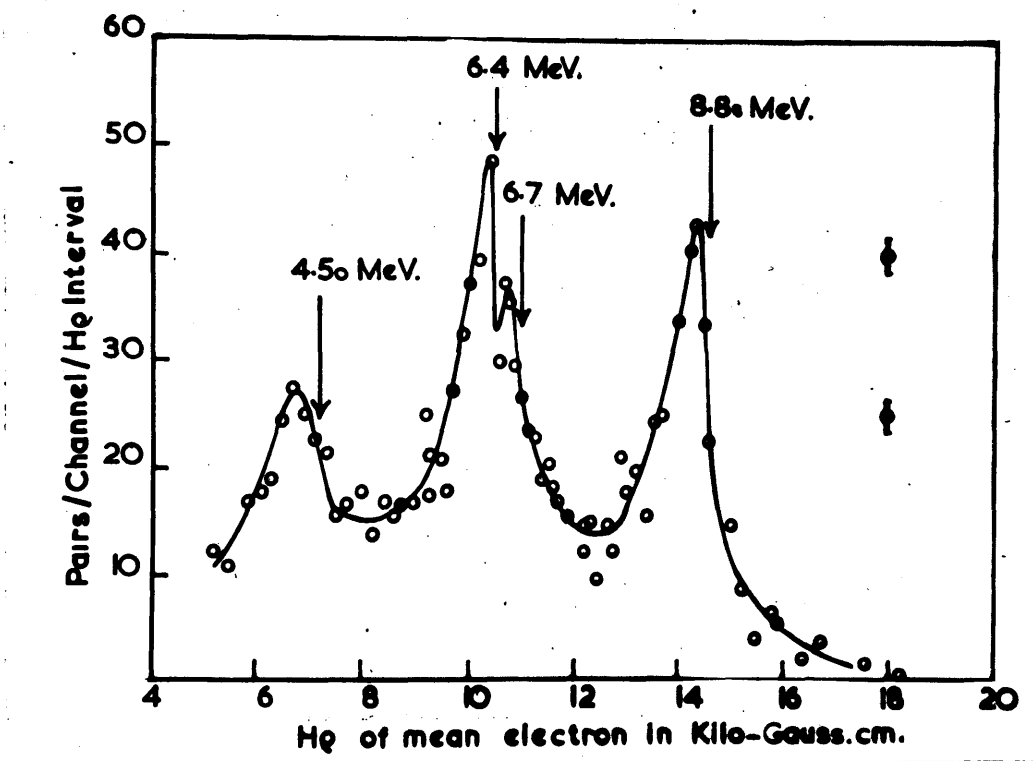

Fig.IV(v). Gamma-Rays from B^{10}+d at 600 kv.

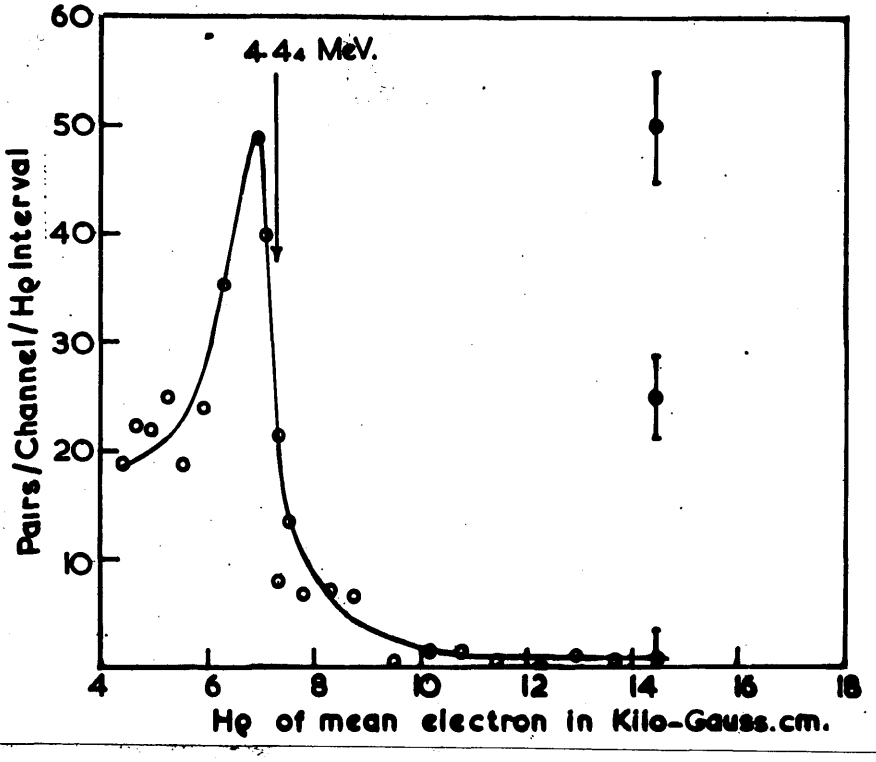

Fig.IV(vi). Gamma-Rays from B^{11} +d at 600 kv.

spectrum shown.

The results of these three runs are summarised in Table I, together with the measurements of previous workers on the same reaction. It will be seen that the majority of the high energy gamma-rays from B + d reactions are due to the B^{10} isotope and that B^{11} + d does not produce any gamma rays of energy greater than 4.44 MeV. The spectrum from B^{10} + d is clearly complex in the region between 6 and 7 MeV and is not completely resolved. However, both the B + d and B^{10} + d runs indicate two gamma-rays of the same order of intensity at 6.4 and 6.7 MeV. There is also a pronounced 'tail' on the high energy side of these peaks which suggests the presence of a gamma-ray of smaller intensity at about 7 MeV.

We can now consider the interpretation of these results. In the case of B^{10} + d, three reactions are energetically possible as shown in the energy level diagram of Fig. IV (vii). These are: $B^{10}(d,p)B^{11}$, Q = 9.24 MeV; $B^{10}(d,\alpha)Be^{8}$, Q = 17.8 MeV; and $B^{10}(d,n)C^{11}$, Q = 6.53 MeV.

The reaction $B^{10}(d,p)B^{11}$ leads to a number of excited states in B^{11}. The most precise measurements of the energies of these proton groups have been made by Buechner and his co-workers using 1.5 MeV deuterons, and his results are shown in Table II, which are taken from the recent review by Hornyak et al (1950). These results

TABLE I.

SUMMARY OF GAMMA-RAY MEASUREMENTS.

Reaction.	Present Work.		Gaerttner et al. 1939.		Halpern and Crane. 1939.	
	E_γ Mev	Relative Intensity.	E_γ Mev	Relative Intensity.	E_γ Mev.	Relative Intensity.
B + d	8.88 ± .06	1	9.1 ± .4	1	8.6	1
	6.7 ± .15	0.8	6.9 ± .4	3	6.0	2
	6.4 ± .15	0.9				
	4.38 ± .05	2.9	4.4 ± .3	10	4.2	6
B^{10} + d	8.88 ± .06	1				
	6.7 ± .15	0.8				
	6.4 ± .15	1.0				
	4.50 ± .05	0.9				
B^{11} + d	4.44 ± .05					
Al^{27} + p	12.12 ± .1	1				
	10.46 ± .07	7.5				
	7.62 ± .1	3.5				

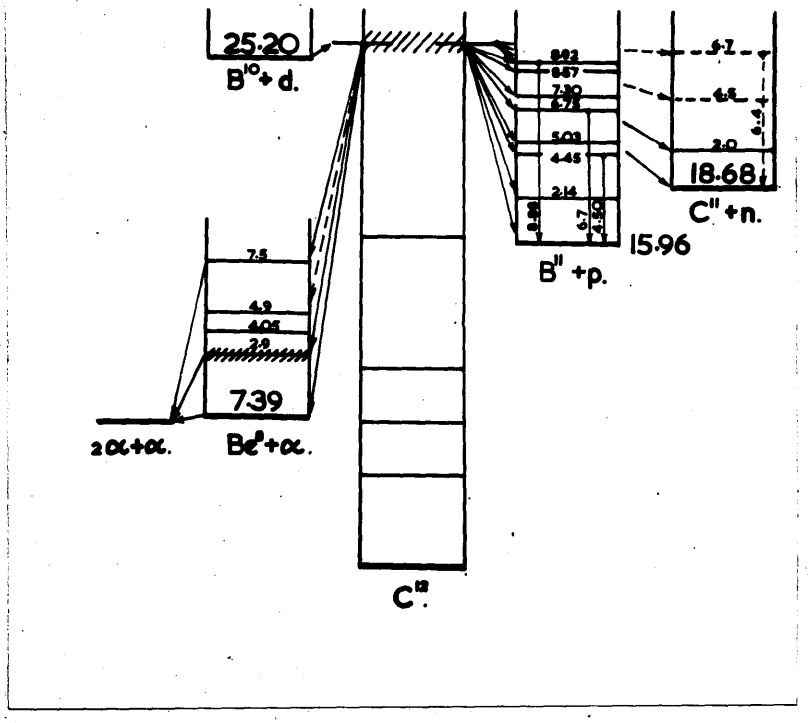

Fig.IV(vii). Energy Level Diagram C^{12}.

TABLE II.

ENERGY LEVELS OF B^{11} FROM THE B^{10} (d,p) B^{11} REACTION.

PROTON MEASUREMENTS			GAMMA RAYS	
Buechner 1950.	Present Work.		Present Work.	
E(level) Mev.	E(level) Mev.	Relative Intensity.	E_γ Mev.	Relative Intensity
0				
2.141				
4.457	4.50	1.9	4.50	0.9
5.033	5.01	0.3		
			6.4	1.0
6.752	6.72	2.1	6.7	0.8
6.802				
7.297	7.26	0.5		
8.565	8.51	0.1		
8.921	8.93	1.0	8.88	1

were not available at the time at which the present measurements were made. We also include in Table II the results of measurements on these proton groups which were made with 600 keV deuterons and will be described later in this section. It will be seen that the energies of the measured gamma rays at 4.5, 6.7 and 8.9 MeV are in good agreement with the energy levels predicted by the three most intense proton groups. The intensities of the remaining proton groups are too small to give observable gamma-rays in this work, but the proton group corresponding to the 7.3 MeV level is almost certainly responsible for the shape of the gamma-ray spectrum on the high energy side of the 6.7 MeV peak.

The $B^{10}(d,\alpha)Be^{8}$ reaction is known to lead to levels in Be^{8} at 7.5 MeV and 2.9 MeV. (Smith and Murrell 1939) but it is almost certain that these levels decay with the emission of two alpha-particles and would not, therefore, contribute to the observed gamma radiation.

The neutrons from $B^{10}(d,n)C^{11}$ have been studied by Gibson (1949) at Ed = 0.93 MeV and by Swann and Hudspeth (1949) at Ed = 1.4 MeV. The former find neutron groups corresponding to the ground state and to a 2.0 MeV excited state in C^{11}. The latter find evidence for only two levels in C^{11} at 4.5 and 6.7 MeV, but there is a possibility that the corresponding neutron groups were due to contamination. If a level exists in the region of 6.7

MeV it may be responsible for the complexity of the gamma-ray spectrum in this region. Our results would be better explained by a level at 6.4 MeV, but this is not outside the experimental error of the measurements of Swann and Hudspeth.

We may summarise these conclusions by saying that the majority of the high energy gamma rays from B^{10} + d arises from transitions between excited states of B^{11} and the ground state, following the $B^{10}(d,p)B^{11}$ reaction, but that there may be some gamma-radiation of energy about 6.4 MeV from the $B^{10}(d,n)C^{11}$ reaction.

In the case of B^{11} + d, we must consider the reactions $B^{11}(d,n)C^{12}$, Q = 13.78 MeV; $B^{11}(d,p)B^{12}$, Q = 1.06 MeV and $B^{11}(d,\alpha)Be^{9}$, Q = 8.03 MeV., as shown in the energy level diagram of Fig.IV (viii). The first reaction has been recently studied by Gibson (1949) and is found to yield neutron groups leading to excited states of C^{12} at 9.72 $\pm$ 0.15 MeV and 4.47 $\pm$ 0.10 MeV with relative intensities of 0.67 : I. The second group corresponds well with the gamma-ray energy of 4.44 $\pm$ 0.05 MeV measured in this work. However, there is no evidence of a gamma-ray at 9.7 MeV. This is not unexpected, since this level can decay by the emission of an alpha-particle to the ground state of Be^{8}, with an energy release of 2.3 MeV and one would expect the lifetime for this process to be very much shorter than that for emission of a gamma-ray. The possibility of a cascade

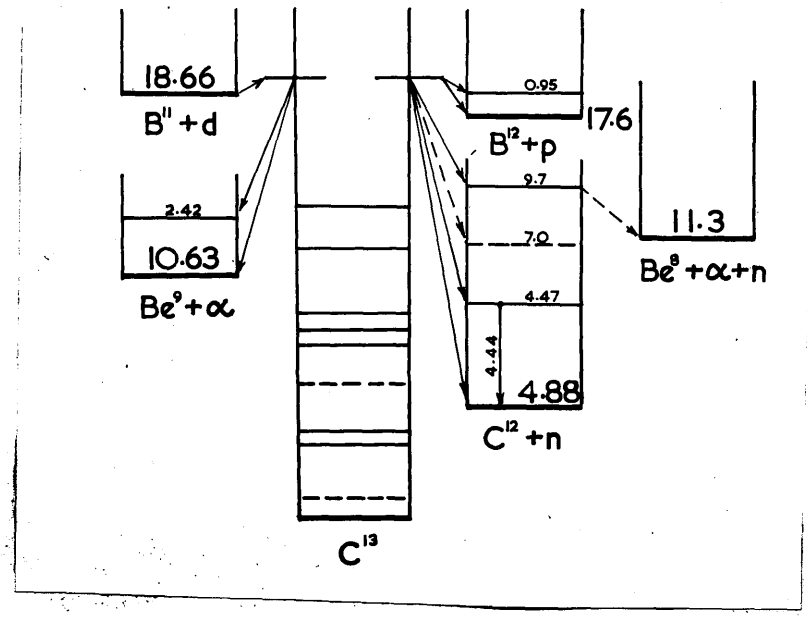

Fig.IV(viii). Energy Level Diagram C^{13}.

transition through the 4.5 MeV level seems to be ruled out by the fact that a gamma ray of energy 5.2 MeV is not observed.

The reaction $B^{11}(d,p)B^{12}$ need not be considered because of its low Q-value. The reaction $B^{11}(d,\alpha)Be^{9}$ has recently been studied by Van Patter and Buechner (Hornyak et al 1950) and has been found to lead only to the 2.4 MeV level in Be^{9}. It would not, therefore, be expected to contribute to the gamma radiation observed in this work.

We may summarise these conclusions by saying that the high energy gamma-radiation from B^{11} + d arises from the transition from the 4.47 MeV level in C^{12} to the ground state and that the 9.7 MeV level in C^{12} decays by alpha-particle emission to Be^{8}.

(b) <u>The Proton Groups.</u>

We have already noted that the proton groups from the $B^{10}(d,p)B^{11}$ reaction have recently been measured by Buechner et al with a high degree of precision. However, his measurements were made at a deuteron energy of 1.2 MeV and no information was given on the relative intensities of the various groups. In order to assist in the interpretation of the gamma-ray measurements we wished to know the relative intensity of the proton groups at a deuteron energy of 600 keV. We therefore made an investigation of these proton groups with the spectrometer

described in Section III.I.

A target of separated B^{10} was bombarded with 600 keV deuterons and the disintegration protons were observed in the proportional counter of the spectrometer. The lowest energy proton group which was to be observed had an energy of only 700 keV and therefore had a considerably smaller $H\rho$ value than that of the highest energy scattered deuterons. However, the range of a 700 kev proton is greater than that of a 600 keV deuteron and hence it was possible to prevent the deuterons from entering the counter by means of a foil of suitable thickness. From the curves of Fig.I (iii) we find that the range of a 700 keV proton is 1.23 cms. of air and that of a 600 keV deuteron is 0.92 cms.

The first measurements were made with a foil of 0.7 cms. air equivalent thickness. The effective stopping power of the counter window itself and the counter gas in the initial insensitive volume of the counter was about 0.3 cms, so that the total effective absorber thickness was about 1.0 cms. The spectrum obtained under these conditions is shown in Fig.IV (ix) (a). It will be seen that groups are found at fluxmeter readings of 56, 68.5, 82.5 and 100, and there is no sign of the presence of scattered deuterons. The window thickness was then reduced, so that the total absorber thickness was of the order of 0.7 cms, and the spectrum shown in Fig.IV (ix)(b) was taken. It will be seen that a very intense broad

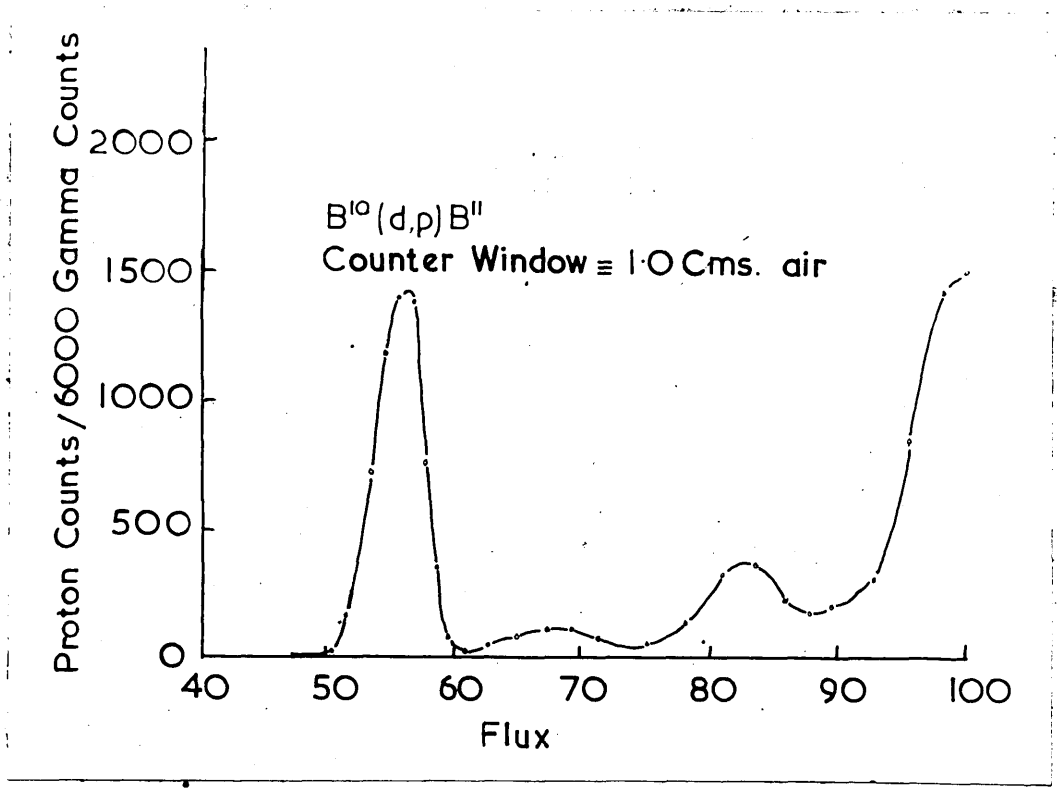

Fig.IV(ix)(a). Proton Groups from $B^{10}(d,p)B^{11}$.

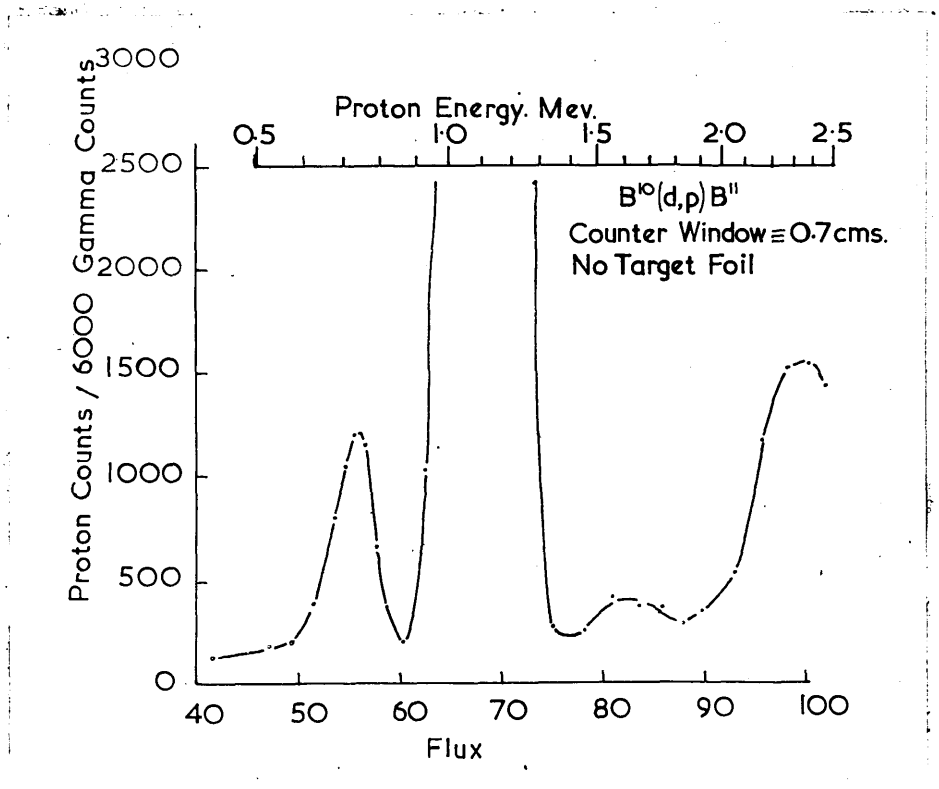

Fig.IV(ix)(b).

group appears, which is due to eleastically scattered deuterons. However, the lowest energy proton group is still clearly separated. This is because the deuterons which have the same $H\rho$ as this 730 keV proton group have an energy of only 365 keV and are therefore completely stopped by the foil.

Before discussing these results we shall describe the measurement of the proton groups of higher energy. The upper energy limit imposed by the maximum field available from the spectrometer magnet is about 2.3 MeV. In order to observe groups of higher energy, aluminium foils of known thickness were placed over the slit at the open end of the tube A in Fig.III (iii). Thus the disintegration protons were slowed down immediately after leaving the target and, by the choice of suitable foils, any desired proton group could be brought within the range of the spectrometer. The thickness of the foils was measured by careful measurement of their mass and area. The energy of the protons leaving the target was then calculated from their measured energy after traversing the foil by means of the published range-energy curves. The proton spectra obtained in this way with foils of thickness 6.3, 12.6, 32.0 and 38.3 Mg/cms^2 are shown in Figs. IV (ix)(c), (d), (e) and (f) respectively. For convenience in reading these graphs a scale is marked along the top of each graph giving the calculated energy

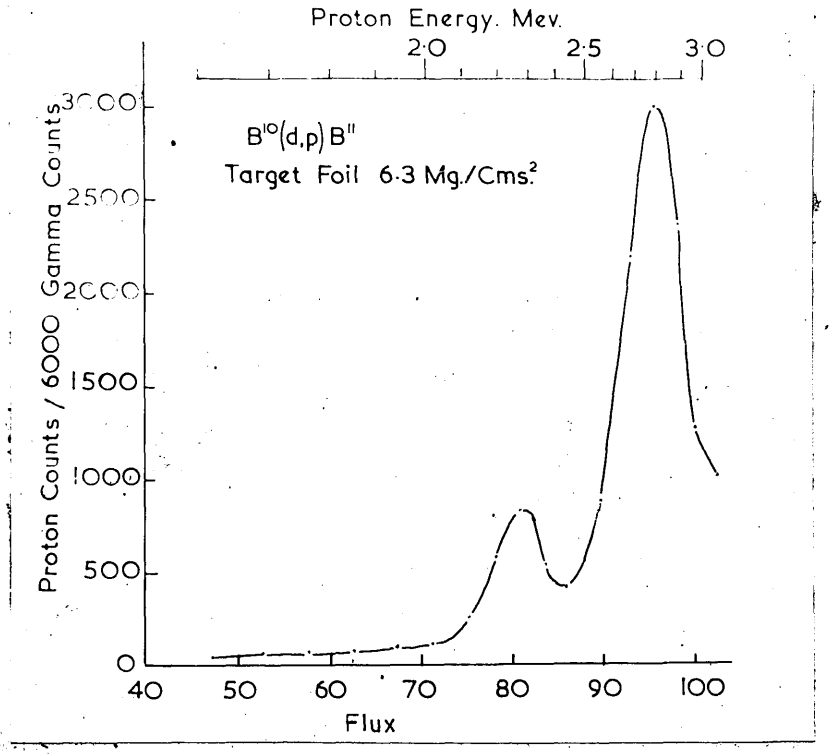

Fig.IV(ix)(c).

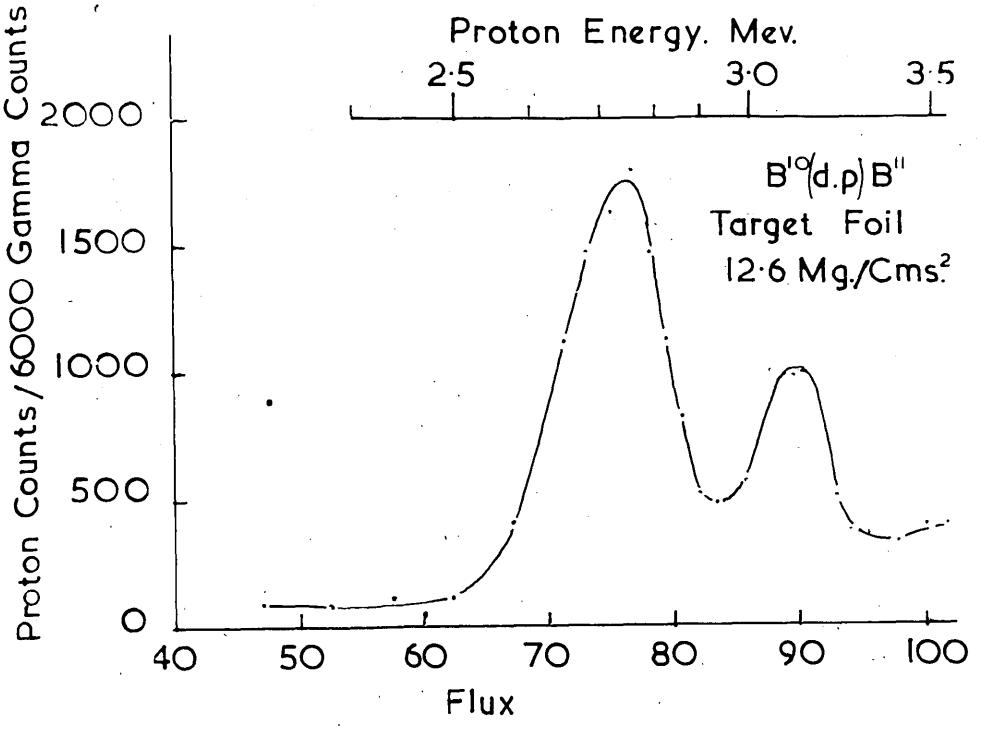

Fig.IV(ix)(d).

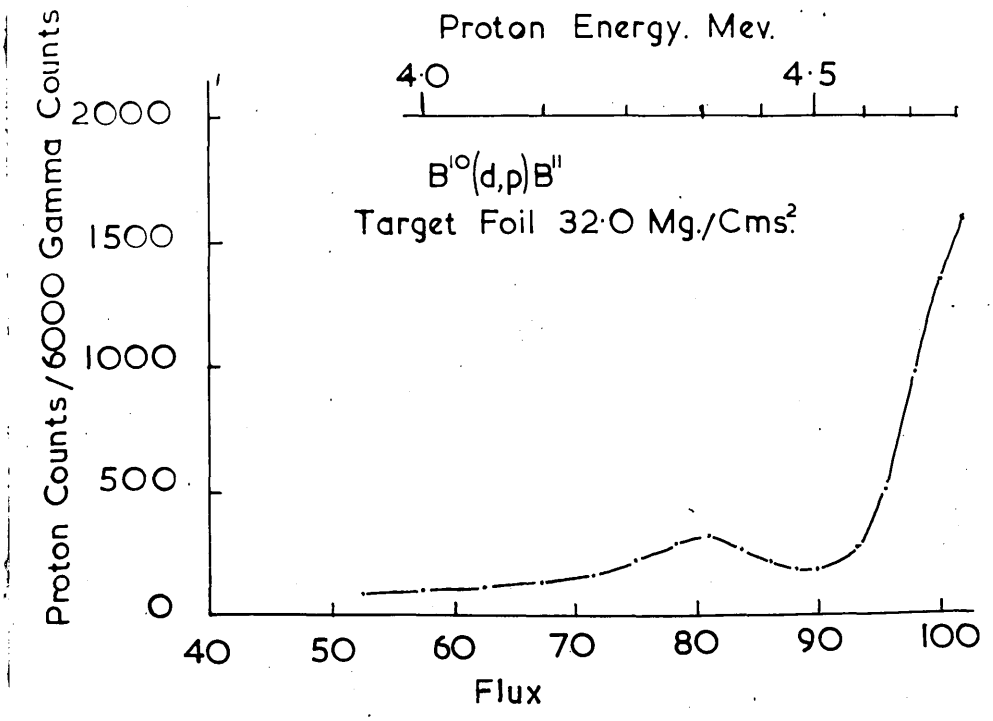

Fig.IV(ix)(e).

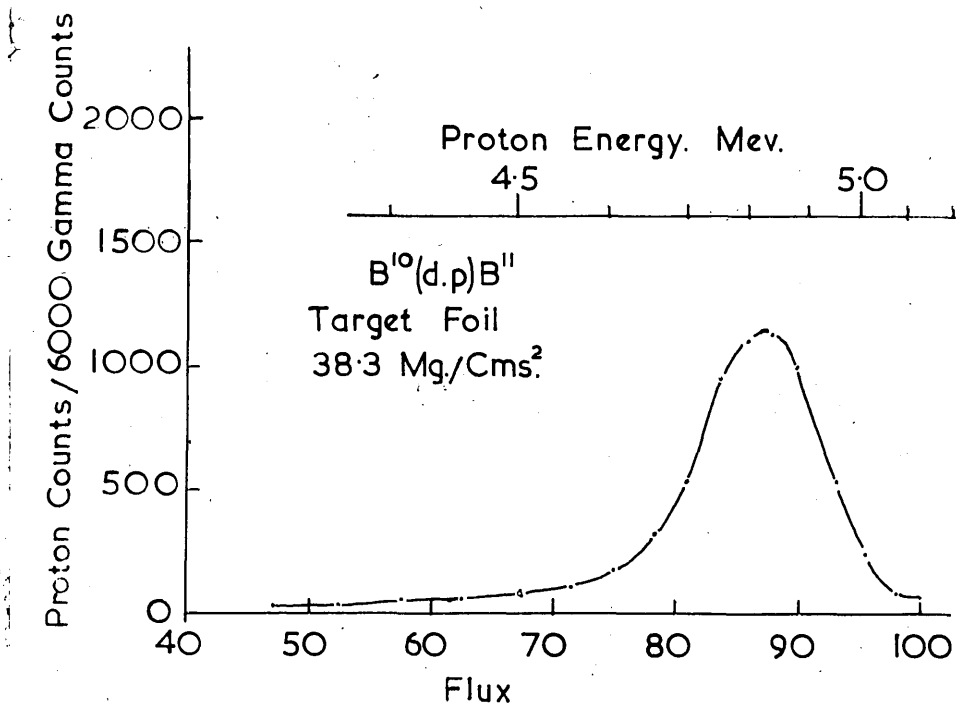

Fig.IV(ix)(f).

of the protons leaving the target. In all these measurements a Geiger counter was used to monitor the gamma-ray output and the ordinates of the graphs are the proton counts for a fixed number of counts in the monitor counter. All the observed proton groups are due to the $B^{10}(d,p)B^{11}$ reaction with the exception of the group at 1.6 MeV, which is due to the $O^{16}(d,p)O^{17}$ reaction, and the group at 3.1 MeV, which is due to the $d(d,p)H^3$ reaction. The results are summarised in Table III, which illustrates the method of calculating the proton energy E_o from the measured energy E and the foil thickness. The Q values are calculated from the formula (i) of section I.5. For comparison, the Q values obtained by Buechner et al (1950) are also listed in Table III. The relative intensities of the various groups are also listed in Table III. These relative intensities were obtained in the usual way by measuring the area under each peak and dividing it by the flux F at the peak, to allow for the fact that the resolution width is proportional to F. It must be noted that these relative intensities refer to protons which leave the target at 90^o to the direction of the incident beam and cannot be precisely related to the total yields without a knowledge of the angular distributions, which is not available at present. However, they give the order of magnitude of the relative yields and we have seen in the preceding part of this section that they are in

TABLE III.

PROTON GROUPS FROM B^{10} (d,p) B^{11}.

Line	E Mev	Range Mg/cms^2	Foil Mg/cms^2	Total R. Mg/cms^2	E_o Mev	Q Mev	Rel. Int.	Buechner Q Mev.
1 (a)	0.730		0		0.730	0.304	1.0	0.311
2 (a)	1.09		0		1.09	0.720	0.1	0.667
3 (a)	1.58		0		1.58			
1 (b)	0.728		0		0.728	0.300	0.9	0.311
3 (b)	1.58		0		1.58			
4 (c)	1.52	6.9	6.3	13.2	2.26	1.97	0.5	1.935
5 (c)	2.12	11.9	6.3	18.2	2.75	2.51	2.3	2.480
5 (d)	1.34	5.6	12.6	18.2	2.75	2.51	2.0	2.480
6 (d)	1.87	9.6	12.6	22.2	3.13			
7 (e)	1.48	7.3	32.0	39.3	4.32	4.22	0.3	4.199
8 (f)	1.75	8.6	38.3	46.9	4.79	4.73	1.9	4.775

qualitative agreement with the relative intensities of the corresponding gamma rays from the de-excitation of the excited states in B^{11}.

* * * * * * *

IV. 3. The Reaction $Al^{27} + p$.

(a) The Gamma-rays from $Al^{27}(p,\gamma)Si^{28}$.

The excitation curve of the gamma-rays from the proton bombardment of aluminium has been studied by a number of workers, but very little was known of the energy spectrum of the gamma-rays prior to the present work. Plain et al (1940) made an estimate of the mean energy of the gamma-rays by the method of coincidence absorption of the secondary electrons from an aluminium converter and showed it to be in the region of 7 MeV, but this method is known to be rather unsatisfactory if the gamma-ray spectrum is complex. The Q-value for the reaction $Al^{27}(p,\gamma)Si^{28}$ was known to be in the region of 12 MeV from the mass values, so it appeared certain that the gamma-ray spectrum must, in fact, be complex. The only other possible reaction in this case is $Al^{27}(p,\alpha)Mg^{24}$, but the Q-value of this reaction is only 1.6 MeV and hence it cannot be responsible for the production of hard gamma-rays.

The principle difficulty in the measurement of this gamma-ray spectrum is that the yield is rather small at low proton energies because of the effect of the potential barrier. The excitation curve shows a number of sharp resonances, whose position and yield have been accurately measured by Brostrom et al (1947). We shall discuss these resonances in more detail in the second part of this section.

However we may note here that even if a thick target is used with a bombarding proton energy of 750 keV, the total yield due to all the resonances below this energy is only about 1/15 of that produced by the 340 keV resonance of $F^{19}(p,\alpha,\gamma)O^{16}$. This intensity was sufficient to allow a measurement of the gamma-ray spectrum to be made with the pair spectrometer, but it was not practical to measure the spectrum from separate resonances.

The spectrum obtained from a thick aluminium target bombarded with 750 keV protons is shown in Fig.IV(X). This spectrum was obtained from twenty separate runs, each of duration of about twenty minutes with a proton beam current of about 150μa. It will be seen that three gamma-ray peaks of energies 12.12 $\pm$ 0.1 MeV, 10.46 $\pm$ .07 MeV and 7.62 $\pm$ 0.1 MeV are clearly resolved, but the background both above and below the 7.6 MeV peak suggests the presence of other weak gamma-rays. The relative intensities of the three main peaks are in the ratio of 1 : 7.5 : 3.5.

The interpretation of these gamma-rays can be discussed in terms of the energy level diagram of Si^{29} shown in Fig.IV$_{\Lambda}^{(XI)}$. The most energetic gamma-ray is presumed to correspond to the direct transition to the ground state of Si^{28}. From the results of Brostrom et al (1948) on the relative intensities of the resonances below our bombarding energy of 750 keV we assume the effective mean

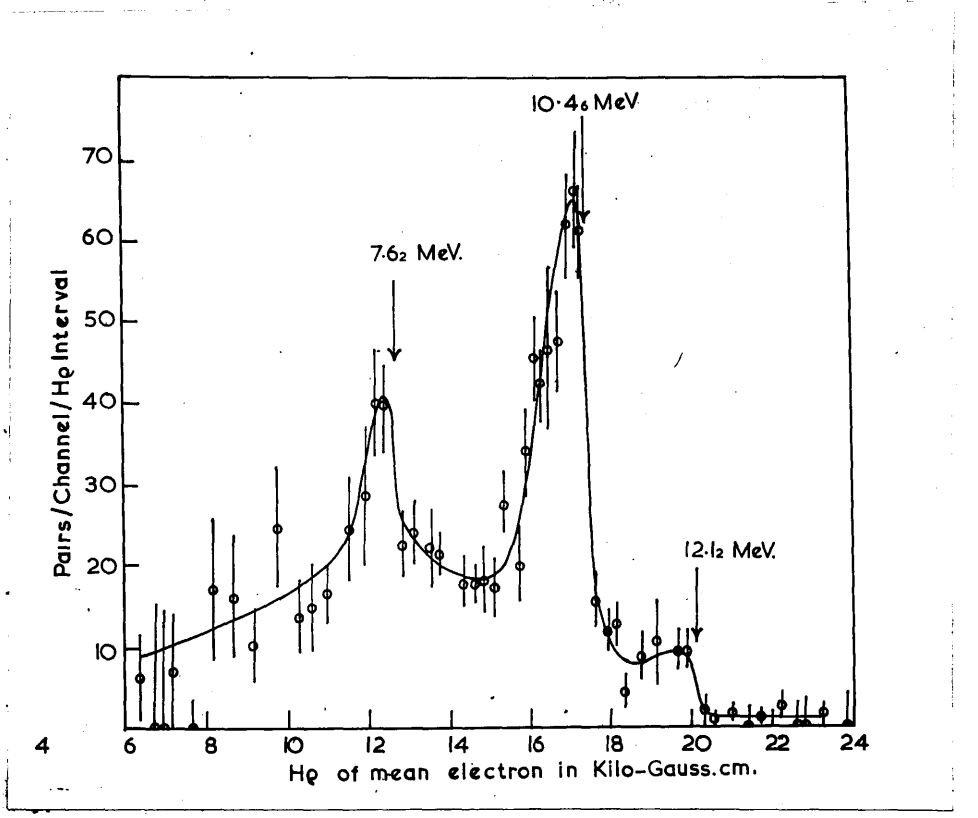

Fig. IV(x). Spectrum of Gamma-Rays from $Al^{27}(p,\gamma)Si^{28}$.

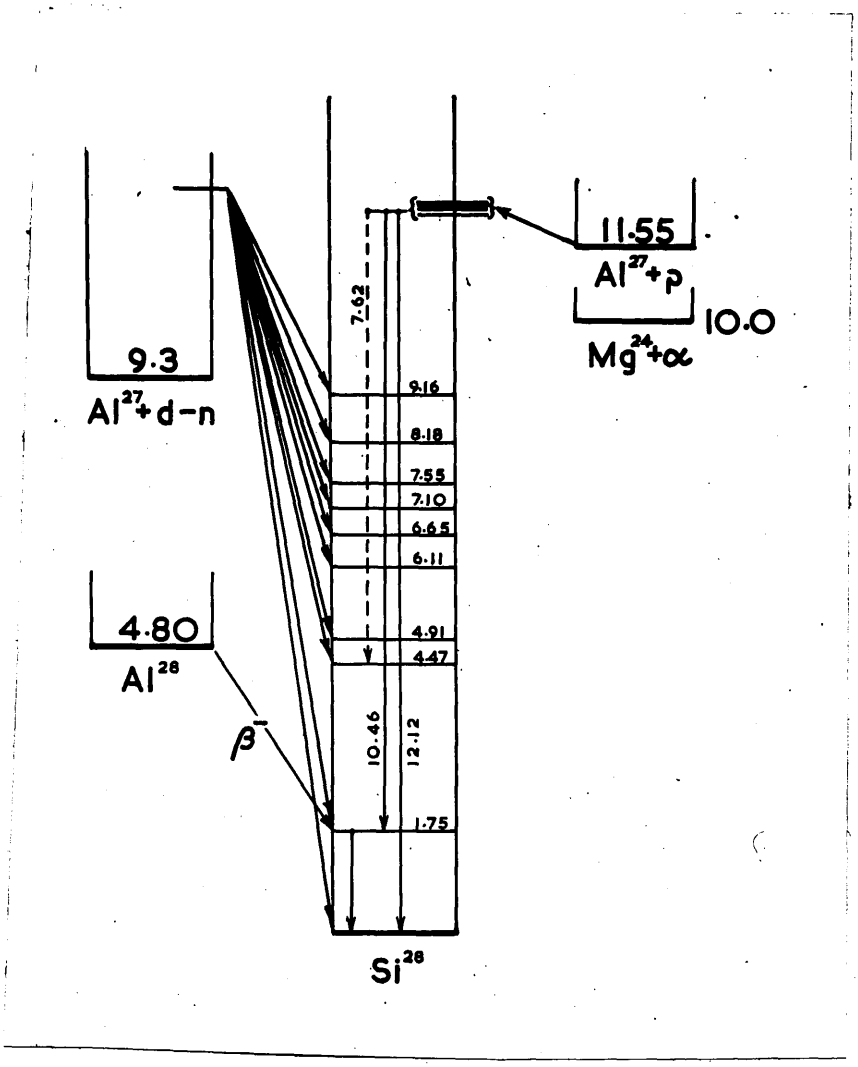

Fig.IV(xi). Energy Level Diagram Si^{28}.

bombarding energy to be 630 keV, which corresponds to an additional excitation energy of 610 keV in centre of mass co-ordinates. We thus obtain a value of 11.51 ± 0.1 MeV for the Q-value of the ground state transition. This Q-value may be calculated by two other methods. First, the reactions $Al^{27}(d,p)Al^{28}$, Q = 5.45 ± 0.05 MeV (Pollard et al 1949) and $Al^{28}(\beta^-)Si^{28}$, Q = 4.80 ± .05 MeV, (Benes et al 1948) predict a Q-value of 11.70 ± 0.1 MeV for $Al^{27}(p,\gamma)Si^{28}$. Second, the reaction $Al^{27}(d,n)Si^{28}$, Q = 9.08 ± 0.2 MeV (Peck 1949) predicts a Q-value of 11.31 ± 0.2 MeV. It will be seen that there is no serious discrepancy between these three determinations and they yield a weighted mean value of 11.55 ± .07 MeV.

The gamma-ray of energy 10.46 ± .07 MeV is almost certainly due to a cascade transition which proceeds through a level in Si^{28} in the region of 1.7 MeV, since it is very unlikely that a gamma ray with an energy as low as 1.7 MeV would be emitted directly from such a highly excited state in competition with high energy gamma-rays. On this assumption our measurements give a value of 1.66 ± 0.12 MeV for this level in Si^{28}. The reaction $Al^{28}(\beta^-)Si^{28}$ proceeds via a level at 1.80 ± .05 MeV (Benes et al. 1948) and the reaction $Al^{27}(d,n)Si^{28}$ proceeds via a level which has been measured as 1.78 ± 0.13 MeV from the neutron groups (Peck 1949) and as 1.72 ± 0.08 MeV from the gamma-radiation (Allburger 1949). Thus, all the

determinations are consistent with a weighted mean value of 1.75 ± 0.04 MeV for the energy of this level in Si^{28}.

The interpretation of the gamma-ray at 7.62 Mev is less certain, but it seems probable that it is due to a cascade transition which proceeds through a level in Si^{28} at 4.50 ± 0.15 MeV. This interpretation is consistent with the level at 4.47 ± 0.13 MeV found by Peck (1949) in the $Al^{27}(d,n)Si^{28}$ reaction.

* * * * * *

(b) The Alpha-Particles from $Al^{27}(p,\alpha)Mg^{24}$.

The alpha-particles from this reaction were first observed by Freeman and Baxter (1948), who measured the Q-value to be 1.32 MeV. They used a magnetic analyser to separate the alpha-particles from the elastically scattered protons but used a range absorption method to measure the energy of the alpha-particles after they emerged from the analyser. In a later paper (Freeman, 1950) they reported a Q-value of 1.585 ± 0.015 Mev, obtained by direct measurement of the $H\rho$ value of the alpha-particles in a magnetic spectrometer. The discrepancy between the two Q-values was attributed to an error in the range-energy relation used in the earlier measurement. In their first paper Freeman and Baxter gave a rough excitation curve, which indicated a resonance at a proton energy of about 730 keV and a weaker resonance in the region of 650 keV. The Cambridge H.T. set, with which this work was performed, is not very suitable for excitation curve measurements because of the rather large energy spread on the proton beam due to the type of ion source. We therefore decided to undertake some measurements on this reaction with a view to obtaining a more precise excitation curve and at the same time checking the Q-value. We have already noted that the excitation curve for the reaction $Al^{27}(p,\gamma)Si^{28}$ shows a number of sharp resonances corresponding to highly excited states of Si^{28},

and it was felt to be of some interest to see whether the same levels decay by alpha-particle emission to Mg^{24} in competition with the gamma-ray emission to lower states of Si^{28}, or whether different levels are involved. These reactions are illustrated in the energy level diagram of Si^{28} shown in Fig.IV(xi).

The heavy-particle spectrometer described in section III.1. was used in this work and the alpha-particles were detected with the proportional counter. A standard Geiger counter was placed close to the target so that the gamma-rays from the reaction $Al^{27}(p,\gamma)Si^{28}$ could be observed at the same time. A thick target of ordinary commercial aluminium was used in preliminary experiments, but was found to be unsatisfactory because of the presence of particle groups due to contaminants, probably mainly of fluorine, in the aluminium. We may mention that the yield of the reaction is very small compared with that in lighter element reactions such as $F^{19}(p,\alpha)O^{16}$. The final results were obtained with thin targets prepared by evaporating spectroscopically pure aluminium in vacuum on to brass backing plates.

The excitation curves obtained for the alpha-particles and gamma-rays are shown in Fig.IV(xii). The target thickness was 10 keV for the measurements below 700 keV and was 5 keV for the measurements between 700 and 750 keV, so that the gamma-ray resonances at 728 and 733 keV could be resolved

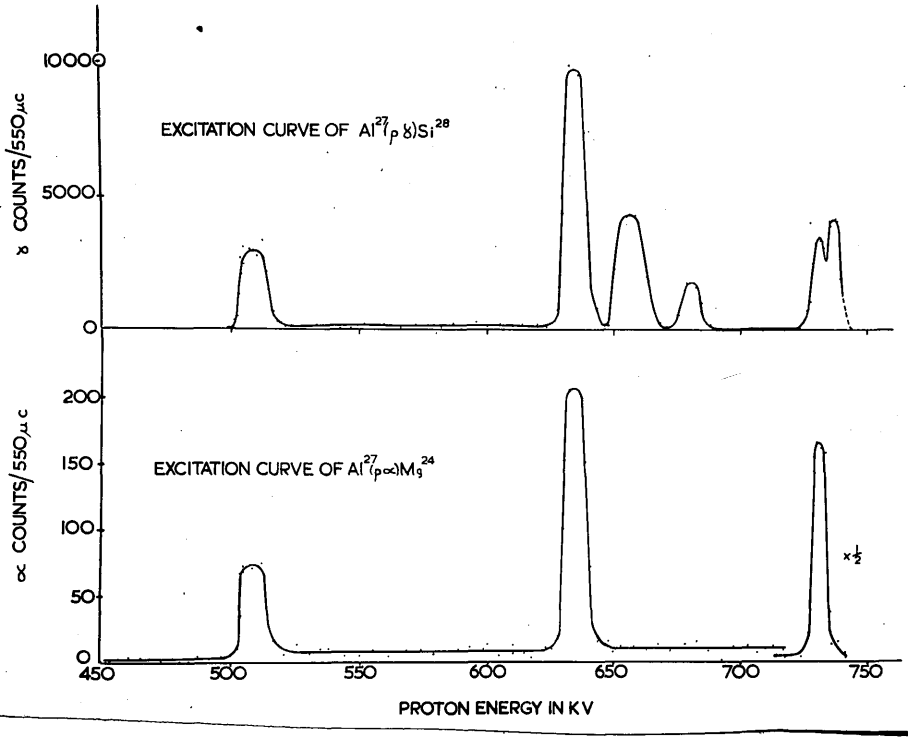

Fig.IV(xii). Excitation Curves of Alpha-Particles and Gamma-Rays from Al^{27}+p.

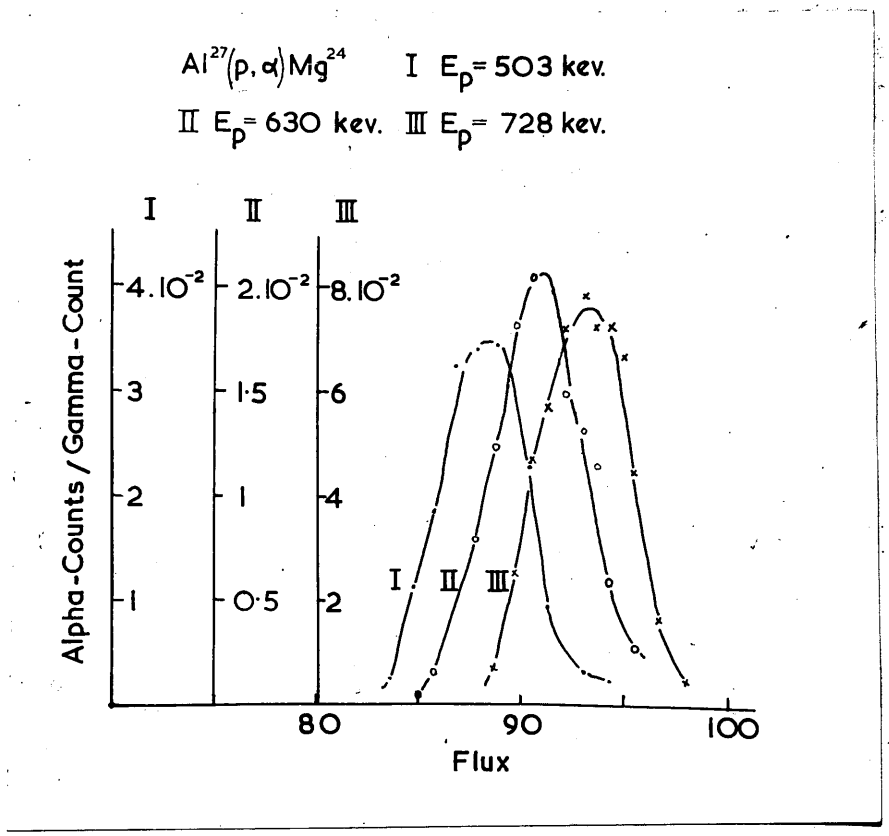

Fig.IV(xiii)Spectra of Alpha-Particles from $Al^{27}(p,\alpha)Mg^{24}$.

from each other. The widths of the peaks in the excitation curve are entirely due to the target thickness and the peaks are approximately flat-topped, as would be expected in this case. The counting rate at each peak therefore gives a measure of the 'thick target' yield of the resonance. The magnet current of the spectrometer was adjusted during the runs so that the magnetic field was always at the value corresponding to the peak of the energy spectrum at the proton bombarding energy used. The appropriate values of the magnet current had already been determined in preliminary measurements. The slope of the front edge of each peak is entirely due to the ripple and voltage fluctuations on the H.T. set, which was about 1.5 keV at the time these measurements were made. It is therefore only possible to say that the actual widths of the nuclear resonances are less than 1.5 keV.

A measurement was made of the energy spectrum of the alpha-particles at each of the three alpha-particle resonances at proton energies of 503, 630 and 728 keV. These spectra are shown in Fig.IV (xiii) . In order to reduce the effects of target deterioration, the gamma-ray counter was used as a monitor in these measurements rather than the current integrator and the ordinates of the graph in Fig.IV (xiii) are therefore the ratio of the alpha-counts to gamma-counts. From the position of the peaks the alpha-particle energies

were calculated to be 1.79, 1.89 and 1.98 MeV at the 503, 630 and 728 KeV resonances respectively. The Q-values calculated from these results are 1.62, 1.60 and 1.61 MeV. We estimate the total probable error of these measurements to be $\pm$ 1% and thus obtain a final Q value of 1.61 $\pm$ .02 MeV. This value is in reasonable agreement with the value of 1.585 $\pm$ .015 found by Freeman (1950) and the value of 1.600 $\pm$ .014 MeV calculated by Strait et al (1951) from their measurements of the Q-values of the reactions $Al^{27}(d,\alpha)Mg^{25}$ and $Mg^{24}(d,p)Mg^{25}$.

Immediately after the above measurements had been made a fluorine target was mounted in the spectrometer for calibration purposes. The purpose of these measurements was two-fold, first to check the energy calibration as described in Section III.1. and second to make an absolute intensity calibration of the alpha and gamma counters used in the aluminium experiments. The absolute yield of the 330 keV resonance in the reaction $F^{19}(p,\alpha,\gamma)O^{16}$ has been accurately measured by Chao et al (1950) to be 0.15 alpha particles per 10^7 protons and, since there is one 6.13 MeV gamma-ray in cascade with each alpha-particle, the yield of gamma-rays will be the same. The curve published by Fowler et al (1948) for the efficiency of an aluminium wall Geiger counter as a function of gamma-ray energy was used to estimate the relative efficiency of the gamma counter for the 12 MeV radiation from $Al^{27}(p,\gamma)Si^{28}$ as compared with

that for the 6.13 MeV radiation from $F^{19}(p,\alpha,\gamma)O^{16}$. It must be noted that the fact that the radiation from aluminium is complex, due to cascade transitions, it is not important because the counter efficiency is almost exactly linear with energy and hence the number of gamma counts per disintegration is independant of the mode of de-excitation to a first order. The results of these yield measurements are summarised in Table IV. The yield measurements of Brostrom et al (1947) for the gamma-rays are also included for comparison purposes. It will be seen that our yield measurements are uniformly lower than those of Brostrom et al. by a factor of about two. Part of this difference is due to the fact that we have used the value of 0.15 disintegrations per 10^7 protons for the $F^{19}(p,\alpha,\gamma)O^{16}$ reaction. (Chao et al 1950), whereas Brostrom et al., who also used this reaction for calibration, used the earlier value of 0.18 (Van Allen and Smith 1941). A further difference of about 20% may be accounted for by the slightly different assumption which they made as to the relative efficiency of their gamma counter for fluorine and aluminium radiation. However, there remains a discrepancy of about 50% for which it is difficult to account. The ratios of alpha-particle to gamma-ray yields are also given in Table IV for the various resonances. It will be seen that the three resonances at 503, 630 and 728 keV give alpha and gamma yields of the same order of magnitude,

TABLE IV.

YIELDS OF Al^{27} + p.

E_r kev.	Yields per 10^{10} protons Y_α	Y_γ	Brostrom Y_γ	$\frac{Y_\alpha}{Y_\gamma}$	$\omega\gamma_\alpha$ e.v.	$\omega\gamma_\gamma$ e.v.
503	1.2	0.95	1.7	1.27	0.14	0.11
630	3.6	3.3	7.0	1.09	0.51	0.47
652	< 0.15	1.4	2.7	< 0.11	< 0.02	0.21
677	< 0.15	0.55	1.1	< 0.28	< 0.02	0.07
728	4.8	1.15	2.5	4.20	0.75	0.18
733	< 0.35	1.4	3.5	< 0.25	< 0.05	0.22

whereas alpha-particle emission appears to be completely forbidden from the three gamma-ray resonances at 652, 677 and 733 keV. No resonances are observed which only emit alpha-particles.

We can now discuss these results on the basis of the theoretical considerations mentioned in Section I.3. We see from equation (2) of that section that if Γ_r, Γ_α and Γ_γ are the partial widths of a given energy level for the emission of a proton, alpha-particle and gamma-ray respectively, then:

$$Y_\alpha = \frac{\lambda^2 \omega}{4\pi E_r \epsilon} \frac{\Gamma_\alpha \Gamma_r}{\Gamma} \qquad (1)$$

and

$$Y_\gamma = \frac{\lambda^2 \omega}{4\pi E_r \epsilon} \frac{\Gamma_\gamma \Gamma_r}{\Gamma} \qquad (2)$$

where

$$\Gamma = \Gamma_r + \Gamma_\alpha + \Gamma_\gamma \qquad (3)$$

and Y_α and Y_γ are the alpha-particle and gamma-ray yields respectively.

For simplicity we write:

$$\gamma_\alpha = \frac{\Gamma_\alpha \Gamma_r}{\Gamma} \qquad (4)$$

and

$$\gamma_\gamma = \frac{\Gamma_\gamma \Gamma_r}{\Gamma} \qquad (5)$$

The qualities $\omega \gamma_\alpha$ and $\omega \gamma_\gamma$ may be calculated directly from the observed yields by the use of equations (1) and (2) and the results are tabulated in Table IV. For the specific

stopping power, ϵ , of aluminium we have used the values given by Parkinson et al. (1937).

It will be seen that the values so obtained for $\omega\gamma_\alpha$ and $\omega\gamma_\gamma$ lie in the range from 0.1 to 0.5 electron volts for most of the resonances for which alpha-particles or gamma-rays are actually observed. We can now consider the relative orders of magnitude to be expected for the partial widths Γ_α , Γ_r and Γ_γ . The values of Γ_α and Γ_r will be determined mainly by the appropriate barrier penetrability factors. We have estimated these factors, G, from the data given by Christy and Latter (1948) and Mattauch (Nuclear Physics Tables). For protons in the range from 400 keV to 800 keV, G is of the order of 10^{-4} to 10^{-2} for aluminium. For alpha-particles of 1.8 MeV, G is of the order of 10^{-6} . These factors are given for S-wave particles, i.e. for transitions with zero change of angular momentum. For P-wave particles ($\Delta l = 1$) the barrier penetrability factors will be lower by a factor of the order of magnitude of ten. Thus it seems certain that the barrier penetrability factors will make the proton widths larger than the alpha-particle widths by a factor of the order of 10^2 to 10^4 . Thus the total width Γ will simply be equal to the proton width Γ_r and we see that equations (4) and (5) become:

$$\gamma_\alpha = \Gamma_\alpha$$

and

$$\gamma_\gamma = \Gamma_\gamma$$

The actual values of the level widths cannot be calculated without making some assumption as to the level widths without barrier. Plausible values for these level widths without barrier are of the order of 10^5 to 10^6 e.v. (Fowler et al.1948). Taking a value of 10^6 e.v. and the penetrability factors to be 10^{-3} for the protons and 10^{-6} for the alpha-particles, we find $\Gamma_p = 10^3$ e.v. and $\Gamma_\alpha = 1$ e.v. Thus we see that the observed values of $\omega\gamma_\alpha$ given in Table IV are of the expected order of magnitude. The present state of the theory does not permit of a more accurate comparison.

We can now attempt to make assignments of the angular momentum and parity of the levels of the compound nucleus Si^{28} involved in these transitions. The ground state of Al^{27} is known from spectroscopic data to be a $D^{5/2}$ state, i.e. it has an orbital angular momentum quantum number of 2 and a total angular momentum of $5/2$. Since it is a D state it must have even parity. The parity of the compound states formed in Si^{28} will therefore be even or odd according to whether the orbital angular momentum of the incoming protons is even or odd. If we assume that the incoming protons have zero angular momentum (S-wave) then the states of Si^{28} will have angular momentum of either 2 or 3 units, depending on whether the proton spin is parallel or anti-parallel to the angular momentum axis of the Al^{27} nucleus. The parity of the states will be

even in both cases. Now it is known that the ground state of Mg^{24}, which is the residual nucleus after the emission of an alpha-particle, is an S-state with zero angular momentum and even parity. Thus in the case considered above, the alpha-particles must be emitted with no change of parity. This is only possible if the alpha-particles carry away an even number of units of angular momentum. Thus if we assume that only S-wave protons are captured to form the compound states in Si^{28} we can say that the levels which are observed to emit alpha-particles must have an angular momentum quantum number of 2 and those which only emit gamma-rays must have an angular momentum quantum number of 3. The ground state of Si^{28} is known to be an S-state with zero angular momentum and even parity. The selection rules for gamma-ray transitions would therefore only allow electric quadrupole radiation to the ground state in the case of the 2(+) levels and magnetic octupole radiation in the case of the 3(+) levels. There is not sufficient information available at present to make definite spin and parity assignments to the level in Si^{28} at 1.8 MeV or to the higher levels but it is quite likely that electric dipole radiation may be allowed from either the 2(+) or 3(+) levels to the level at 1.8 MeV and to the intermediate levels. We have seen that the gamma-ray spectrum from all the levels excited by 750 keV

protons shows that the cascade transitions are more favoured than the ground state transition, which is consistent with this picture. If the gamma-ray spectrum could be measured from the separate levels by the use of a thin target and the appropriate proton energy, a more definite check on these assignments could be made, since one would only expect to observe the ground state transitions in appreciable intensity from the 2(+) levels, i.e. from those levels which also emit alpha-particles.

If we allow the capture of P-wave protons, which is less probable than S-wave capture on account of the barrier penetrability effects, but which cannot be completely ruled out, then a greater variety of levels in Si^{28} are possible. The various possibilities are summarised in Table V, together with the possibilities already discussed for S-wave capture. It will be seen that in the case of P-wave capture the alpha-emitting levels can be either 1(-) or 3(-), but the former would allow electric dipole gamma-radiation to the ground state, which seems unlikely in view of the observed low intensity. It may be mentioned that a measurement of the angular distribution of the gamma-rays relative to the direction of the incoming protons should provide further information, since one would expect this distribution to be isotropic for S-wave capture but not for P-wave capture. It is hoped to make this measurement in this laboratory shortly.

* * * * * *

TABLE V.

Incoming Protons	Possible Levels in Si^{28}.	Alpha-Emission Possibility.	Gamma-Rays to Ground State.
S	2 +	Yes	E.Q.
S	3 +	No	M.O.
P	1 -	Yes	E.D.
P	2 -	No	M.Q.
P	3 -	Yes	E.O.
P	4 -	No	M^4 pole.

Part V. Conclusion.

In this thesis we have described the experimental work which has been performed with the Glasgow H.T. and discussed the new knowledge which has been obtained from this work. There is now a very considerable amount of information on the energy levels of nuclei which has been obtained from experiments of this type. Excellent summaries of this information have been made from time to time, notably by Bethe (1937), Hornyak and Lauritsen (1948), Hornyak et al (1950) and Alburger and Hafner (1950). It was from information of this type that the Rutherford-Bohr theory of the atom was developed and we might hope that similar information about nuclear energy levels would lead to some similar theory of nuclear forces and nuclear structure. Unfortunately this is not at present the case.

In the case of the atom, the problem is very much simplified by the fact that the electrons move in a central field of force and are very little influenced by each other. This results in a series of energy levels which have simple integral relations to each other and this characteristic feature, of which the Rhydberg relation for the hydrogen spectrum is an obvious example, was quickly observed from the experimental data and formed one of the starting points of the Rutherford-Bohr theory.

In the case of the nucleus there is no such central field of force and the theory therefore has to deal with a 'many-body' problem of an extremely complicated nature. Exact calculations have been attempted for the very simplest of nuclei, such as H^2, but even here they have met with very limited success. A study of the empirical data on nuclear energy levels does not, in general, yield any simple integral relations similar to the Rhydberg relation, which might give a lead to theoretical interpretations.

In view of the difficulties associated with the formulation of any exact theory, a considerable amount of effort has been devoted to 'nuclear model' theories. These theories make simplifying assumptions which allow the problem to be treated in terms of a simple dynamical model about which calculations can be made. These theories have had a certain limited degree of success in the qualitative explanation of particular features of nuclei. For example, the 'liquid drop' model developed by Bohr gives a qualitative description of the stability of heavy nuclei and of the phenomenon of nuclear fission which is in reasonable agreement with the observed data. Nuclear 'shell' models have also had some success in explaining the general features of the ground states of nuclei, such as the spin and magnetic moment and the particular stability of nuclei with certain numbers of

neutrons and protons. However, none of these models are able to make quantitative predictions about the energy levels of nuclei because of the drastic nature of the assumptions on which they are based.

The experimental data on the energy levels of nuclei, although very considerable in quantity, is very far from complete and we must hope that when further data is obtained it will give a lead to the development of more fruitful theories of nuclear structure and to a better understanding of nuclear forces.

* * * * * * *

References.

Alburger, D.E. (1949).	Phys.Rev., 75, 51.
Bayley, A.J. and Ward, A.G. (1948).	Can.Jour.Res. A26, 69.
Benes, J., Hedgram, A., and Hole, N., (1948).	Arkiv.Mat.Astron.Fysik, 35A, No.12.
Bethe, H.A., (1937).	Rev.Mod.Phys. 9, 69.
Brostrom, K.J., Huus, T., and Tangen, R. (1947).	Phys. Rev., 71, 661.
Buechner, W.W., Strait, E.N., Stergiopoulous, C.G., and Sperduto, A. (1948).	Phys.Rev., 74, 1569.
Burcham, W.E., and Freeman, J.M. (1949).	Phil.Mag. 40, 807.
Burcham, W.E., and Freeman, J.M. (1950).	Phil.Mag. 41, 921 and 337.
Chao, C.V., Tollestrup, A.V., Fowler, W.A., and Lauritsen, C.C. (1950).	Phys. Rev. 79, 108.
Christy, R.F. and Latter, R. (1948).	Rev.Mod.Phys. 20, 185.
Cockroft, J.D. and Walton, E.T.S. (1932).	Proc.Roy.Soc. A136, 619 and A137, 229.
Dee, P.I., and Gilbert, C.W. (1936).	Proc.Roy.Soc., A154, 279.
Delsasso, L.A., Fowler, W.A., and Lauritsen, C.C. (1947).	Phys.Rev. 51, 391.
Devons, S. (1949).	"Excited States of Nuclei". Camb.Univ.Press.
Devons, S., and Hine, M. (1949).	Proc.Roy.Soc. A199, 56.
Epstein, D.W. (1936).	Proc.Inst.Rad.Eng. 24, 1095.
Fowler, W.A., Lauritsen, C.C. and Lauritsen, T. (1948).	Rev.Mod.Phys. 20, 236.

References. (Continued).

Freeman, J.M., (1950).	Proc.Roy.Soc. A63, 668.
Freeman, J.M., and Baxter, A.S. (1948).	Nature, 162, 696.
Gaerttner, E.R., Fowler, W.A., and Lauritsen, C.C. (1939).	Phys.Rev. 55, 27.
Gibson, W.M., (1949).	Proc.Phys.Soc., A62, 586.
Halpern, J., and Crane, H.R. (1939).	Phys.Rev. 55, 415.
Heitler, W. (1944).	"Quantum Theory of Radiation". Oxford University Press.
Hornyak, W.F., and Lauritsen, T. (1948).	Rev.Mod.Phys. 20, 191.
Hornyak, W.F., Lauritsen, T., Morrison, P., and Fowler, W.A. (1950).	Rev.Mod.Phys., 22, 291.
Lewis, W.B. (1942).	"Electrical Methods of Counting". Camb.Univ.Press.
Lamar, E.S., Buechner, W.W., and Compton, K.T. (1937).	Phys.Rev. 51, 936.
Lawrence, E.O., and Livingstone, M.S., (1932).	Phys.Rev. 40, 19.
Livingstone, M.S., and Bethe, H.A. (1937).	Rev.Mod.Phys. 9, 245.
Mattauch.	"Nuclear Physics Tables".
Mayer, M.G. (1950).	Phys.Rev. 78, 16.
Oliphant, M.E.L. and Rutherford, Lord. (1933).	Proc.Phys.Soc.141, 259.
Parkinson, D.B., Herb, R.G., Bellamy, J.C., and McHudson, C.M. (1937).	Phys.Rev. 52, 75.
Peck, R.A. (1949).	Phys.Rev. 76, 1279.
Plain, G.P., Herb, R.G., Hudson, C.M., and Warren, R.E. (1940).	Phys.Rev. 57, 187.

References. (Continued).

Rae, E.R., Rutherglen, J.G., and Smith, R.D. (1950). Proc.Phys.Soc. A63, 775.

Rumbaugh, L.H., Roberts, R.B., and Hafstad, L.R. (1938). Phys.Rev. 54, 654.

Rutherglen, J.G., and Cole, J.F.I. (1947). Nature, 160, 545.

Smith, C.L., and Murrell, E.B.M. (1939). Proc.Camb.Phil.Soc. 35, 298.

Smyth, H.D. (1931). Rev.Mod.Phys. 3, 347.

Strait, E.N., Van Patter, D.M., Buechner, W.W., and Sperduto, S. (1951). Phys.Rev. 81, 749.

Swann, C.P. and Hudspeth, E.L., (1949). Phys.Rev. 76, 168.

Tollestrup, A.V., Fowler, W.A., and Lauritsen, C.C. (1949). Phys.Rev. 76, 428.

Tuve, M.A., Dahl, O., Hafstad, L.R. (1935). Phys.Rev. 48, 241.

Van Allen, J.A., and Smith, N.M. (1941). Phys.Rev. 59, 501.

Van der Graaff, R.J. (1931). Phys.Rev. 38, 1919.

Van der Graaff, R.J., Compton, K.T., and Van Atta, L.C. (1933). Phys.Rev., 43, 149.

Walker, R.L. and McDaniel, B.D. (1948). Phys.Rev. 74, 315.

* * * * *